

740-3

JPL RELEASE
7N-89
63002-CR
92P

SUBMILLIMETER WAVELENGTH ASTRONOMY FROM SPACE

REPORT OF THE SUBMILLIMETER SPACE TELESCOPE WORKING GROUP

R-0
5-28-85
10-15
11-28
1-30
4-10
9-17

K

10 April 1978

(NASA-CR-180268) SUBMILLIMETER WAVELENGTH
ASTRONOMY FROM SPACE. REPORT OF THE
SUBMILLIMETER SPACE TELESCOPE WORKING GROUP
(Jet Propulsion Lab.) 92 p

N87-70356
63002

Unclas
00/89 45002

Jet Propulsion Laboratory
California Institute of Technology
Pasadena, California

740-3

SUBMILLIMETER WAVELENGTH ASTRONOMY FROM SPACE

REPORT OF THE SUBMILLIMETER SPACE TELESCOPE WORKING GROUP

10 April 1978

**Jet Propulsion Laboratory
California Institute of Technology
Pasadena, California**

PREFACE

A low level study was funded by the Office of Space Science in FY 76 to make a preliminary investigation of the requirements and technical feasibility of a space telescope for submillimeter wavelengths. As a result of this early study, funding was made available from Dr. Frank Martin in the Office of Space Science in FY 77 to form a small working group at the Jet Propulsion Laboratory. The main charge of this group was to develop a strong science rationale for a submillimeter space telescope. In response to this request, a Submillimeter Space Telescope Working Group was formed in May 1977. The following twelve members participated in the study.

R. L. Brown - National Radio Astronomy Observatory
 D. Buhl - Goddard Space Flight Center
 T. de Graauw - European Space Agency
 S. Gulkis - Jet Propulsion Laboratory (Chairman)
 T. Kuiper - Jet Propulsion Laboratory
 R. Leighton - California Institute of Technology
 D. Staelin - Massachusetts Institute of Technology
 P. Swanson - Jet Propulsion Laboratory
 P. Thaddeus - Goddard Institute for Space Studies
 B. Turner - National Radio Astronomy Observatory
 J. Waters - Jet Propulsion Laboratory
 M. Werner - California Institute of Technology

These twelve members have diverse interests which span the fields of star formation, molecular astrophysics, physics, galactic and extragalactic radio physics, planetary astronomy, and radio engineering. In addition to the working group members, B. Gary, M. Janssen, M. Klein, and E. Olsen, all from the Jet Propulsion Laboratory, also attended meetings and supported the study.

The primary functions of the working group were:

- a. To develop the science rationale for a shuttle-launched submillimeter telescope, and
- b. to define a nominal telescope configuration and typical set of receivers for various types of experiments as a guideline for future studies.

The working group was asked to provide a written report of its findings to NASA by the end of calendar year 1977. To fulfill the above goals the working group held the following meetings during which the contents of the report were developed.

May 12-13, 1977	Shuttle Orientation and Organization
July 27-28, 1977	Science Objectives Discussion and Report Outline
Oct. 5-6, 1977	Discussion of Final Report

CONTENTS

I.	INTRODUCTION-----	1-1
II.	SUMMARY OF MAJOR CONCLUSIONS AND RECOMMENDATIONS -----	2-1
A.	CONCLUSIONS -----	2-1
B.	RECOMMENDATIONS -----	2-2
III.	SCIENTIFIC OBJECTIVES -----	3-1
A.	INTRODUCTION AND SUMMARY -----	3-1
B.	THE COSMIC BACKGROUND -----	3-3
C.	EXTRAGALACTIC RADIO SOURCES -----	3-5
D.	THE STRUCTURE OF GALAXIES -----	3-6
	1. The Lines of Neutral Carbon -----	3-7
	2. Molecular Observations in External Galaxies -----	3-9
	3. Dust in External Galaxies -----	3-12
E.	THE EVOLUTION OF MOLECULAR CLOUDS -----	3-12
	1. Physical Properties of Clouds -----	3-13
	2. Internal Motions of Clouds -----	3-14
	3. Interstellar Chemistry -----	3-14
	4. Heating and Cooling of Clouds -----	3-18
F.	STAR FORMATION -----	3-21
G.	COMETS -----	3-24
H.	PLANETS -----	3-24
	1. Venus -----	3-24
	2. Outer Planets -----	3-28

I.	POST-MAIN-SEQUENCE EVOLUTION -----	3-31
1.	Red Giants -----	3-32
2.	Carbon and S-type Stars -----	3-35
3.	Early-Type Emission Line Stars -----	3-37
4.	Novae -----	3-37
IV.	TECHNICAL REQUIREMENTS AND FEASIBILITY -----	4-1
A.	GENERAL CONSIDERATIONS -----	4-1
B.	SCIENCE CONSIDERATIONS -----	4-1
C.	SUBMILLIMETER TELESCOPE CONCEPT -----	4-2
D.	ANTENNA -----	4-2
E.	ANTENNA POINTING AND CONTROL -----	4-8
F.	RECEIVERS -----	4-8
V.	FOLLOW-UP POSSIBILITIES -----	5-1
A.	ANTENNAS -----	5-1
B.	COHERENT RECEIVERS -----	5-3
VI.	BIBLIOGRAPHY -----	6-1
APPENDICES		
A.	EFFECT OF THE ATMOSPHERE ON GROUND-BASED AND AIRBORNE OBSERVATIONS -----	A-1
B.	THE PHYSICAL LIMITATIONS OF GROUND-BASED ANTENNAS -----	B-1
C.	REVIEW OF SUBMILLIMETER WAVE MIXERS -----	C-1

Figures

2-1.	Artist's Conception of 4.2 m Diameter Submillimeter Telescope Which Would have Applications in Astronomy and Upper Atmospheric Research -----	2-3
------	--	-----

3-1. Cosmic Background Anisotropy Predicted by Silk (1974) for a Typical Model Universe -----	3-4
3-2. The Spectrum of the Extragalactic Source NGC1068. Original figure is from Telesco, Harper, and Stein (1976). Additional points at 390 μm and 540 μm from Hildebrand et al (1977) have been added. -----	3-5
3-3. Spectra of non-thermal extragalactic sources with substantial millimeter and submillimeter fluxes -----	3-7
3-4. Two galaxies which have been partially mapped in the J=0-1 line of CO with an angular resolution of 1 arc minute. (After Rickard <u>et al</u> , <u>Ap. J.</u> , 213, 673, 1977) -----	3-11
3-5. Spectra of HII regions W3(A) and W3(OH), (Mezger, 1975). Dashed region shows anticipated submillimeter space telescope coverage -----	3-15
3-6. Continuum emission from the Orion Nebula complex at 20 μm , 100 μm , 1 mm, and 6 cm -----	3-16
3-7. Spectrum of the excess infrared emission from an HII region. The dashed line is a black-body curve at 70 K and the solid line the theoretical curve for emission from electron transitions in a plasma (Wynn-Williams and Becklin 1974). The dotted line shows the submillimeter spectral dependence, approximately λ^{-3} -----	3-20
3-8. Radio Continuum Spectrum of MWC 349 -----	3-22
3-9. Schematic diagram of the structure of Comet Encke -----	3-25
3-10. Signal-to-noise ratio obtained on various Solar System Bodies in 1-hour integration with 500 MHz bandwidth -----	3-26
3-11. Pioneer II Photo of Jupiter. Resolution of 10-m telescope at 500 and 1000 GHz are indicated ----	3-27
3-12. Theoretical phosphine and ammonia spectrum on Saturn. (After Encrenaz and Combes, 1975) -----	3-33
3-13. Shaded region shows approximate shape of Jovian spectrum. Insert illustrates virtually unexplored spectral region which could be studied with a submillimeter space telescope -----	3-34

3-14a.J=0-1 profile of $^{12}\text{C}^{16}\text{O}$ in IRC+10216 -----	3-36
3-14b.J=0-1 profile of $^{13}\text{C}^{16}\text{O}$ in IRC+10216 -----	3-36
3-15. Radio Spectra of Nova Delphini 1967 and Nova Serpentis 1970 as measured from June to October 1970. (C.M. Wade and R. M. Hjellming, 1971) ---	3-38
4-1. 10-m diameter orbiting submillimeter telescope concept -----	4-3
4-2. 10-m diameter orbiting submillimeter telescope being serviced by shuttle -----	4-4
4-3. 10-m millimeter wavelength telescope at Owens Valley Radio Observatory, constructed of hexagonal modules -----	4-6
4-4. Receiver noise temperature versus frequency for a number of receivers -----	4-10
5-1. 24 m diameter Space-Erectable Antenna Consisting of 37 Hexagonal Penals -----	5-2
A-1. Vertical Atmospheric Opacity from Sites Given in Table A-1 -----	A-2
A-2. Effective System Temperature for a Highly Sensitive Receiver ($T_{\text{rec}} \text{ (K)} = \nu \text{ (GHz)}$) Located at the Sites Given in Table A-1 -----	A-3
A-3. Effective Antenna Diameter of the Largest Antennas Possible with Present Technology, when Such Antennas are Located on Kitt Peak -----	A-6
B-1. Efficiency of a Reflecting Antenna as a Function of its Surface Irregularities -----	B-3
B-2. Relationship between the Diameter of a Reflecting Antenna and its Minimum Operating Wavelength ---	B-4
C-1. Intrinsic conversion loss as a function of local oscillator drive for a Schottky-barrier mixer with optimum coupling -----	C-2
C-2. Equivalent circuit of a Schottky-barrier diode -----	C-2
C-3. The structure of an epitaxial Schottky-barrier diode. With n-GaAs the epilayer doping is 1 to $4 \times 10^{17} \text{ cm}^{-3}$ and the substrate doping is 2 to $5 \times 10^{18} \text{ cm}^{-3}$. -----	C-3

C-4.	The structure of a contact array diode. To reduce skin effect losses, ohmic contacts are made on the top surface encompassing the linear array on both sides -----	C-4
C-5.	An SEM photograph of preliminary linear contact-array diodes. The insulating layer normally present has been stripped away to permit viewing of the entire structure -----	C-4
C-6.	Current voltage characteristics of a Josephson junction. Curves A and B are with and without local oscillator power, respectively -----	C-5
C-7.	Reported values of mixer minimum detectable power (MDP) as a function of wavelength. The two filled-in data points refer to values of receiver MDP. The Schottky-barrier mixer results were obtained with room temperature operation. The remaining devices were cooled to 4.2 K, or below. -----	C-8

Tables

3-1.	Fine Structure Levels of Neutral Carbon -----	3-8
3-2.	Transitions Between $2p^2$ Fine Structure Levels of Neutral Carbon -----	3-8
3-3.	Sensitivity of 10-m Telescope for Continuum Studies -----	3-12
3-4.	Molecular Lines Detected in Interstellar Clouds -----	3-17
3-5.	Interstellar Hydrides -----	3-19
3-6.	Typical Transitions for Hydrides -----	3-19
3-7.	Composition of the Venus Atmosphere -----	3-29
3-8.	Transitions of Water to 1000 GHz -----	3-30
3-9.	CO Spectral Lines -----	3-31
3-10.	Rotational Transitions of Phosphine -----	3-32
4-1.	Parameters of Some Submillimeter Telescopes ----	4-5
4-2.	Antenna Requirements and Parameters -----	4-8

4-3. Submillimeter Receiver Sensitivity Based on Expected Noise Performance, Required Bandwidth and a 10 m Antenna -----	4-12
A-1. Parameters of Sites used in Atmosphere Model Calculations -----	A-4
B-1. Performance Parameters of Selected Filled Aperture Millimeter Radio Telescopes -----	B-2
C-1. Reported results with room temperature n-type GaAs Schottky-barrier mixers -----	C-4
C-2. Reported results with Josephson junction mixers at 4.2 k -----	C-6
C-3. Reported results with extrinsic photoconductive mixers -----	C-7
C-4. Reported results with hot electron photoconductive mixers 4.2 K -----	C-7
C-5. Reported results with MOM and pyroelectric mixers. Operating temperature is at room ambient -----	C-7

SECTION I

INTRODUCTION

The submillimeter and far infrared* region of the electromagnetic spectrum include more than 10 virtually unexplored wavelengths that are rich in astronomical information. Earth-based observations at these wavelengths have been severely restricted by atmospheric absorption, which varies radically with wavelength and weather conditions (Appendix A). Nevertheless, a large amount of work has been done exploring this spectral region from the ground within the spectral windows where the atmosphere is not completely opaque and from balloons and aircraft using small (~ 1 m aperture) telescopes. Based on these pioneering research efforts, astronomers have learned that the submillimeter spectral region offers a new perspective of the universe with new information that can next answer many of the fundamental questions of astronomy and cosmology. What was the nature of the universe in the very early stages of evolution of the primeval fireball? How and when did galaxies and clusters of galaxies form? How do stars and planetary systems form? What is the origin and the nature of comets and what information do they hold regarding the formation of planetary systems? What is the distribution and abundance of those chemical elements that are prerequisites for life?

From the few measurements which have been possible working through the millimeter and submillimeter windows, astronomers in the last decade have been able to sample the interiors of highly obscured dust regions near the center of our galaxy, HII regions, dense dark clouds and suspected protostars. Estimates of densities, temperatures, abundance ratios, kinematics, and grain properties have been made possible for the first time. Astronomers have learned that a number of extragalactic objects emit most of their energy in the far infrared spectral range. They have made preliminary and suggestive measurements of the large-scale anisotropy and have placed stringent limits on the small-scale isotropy of the 2.7 K background radiation.

We are now reaching the limitations imposed by our atmosphere, not in the sense that we have reached the limits of possible research, for there will always be opportunities for clever innovations, but rather in the sense that we can now formulate questions whose answers can best be obtained from a space platform. The NASA Space Shuttle, scheduled to begin routine operation in the early 1980's, will provide the first opportunity to place a large submillimeter telescope in Earth orbit. Operating in the space environment, the entire submillimeter spectral range will be accessible for the first time. Our belief is that a large submillimeter telescope in Earth orbit will open up a whole new regime of astronomical observations which can only be carried out

*The 40 μm to 1000 μm spectral region has been termed either the far infrared or submillimeter wave region reflecting the dual optical/microwave character of the techniques employed. In this document the term submillimeter refers to the range 100 to 1000 μm .

from space. A large submillimeter space telescope will also close the gap that exists between the radio and the infrared spectral regions.

This report shows how an orbiting submillimeter space telescope can be developed and how it will contribute to a number of important scientific questions relating to the origin and evolution of the universe. We recognize that new observational instruments in astronomy invariably yield surprising results which often open up new vistas and unexpected opportunities. Thus we believe that any arguments we can advance for a new facility can only be conservative: the return could be far greater than we can predict.

The outline of this report is as follows. In Section II we list our major conclusions and recommendations in summary form. In Section III, we present the scientific motivation for an orbiting submillimeter telescope. The section begins with an introduction which identifies the major research areas in general terms, relating them to an overall investigation into the evolution of the universe. Subsequent sections treat each of these areas in greater detail. The introduction to Section III may be read as an overview of the section; the following subsections skipped unless greater detail is desired by the reader.

Section IV assesses the current state of key areas of technology, notes developments that may be anticipated in the near future, and describes the concept for an orbiting submillimeter telescope which the working group feels is adequate to meet the scientific objectives.

In Section V we note how the scientific and technical experience to be derived from this instrument may lead to future opportunities for more sensitive telescopes and planetary probes.

Appendix A discusses the limits to ground-based radio observations imposed by the earth's atmosphere, and Appendix B discusses these and the gravitational limits in terms of maximum antenna gain for ground based antennas.

Appendix C is a recent review of submillimeter wave mixer technology.

SECTION II

SUMMARY OF MAJOR CONCLUSIONS AND RECOMMENDATIONS

This section contains the principal product of the deliberations of the Submillimeter Space Telescope Working Group. The working group has summarized its deliberations in the form of specific conclusions and recommendations after reviewing the scientific and technological material. Support for these conclusions is given either in Section III, which discusses scientific rationale, or in Section IV, which discusses technological capabilities and feasibilities. Cross-references to the appropriate subsections are noted in square [] brackets.

A. CONCLUSIONS

CONCLUSION 1: The Submillimeter Spectral Region

The submillimeter spectral band between wavelengths of 100 μm and 1 mm is of key importance for the investigation of a wide range of astronomical subjects, including:

- Cosmic microwave background [III-B].
- Emission mechanisms and physical conditions in quasars and other extragalactic radio sources [III-C].
- Structure and evolution of galaxies [III-D].
- Composition and evolution of interstellar clouds [III-E].
- Investigation of both early and late stages of stellar evolution [III-F,I].
- Composition of comets and planetary atmospheres [III-G,H].

CONCLUSION 2: Requirement for Submillimeter Observatory in Space

A large space telescope 10 m in diameter or larger, dedicated to astronomical studies in the submillimeter band, is needed for astronomy to provide both sufficient collecting area and adequate spatial resolution. No instrument with such capability is currently planned, but experience gained from constructing ground-based and space antennas indicates that such a space telescope is feasible [IV-C,D].

CONCLUSION 3: Availability of Receivers

Submillimeter receiver technology is now experiencing a period of very rapid development. Broadband superheterodyne receivers capable of making useful astronomical measurements to wavelengths as short as 0.6 mm are now being constructed. Receivers operating up to 1000 GHz (0.33 mm) with a sensitivity comparable to current millimeter wavelength

receivers may be anticipated within 5 years. Bolometers are available throughout the entire submillimeter spectral range [IV-F App. C].

CONCLUSION 4: Serendipity

The band between 100 μ m and 1 mm is a largely unexplored region of the electromagnetic spectrum. The history of astronomical research suggests that observations in this spectral window have a high probability of uncovering previously unsuspected astronomical phenomena.

B. RECOMMENDATIONS

Recommendation 1: Ten-meter Diameter Ambient Temperature Telescope

We recommend the initiation of design studies of a 10-m free-flying submillimeter telescope for astrophysical applications [IV-D].

Recommendation 2: Continued Program of Submillimeter and Infrared Astronomy

We recommend that a vigorous program of ground-based and aircraft observations in the submillimeter and infrared spectral regions be pursued in the immediate future in order to build the astronomical and instrumental foundation required to ensure the most effective utilization of a submillimeter space telescope.

Recommendation 3: Early Shuttle Missions

We recommend the use of a small (~ 2 -4 m) shuttle fixed, submillimeter telescope on early shuttle missions for astronomical research and for engineering tests of submillimeter space systems. A small shuttle fixed telescope could also be used for earth atmospheric research, in which case the program costs might be shared. (Figure 2-1 illustrates one configuration of a shuttle fixed 4.2 m diameter submillimeter telescope which could be used on an early mission.)

Recommendation 4: Receiver Development Program

We recommend that increased resources be devoted to the development of low-noise, coherent, submillimeter receivers. Such receivers will have a wide range of applications including astronomy, earth remote sensing, satellite communications, and laboratory plasma physics [IV-F]. Additional development of far infrared incoherent detectors, in particular arrays for imaging, will also enhance the utilization of space telescopes.

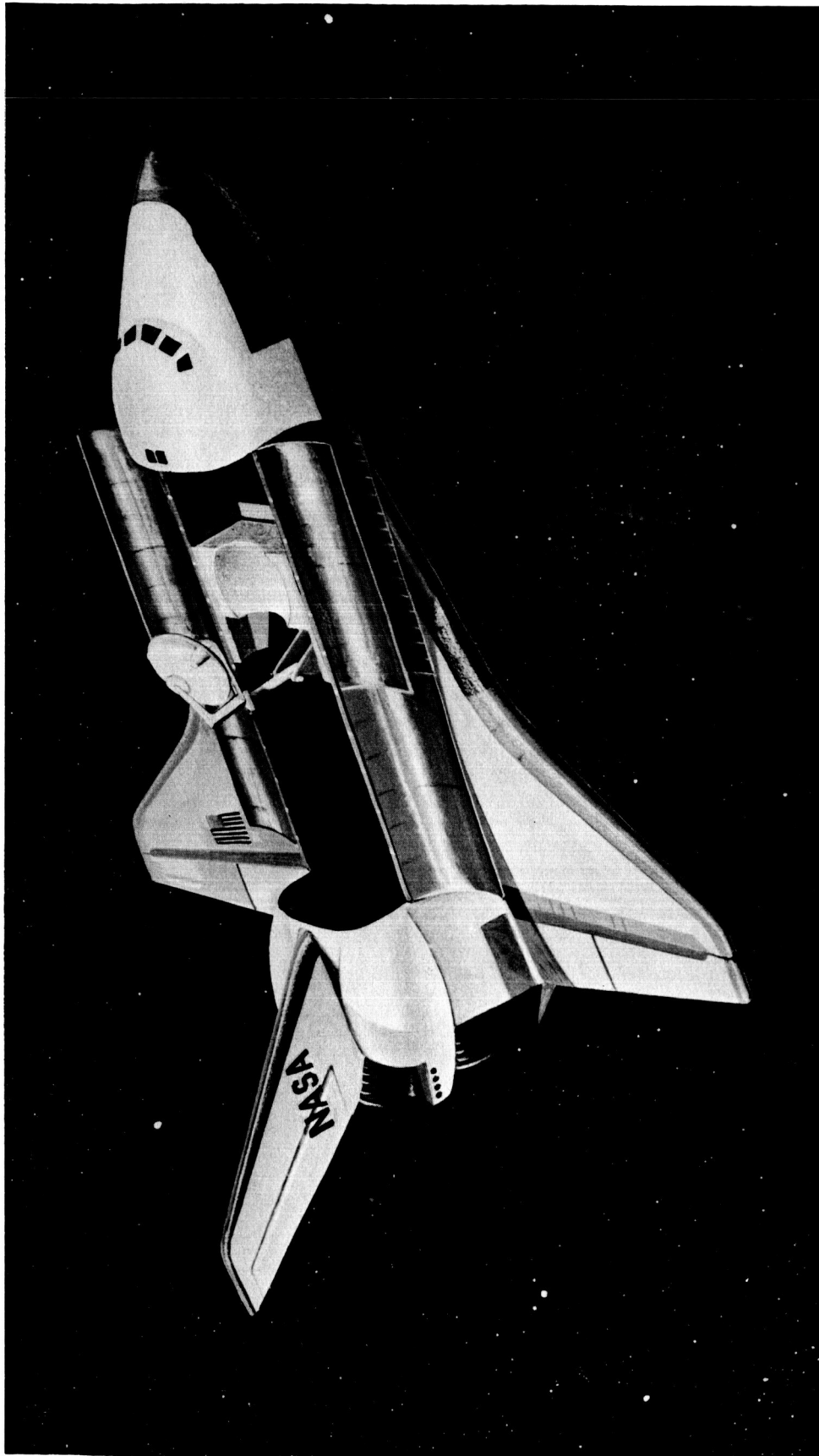


Figure 2-1. Artist's Conception of 4.2 m Diameter Submillimeter Telescope Which Would Have Applications in Astronomy and Upper Atmospheric Research

SECTION III

SCIENTIFIC OBJECTIVES

A. INTRODUCTION AND SUMMARY

Although astronomers have constructed a rather general overview of the evolution of the universe, crucial questions bearing on the validity of particular models remain unanswered. Many questions, whose answers probably lie in the submillimeter and infrared portions of the electromagnetic spectrum, have been formulated. Since the terrestrial atmosphere severely limits the ground-based observations which can be conducted between wavelengths of 10 μ m to 1000 μ m (Appendix A), a space telescope is required to explore this spectral region systematically.

The discovery at centimeter wavelengths of the universal background radiation has yielded probably the single most convincing evidence that the universe has its origin in a dense hot nuclear gas, and that the universe as we observe it today is the consequence of the expanding and cooling of that gas. In order for galaxies and clusters of galaxies to have condensed gravitationally, there must have been density inhomogeneities in this primordial fireball. These inhomogeneities should, in turn, be reflected in small scale anisotropy of the cosmic background radiation. The degree and angular scale of this isotropy have eluded measurement, primarily because of the instability of the atmosphere through which these measurements are made. In the early 1980's, the Cosmic Background Explorer using small horn antennas will survey the sky for anisotropy on an angular scale of $\sim 10^\circ$ or larger, but a larger instrument is needed to measure the smaller structure, which is important to the understanding of galaxy formation.

The discovery of quasars, whose large redshifts suggest that they are located at remote extragalactic distances, led to the suspicion that these objects represent some phenomenon in the early evolutionary stages of galaxies. It is generally believed that these objects emit primarily by non-thermal radiation, but the details of the emissions, the physical conditions which give rise to them, and the subsequent evolution of these sources are still unknown. The shape of the spectra at radio wavelengths and in the visual and near infrared indicate that a subclass emits very strongly in the infrared; but even the largest telescopes, when looking through windows in the atmosphere, do not have enough sensitivity in the far infrared to measure more than the strongest sources. The link, if any, between variability in the visual and radio is also missing because of the large spectral range between them that is obscured by the atmosphere. Submillimeter observations, including measurements of polarization and variability, will enable astronomers to have a more complete picture of these sources.

With the development of aperture synthesis radio telescope arrays, astronomers achieved the sensitivity and angular resolution to study the structure of nearby galaxies at radio wavelengths. The positions of the clouds of neutral hydrogen, and of synchrotron emission relative to the dust clouds and stars have supported the spiral density wave theory

and its role in star formation. In order to follow the subsequent evolution of these clouds, it will be necessary to observe a number of spectral lines, such as those of neutral carbon. High angular resolution on the order of 10 arc seconds, which can be achieved at high frequencies, is an important asset in such studies.

Our understanding of these processes on a galactic scale in turn hinges on what we know of the processes within individual clouds. Access to many important spectral lines will enable astronomers to focus more clearly on a variety of phenomena. The lines of neutral carbon at 491 and 812 GHz may serve to delineate the boundaries of major clouds. The ground state transitions of water (557 GHz) and ammonia (573 GHz) will identify regions of high density (shock fronts, protostars) and those excited by infrared sources. It will be possible to search for new molecules such as HCl (626 GHz), NH (975 GHz), NH^+ (391 GHz), OH^+ (~900 GHz), SiH^+ (453 GHz), and thus come to a clearer understanding of the mechanisms by which inter-

molecules already observed at millimeter wavelengths will advance our understanding of the excitation mechanism, and thus such physical conditions as molecular density, kinetic temperature, and infrared flux on an angular scale of tens of arc seconds. A space telescope will also provide greatly increased sensitivity and precision in the determination of the infrared continuum radiation from dust within the clouds, yielding information on the nature of dust grains, the gas-to-dust ratio, and the scale of clumping.

An orbiting telescope would be an important tool in the investigation of many stages of stellar evolution. Observations of a wide variety of molecules in many spectral lines and with high angular resolution will make it possible to investigate the physical conditions, chemistry, and kinematics of the high density, high temperature cores of clouds (such as the Kleinmann-Low nebula in Orion) that are suspected to be sites of star formation. Radio continuum studies of the submillimeter spectrum of pre-main sequence mass-loss stars (e.g., T Tau, P Cyg, Lk Ha 101, MWC 349) yield information about the conditions in the densest parts of their ionized envelopes. Molecular line studies into the composition of envelopes of late spectral-type stars undergoing mass-loss (such as IRC+10216 and CIT6) bears on the formation of planetary nebulae and the return of material to the interstellar medium. The molecular excitation and composition of envelopes of red giants showing maser emission in OH, H_2O , and SiO can be investigated using submillimeter spectral lines. The submillimeter radio continua of post-red-giant mass-loss stars of early spectral type (such as V 1016 Cyg), which are possibly the immediate predecessors of planetary nebulae, need to be examined for turn-over. Study of the excitation of molecules in the outer envelopes of planetary nebulae (e.g., NGC 7027) can be conducted using submillimeter spectral lines which connect the higher rotational energy levels.

The formation of stars is, of course, linked with the origin of our solar system. The composition of comets, which may be remnants of the primordial solar nebula, can be effectively studied by means of the submillimeter spectral lines of the gases surrounding the nucleus. The atmospheres of the "gas giant" planets, which can also be studied in a unique way by submillimeter spectral lines, represent another view of the composition of

the primordial nebula. Similar techniques can also be applied to the study of the atmosphere on Venus, yielding information on its composition, structure, weather and climate.

The topics which have been briefly presented in this summary represent different phases in the physical evolution of the universe. Accordingly, we have structured this chapter on an evolutionary sequence, taking note of the contributions that can be made to our understanding of the various evolutionary stages by means of a submillimeter space telescope. We have endeavored to note the technical requirements - antenna size, receiver sensitivity, bandwidth, spectral resolution - for the investigation of subjects we have identified. However, our selection of problems has been tempered by our assessment of what is technically feasible with instrumentation that has been demonstrated or seems feasible in the near future. An assessment of the technology is presented in Chapter IV.

B. THE COSMIC BACKGROUND

It is generally accepted that some 10 to 20 billion years ago, the universe was a compressed nuclear fluid (the primeval fireball) undergoing an explosive-like expansion. The remnants of the explosion are still seen today in the Hubble expansion. According to current ideas, massive extragalactic systems such as galaxies and clusters of galaxies formed as a result of small fluctuations in density which were present in the early stages of expansion of the universe. Presumably these density fluctuations are still manifested in the angular distribution of the background radiation. A space telescope can easily measure small scale anisotropy and thereby study galaxy formation. Galaxy formation is of fundamental importance and is not yet understood.

An observational test of the main ideas of galaxy formation can be provided by measurements of the residual small-scale fluctuations in the microwave background. Peebles and Yu (1970), Sunyaev and Zel'dovich (1970), Silk and Ames (1972), Silk (1974) and others have investigated the evolution of fluctuations in the primeval plasma in the hot Big Bang cosmology with the hope of accounting for the development of galaxies and clusters of galaxies. Figure 3-1 shows the anisotropy predicted by Silk for a typical model universe. The figure illustrates the strong dependence of the anisotropy on angular scale and the high precision which is required to detect the fluctuations. The existing measurements of Pigg (1976), Carpenter, Gulkis, and Sato (CGS) (1973), Conklin and Bracewell (CB) (1967), and Paryskii (P_a and P_b) (1967) shown on the figure do not have the required precision to confirm this theory although the measurements already rule out certain other models.

In order to make a significant improvement in the sensitivity, measurements must be made from space. Fluctuations in the atmospheric transparency will probably limit the sensitivity of millimeter and submillimeter ground-based measurements to about 0.5×10^{-3} K or $\Delta T/T \approx 2 \times 10^{-4}$ for scales of the order of 1 arc minute. A relatively sophisticated but technologically feasible Josephson junction receiver or maser receiver with $T_{\text{sys}} \sim 100$ K and a bandwidth of 1 GHz would achieve this limit in about one minute. A telescope of ~ 10 m diameter will provide a sufficient resolution capability to examine a wide variety of models. The line marked "OST"

in Figure 3-1 shows the limits which could be achieved by an orbiting submillimeter telescope in an hour long integration time. Thus we believe that a submillimeter telescope in space will be an important tool for the investigation of the small-scale structure of the cosmic background. These measurements will not be provided by the Cosmic Background Explorer Satellite (scheduled for launch in 1983) which surveys the sky on an angular scale of 10° .

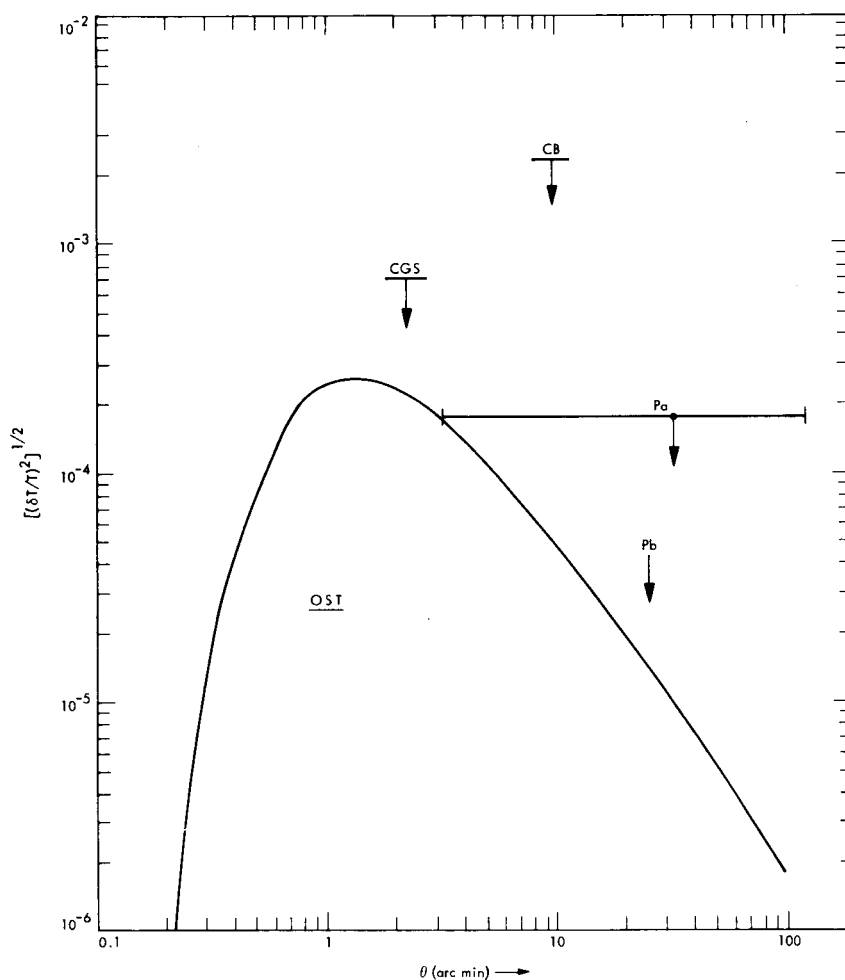


Figure 3-1. Cosmic Background Anisotropy Predicted by Silk (1974) for a Typical Model Universe

C. EXTRAGALACTIC RADIO SOURCES

While it is generally accepted that quasars, the nuclei of radio galaxies, BL Lacertae objects, Seyfert galaxies, etc. emit large amounts of radio radiation by the synchrotron mechanism, the details of this mechanism, the physical conditions which give rise to it, and the temporal variations and evolution of such objects are not understood. The discovery by Pacholczyk and Wisniewski (1967), Kleinmann and Low (1970a; 1970b) and Rieke and Low (1972; 1975) that many of the extragalactic objects are strong emitters at 2-25 μm and that in some cases the infrared emission dominates the total luminosity has given great impetus to efforts to close the gap between the millimeter and infrared spectral domains.

Of the nearly one hundred extragalactic sources which have been measured at 10 μm , about two dozen have now been detected in the range 40 - 1100 μm . The sources detected in this spectral band include galaxies similar to our own, Seyfert galaxies and radio galaxies, and several quasi-stellar and BL Lacertae-type objects. The studies carried out so far in this spectral band have yielded important results concerning the nature of the brightest extragalactic radio sources. For example, luminous galaxies such as NGC 1068, NGC 253, and M 82 exhibit peaks in the far infrared near 100 μm (Fig. 3-2), and the spectra have been

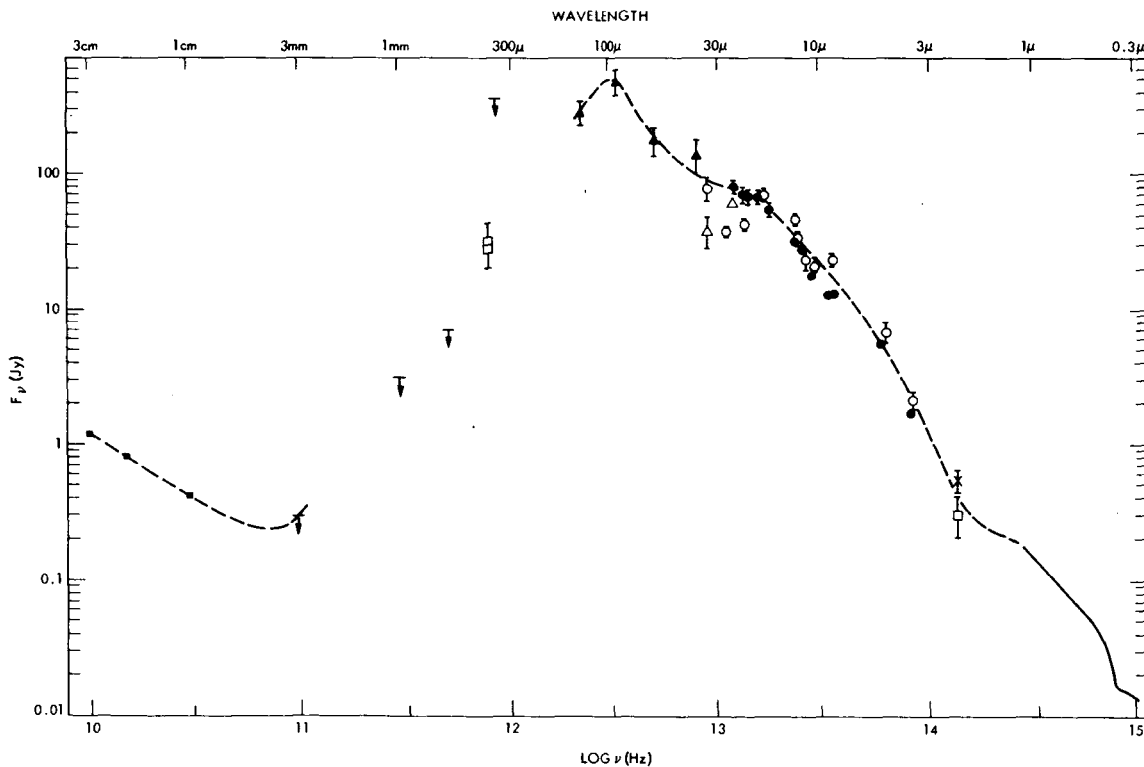


Figure 3-2. The Spectrum of the Extragalactic Source NGC1068. Original figure is from Telesco, Harper, and Stein (1976). Additional points at 390 μm and 540 μm from Hildebrand et al. (1977) have been added.

extended far enough into the submillimeter domain to allow a definitive conclusion to be reached as to the source of emission (Hildebrand et al 1977; Elias et al 1978). In these objects the steepness of the spectrum at sub-millimeter wavelengths indicates that the far infrared peak is the result of re-radiation by optically thin dust, rather than the signature of a self-absorbed non-thermal source. The high spatial resolution at submillimeter wavelengths of the orbiting 10 m reflector considered in this study will permit measurements of the sizes of these thermally emitting sources, which will be extremely useful in determination of the dust densities and analysis of the mechanisms which heat the dust. Additionally, the high sensitivity of such a telescope (see Table 4-3) for both molecular line and thermal continuum observations will permit a study of the apparent correlation between thermal infrared emission and molecular emission which appears to be emerging from the early studies of the nuclei of galaxies (cf. III-C-2).

A second class of extragalactic objects, which includes BL Lacerta and the QSOs 3C273 and 3C279, as well as several radio galaxies, shows submillimeter spectra suggestive of non-thermal emission; the submillimeter flux in these sources does not appear to be significantly above that expected from a smooth extrapolation of the non-thermal spectra observed at radio wavelengths (Fig. 3-3). The 100-fold increase in sensitivity attainable with the orbiting 10-m telescope will permit an extension of these observations to shorter wavelengths, as well as a vast increase in the number of objects which can be studied in this spectral band. Observations at the higher frequencies sample the synchrotron radiation from electrons of higher energy, which have shorter lifetimes in a fixed magnetic field; thus extension of these energy distributions into the submillimeter will provide ever tighter constraints upon the models and radiation mechanisms for these sources. In the case of sources with extended radio lobes, such as Cygnus A for example, it is in the submillimeter domain where the electron radiation lifetimes become less than the time for a relativistically moving electron to cross the radio lobes. Thus investigation of these extended sources at submillimeter wavelengths will help to discriminate between injection and in situ acceleration models for the replenishment of the relativistic particles.

D. THE STRUCTURE OF GALAXIES

The spiral structure of galaxies has been studied by means of the distribution of young stars, HII regions, and dust complexes. In recent years, aperture synthesis radio astronomy has added maps in the radio continuum, and in the 21 cm line of hydrogen, with sufficient angular resolution to make meaningful comparisons with optical data. Within the last 2 years, the first extragalactic molecular line studies have been conducted, although these still suffer from relatively low angular resolution. Access to submillimeter wavelengths with a large telescope will greatly enhance the angular resolution with which molecular studies can be conducted. Key submillimeter lines, such as the lines of neutral carbon, will provide unique views of the clouds in external galaxies.

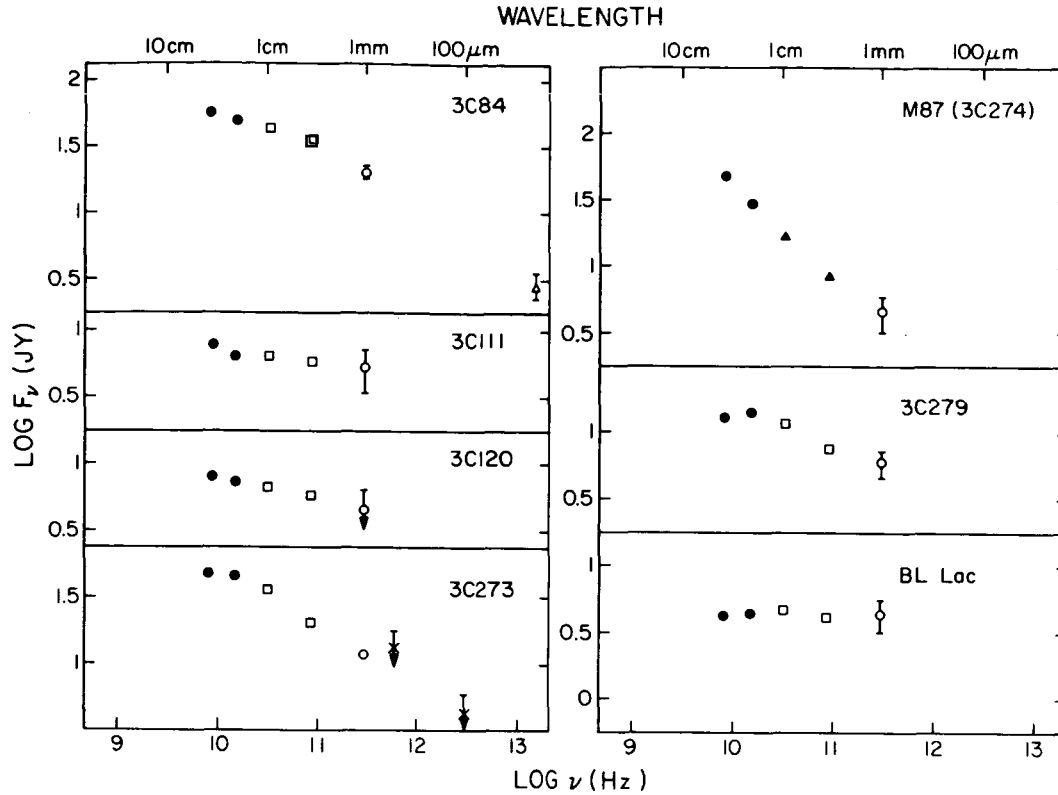


Figure 3-3. Spectra of non-thermal extragalactic sources with substantial millimeter and submillimeter fluxes.

1. The Lines of Neutral Carbon

The transition from ionized carbon to carbon monoxide represents a critical stage in the chemical evolution of clouds, and consequently has great impact on our understanding of galactic structure. Neutral atomic carbon (CI) might be a very efficient coolant of those interstellar clouds having sufficient opacity to the $\lambda < 1100 \text{ \AA}$ radiation which photo-ionizes CI. Consequently, it may permit such clouds to cool and collapse to densities at which CO forms. It is precisely this sensitivity of CI to the opacity and evolutionary state of interstellar clouds that makes a determination of its abundance, taken in concert with those of C^+ and CO, crucial to our understanding of the thermal, chemical and dynamical development of interstellar clouds.

CI may be an efficient coolant in low-temperature neutral clouds because its ground-state is split into three low-lying fine-structure levels (Table 3-1). Two magnetic-dipole transitions are permitted among these levels (Table 3-2).

Table 3-1. Fine Structure Levels of Neutral Carbon

Designation	Excitation (cm^{-1})	Energy (K)
$2p^2 \ ^3P_0$	0	0
$2p^2 \ ^3P_1$	16.4	23.4
$2p^2 \ ^3P_2$	43.5	62.6

Table 3-2. Transitions Between $2p^2$ Fine Structure Levels of Neutral Carbon

Transition (ΔJ)	$\lambda(\mu\text{m})$	$\nu(\text{GHz})$
(1-0)	610	491
(2-1)	369	812

The ionization state of interstellar carbon was first treated by Werner (1970). Later the conversion of C to CO in equilibrium dense clouds was added by Glassgold and Langer (1975) and finally the time-dependent abundance of CI in neutral clouds was computed by Oppenheimer and Dalgarno (1975). Although, as these works point out, the CI abundance may show wide variations, we may nevertheless make a crudely reliable estimate by noting that neutral carbon may be expected in clouds having $\tau_{UV}(\lambda = 1100\text{\AA}) \gtrsim 1$. Using the OAO/Copernicus result that $\tau_{UV} \simeq 2.5 A_V$, we expect to find CI in all clouds for which the total visual extinction, A_V is $\gtrsim 1/2$ magnitudes or alternately in the outer $A_V \sim 1-2$ regions of more opaque clouds. Such clouds are very numerous in our galaxy, or external galaxies.

The optical depth of the 491 GHz line may be computed in the manner described by Penston (1970):

$$\tau(491 \text{ GHz}) \gtrsim 3 \times 10^{-21} N \delta$$

where N is the total gas column density and δ is the fractional depletion of gaseous carbon (= abundance of carbon in the gas phase/total cosmic carbon abundance). Using the result from 21 cm observations that

$$N \simeq 1.7 \times 10^{21} \text{ A}_V$$

we find $\tau(495 \text{ GHz}) \simeq 58$. Recent observations suggest that $1/50 < \delta < 1/5$ (with $1/5$ being more characteristic of tenuous clouds, i.e., $n < 10^3 \text{ cm}^{-3}$). Thus, we expect

$$0.1 < \tau(491 \text{ GHz}) < 1$$

For extended clouds of the type giving rise to 21-cm emission, $T \sim 100 \text{ K}$, where as for smaller, denser clouds, $T \sim 10 \text{ K}$. Thus, the brightness temperature of the line should typically fall in the range of 1-100 K. Therefore, we expect the line to be a major tracer of interstellar gas, comparable to the 21 cm line of hydrogen, but representing physically different regions as noted above.

In order to observe this line, it is necessary to be above the troposphere. At an altitude of 4 km, with 1.2 mm of precipitable water above the telescope (corresponding to near ideal conditions at Mauna Kea or White Mountain), the optical depth along a 45° elevation path through the atmosphere is 2.6 (see Appendix A), corresponding to a loss of more than 11 dB. A receiver with a 6000 K noise temperature would experience an effective system temperature of 85,000 K.

For studies of our own galaxy, it is worth noting that a 30 cm telescope operating at 491 GHz gives the same angular resolution as the 100-m Bonn telescope at 1.4 GHz. Thus, a smaller submillimeter airborne or balloon instrument can make useful galactic studies. For external galaxies, however, a much larger instrument is needed. A 10-m space telescope would resolve typical interstellar clouds of 10-20 pc diameter at the distance of M31. Such a telescope would therefore provide an entirely new view of external galaxies on a scale achieved only by aperture synthesis instruments at centimeter wavelengths.

2. Molecular Observations in External Galaxies

The recent detection of CO (and HCN) in external galaxies has shown that certain aspects of galactic structure may best be understood by high-resolution CO studies of these galaxies. The presently studied objects (about a dozen) are limited by beam dilution to distances of ~ 20 Mpc or less. Furthermore, they show extended molecular sources ($\gtrsim 3'$) that represent the integrated emission of many clouds, each individually unresolved ($< 3''$). CO has been observed in what apparently are quite different types of clouds in the nuclear regions, on the one hand, and the spiral arm regions, on the other. This conclusion is based on studies of our own galaxy, and can be tested by higher resolution observations of external galaxies. With present resolutions one can distinguish these different regions for only a few nearby galaxies, and one cannot resolve the spiral structure adequately to test models of this phenomenon (Fig.3-4).

Observational and theoretical studies of CO in our own galaxy indicate that emissions from rotational levels up to at least $J = 5$ or so occur in optically thick lines with intensities similar to that of the $J = 1-0$ transition, while in optically thin lines the intensities increase

approximately as J^2 . (Although we generally expect ^{12}CO lines to be optically thick, recent observations of the $J = 1-2$, and $2-3$ transitions in Orion show that our expectations can be erroneous.) The proposed 10-m telescope will have a resolution of $13''$ at 576.4 GHz, the frequency of the $J = 5-4$ transition. Many problems, presently out of reach, can be studied with this resolution. Hopefully, future ground based telescopes will provide complementary angular resolution at lower J , to permit studies of molecular excitation and radiative transfer on this angular scale.

The density-wave picture of galactic spiral arm, formation, and maintenance can be studied. In one nearby spiral galaxy, M31, current observations suggest that CO emission arises along, and possibly on the inner edges of, the spiral arms. This possibility can be checked and the question applied to other, more distant galaxies. In view of the well-known, possibly intractable problem of locating gas with precision in our own galaxy, such high-resolution studies of CO in external galaxies may well be one of the few ways to test the density-wave theory, particularly the critical question of where shocks (hence compression and molecule production) occur relative to spiral arms.

High resolution will permit the study of CO in objects beyond the present ~ 20 Mpc limit. The study of many more objects will test the present tentative conclusion that molecular activity in galaxies is correlated with infrared activity and possibly with the integrated strength of non-thermal continuum sources (Rickard *et al* 1977). In the case of the important Seyfert galaxies, higher resolution should determine whether the CO emission comes from the very turbulent inner regions (radius $\sim 5''$) characterized by broad optical emission lines, or from a more widespread region, since the present beam-smeared CO observations are also consistent with an average over the narrower optical emission lines that arise in the outer regions.

Higher resolution will greatly facilitate the study of rotation curves, and of the detailed distribution of molecules. Are molecules located in ring structures, as appears to be the case in the inner part of our own galaxy, and are these rings expanding as a result of bygone nuclear activity?

The detection of the weak ^{13}CO species, not yet accomplished, will be facilitated by the higher resolution and frequency. The question whether the $^{13}\text{CO}/^{12}\text{CO}$ ratio is the same in external galaxies and in our own galaxy is important. Because the $^{13}\text{CO}/^{12}\text{CO}$ ratio depends on stellar processing, such studies will impact cosmological questions such as whether stellar evolution has pursued similar tracks in very distant galaxies. Another important question is how $^{13}\text{CO}/^{12}\text{CO}$ varies across a galaxy. This question, not directly answered in our own galaxy, bears on how the rates at which material is processed through stars are distributed within individual galaxies, and how they vary from galaxy to galaxy. Such studies constitute a powerful tool for the investigation of how galaxies form and evolve.

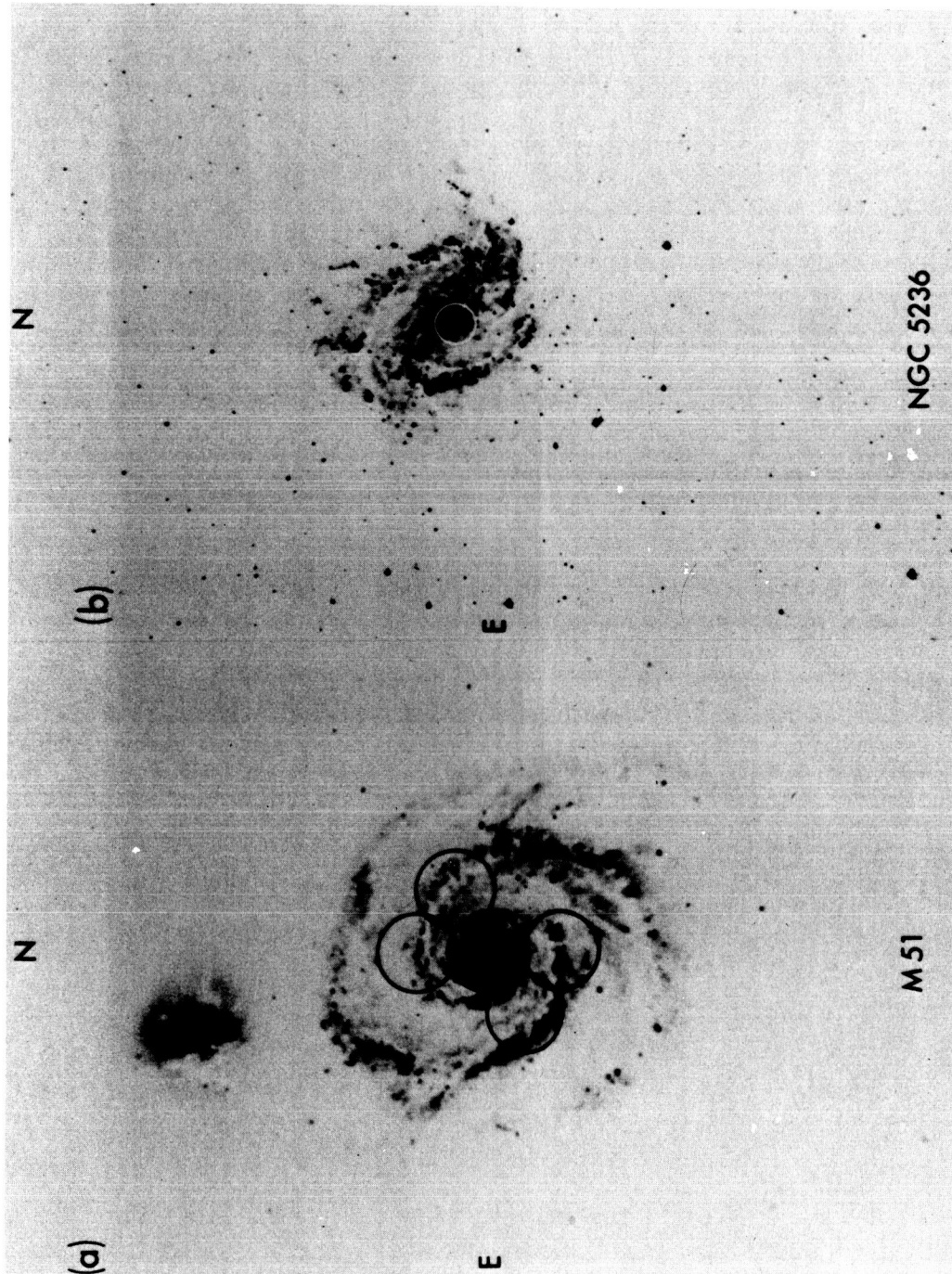


Figure 3-4. Two galaxies which have been partially mapped in the J=0-1 line of CO with an angular resolution of 1 arc minute. (After Rickard *et al*, *Ap. J.* 213, 673, 1977).

3. Dust in External Galaxies

A 10 m telescope, capable of diffraction-limited operation at a wavelength of $300\ \mu\text{m}$, would also offer a unique view of the dust in external galaxies. Assuming a detector system sensitivity of $10^{-14}\ \text{W Hz}^{-1/2}$ (well within the range of current technology) and $\Delta\lambda/\lambda \sim 0.1$, such a telescope would have a 10σ sensitivity of $\approx 0.1\ \text{Jy}$ (Table 3-3). For comparison, NGC 253, a dusty galaxy at 3.4 Mpc distance, has a flux of 125 Jy at $350\ \mu\text{m}$ and 3 Jy at 1 mm; NGC 1068, a dusty Seyfert galaxy at 18 Mpc distance, has a $350\ \mu\text{m}$ flux of 32 Jy and is not detectable at 1 mm with a current sensitivity limit of $\sim 1\ \text{Jy}$ (see Fig. 3-2). Another way to consider this is that, at a typical distance of 5 Mpc and assuming a dust temperature of 25 K, $2.8 \times 10^5\ M_{\odot}$ of dust could be detected. Since this is much less than the gaseous content of a spiral galaxy, one could, for example, investigate the gas-to-dust ratio and the distribution of dust as a function of morphological type. At $300\ \mu\text{m}$, the angular resolution corresponds to 175 pc at a distance of 5 Mpc, making it possible to map the distribution of individual major dust cloud complexes of the size of Sgr B2.

E. THE EVOLUTION OF MOLECULAR CLOUDS

The vast clouds of gas and dust within our galaxy constitute one of the most interesting areas of astronomical research. These dust complexes, which were once thought to be empty regions, are now known to represent a vital component of galaxies, important in determining the dynamics, energy transfer, magnetic fields, and star formation. Comprising a significant fraction of the interstellar medium, these clouds are believed to be concentrated along the leading edge of the spiral arms which sweep up matter as the galaxy rotates. Some of these clouds contain so much dust that no visible light enters or leaves their interior regions: extinctions have been estimated to be as high as 100 magnitudes (larger values are occasionally mentioned), or a factor of 10^{40} . Thus, the study of the interior of these regions requires wavelengths long enough (far infrared or longer) so that the dust no longer attenuates the radiation.

Table 3-3. Sensitivity of 10-m Telescope for Continuum Studies

Wavelength (μm)	f (GHz)	Field-of-View (arc sec)	10σ Flux (in 1 hr) (m Jy)
300	1000	8	80
1000	300	24	140

Since the evolution of clouds proceeds on a time scale of hundreds of thousands of years, their development can be determined only by noting a systematic progression of properties from one kind to the next, and inferring their evolutionary relationship, supported by a good physical and chemical understanding of these objects. This task has barely begun.

The submillimeter spectrum is important for such studies in several ways. It provides access to key spectral lines needed for the determination of abundances and the physical conditions in the gas. At these wavelengths, a telescope of 10 m diameter would have as much as 10 times the angular resolution of existing single-dish telescopes, permitting astronomers to examine more precisely such phenomena as clumping, the heating of gas near embedded stars, the cores of dense molecular clouds, and shock fronts. At these wavelengths, it is also possible to make simultaneous measurements of the continuum emission by dust, so that it will be possible to focus on variations in the gas-to-dust ratio, the association between infrared emission and molecular excitation, and the density and temperature gradients within clouds.

1. Physical Properties of Clouds

We are beginning to understand the physical properties of clouds: temperature, density, size, and energy sources. By comparing different transitions of one molecule, or the same transition of isotopically substituted species of a molecule, we gain information about molecular column density, gas temperature, and isotopic abundances, though not very precisely as yet because of uncertainties in the excitation of the molecule. By knowing the radiative lifetime of a transition, we can estimate the gas number density, by requiring the collisional excitation rate to equal or exceed the radiative decay rate, a process again uncertain. Nevertheless, the comparison of lines which are excited with these which are not, particularly for molecules with simple spectra like diatomic and linear molecules, is a good qualitative guide. Thus we differentiate between clouds with densities in the range $10^3 - 10^4 \text{ cm}^{-3}$ and those with densities of $10^5 - 10^6 \text{ cm}^{-3}$. We can also determine the temperature to within a factor of about two by using optically thick lines.

Improving our understanding of the physical properties of clouds hinges on our ability to determine the molecular excitation more precisely. Basically, this means that carefully calibrated measurements of a reasonable fraction of the rotational transitions of the molecule must be fitted to a model which simultaneously treats the radiative transfer and statistical equilibrium problems. The number of observed spectral lines must at least equal the number of parameters to be determined, and hopefully should exceed it. Even for the simplest and most ubiquitous cloud tracer, CO, the observational problem appears very difficult from the ground, because only three lines can be observed, and the calibration through our variable atmosphere appears rather uncertain. The situation is comparable for other basic molecules: the $J = 1-2$ transitions of HCN, HCO^+ , N_2H^+ and HNC are all obscured by a telluric water line. Thus, it appears that an accurate determination of gas cloud properties from rotational line observations will require a space telescope.

The determination of physical properties via the continuum radiation would also benefit from a space telescope. Figure 3-5 shows that the submillimeter range is very significant in the spectra of major HII/cloud complexes. For studies of such regions we need both high spatial resolution and high frequencies, which cannot both be obtained from ground-based or airborne observatories. For example, with the 7" resolution at 300 μm wavelength it would be possible to define the density gradients in such clouds as the Orion molecular cloud. Figure 3-6 shows the inadequacy of present angular resolution at submillimeter wavelengths, relative to the wealth of detail seen optically or with aperture synthesis at 6 cm wavelength. In another example, in a 25 K cloud at a distance of 10 kpc, one could detect a total mass (gas and dust, assuming the nominal gas-to-dust ratio) of $50M_{\odot}$ within a 1.2 pc region at 1 mm wavelength, corresponding to a density of $\sim 250 \text{ cm}^{-3}$. One could thus study the density inhomogeneity of clouds, and in conjunction with determinations of the gas content, determine the gas-to-dust ratio under a wide variety of physical conditions.

2. Internal Motions of Clouds

One of the great potentials of molecular line observation is the use of Doppler shifts, manifested in the shape of spectral lines, to determine the internal motions of clouds. How rapidly the contraction of clouds proceeds has an important bearing on the determination of the efficiency of star formation. The amount of internal turbulence may be related to such phenomena as the energy input from embedded stars and cloud-cloud collisions. The presently available data do not appear to give unambiguous answers. Because of insufficient spatial resolution, the importance of turbulence and its effect on the line shape, as well as systematic variations of linewidth with position cannot be adequately assessed. Also, because of the relatively few transitions per molecule now available, the details of the radiative transfer and molecular excitation cannot yet be properly evaluated. Thus, there is need both for higher frequencies and large telescope aperture, which can only be simultaneously satisfied in space.

3. Interstellar Chemistry

The chemistry of clouds has an important bearing on cloud evolution, in that the spectral lines of the molecules which comprise the gas are the means by which the gas couples to the radiation field, and thus the means by which the cloud is heated or cooled. Interstellar chemistry is also intensely interesting because the formation of organic compounds (see Table 3-4) occurs under conditions very different from those on Earth and thus elucidates fundamental reaction mechanisms not readily isolated in the laboratory. Some of the interstellar chemistry, involving molecular species believed to be biologically fundamental, may shed light on the process by which life evolved.

One very important type of molecule about which we have very little information is that containing only one heavy atom. These molecules are important in the chemistry of interstellar clouds because they

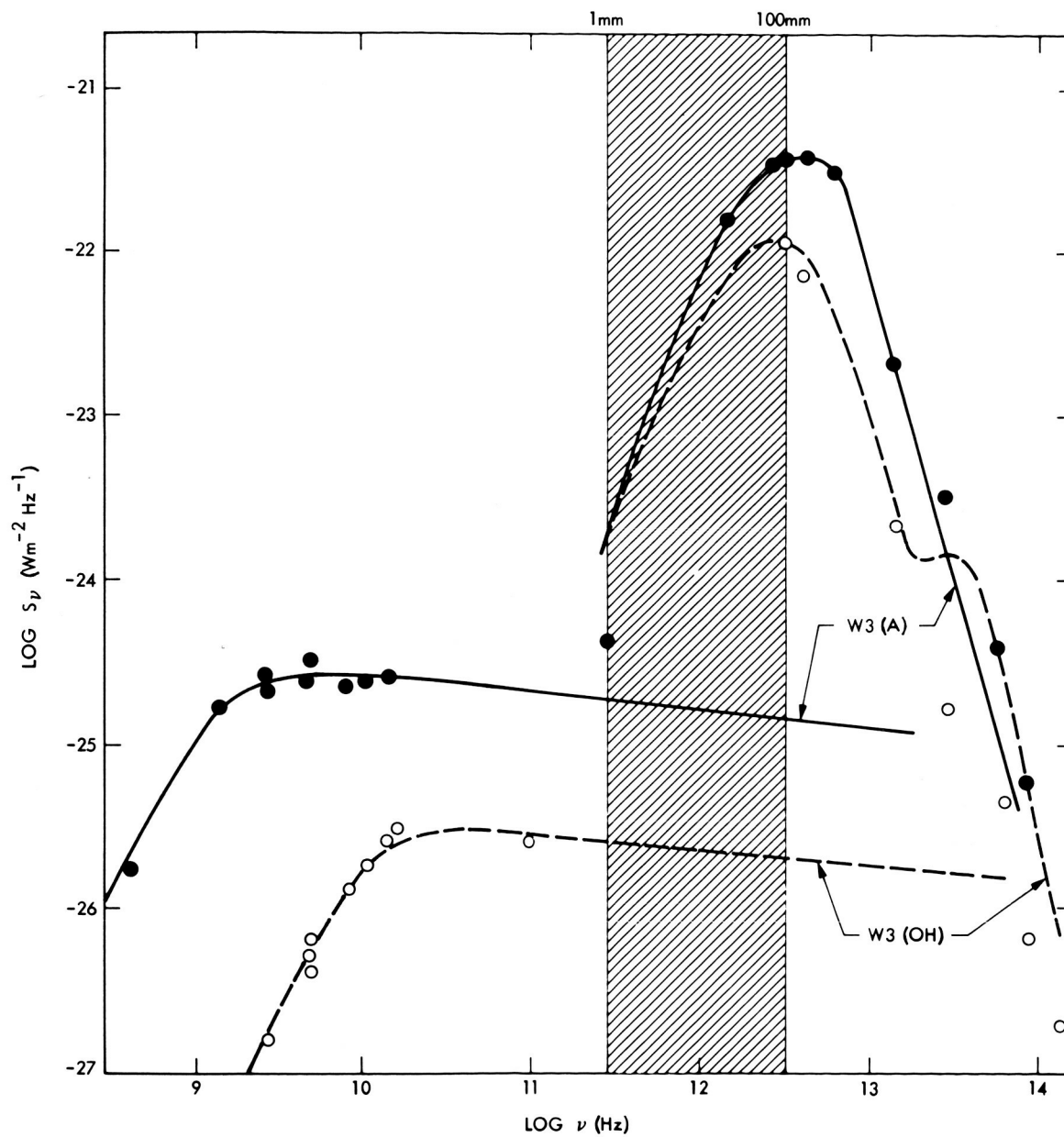


Figure 3-5. Spectra of HII regions W3(A) and W3(OH) (1975). Dashed region shows anticipated submillimeter space telescope coverage.

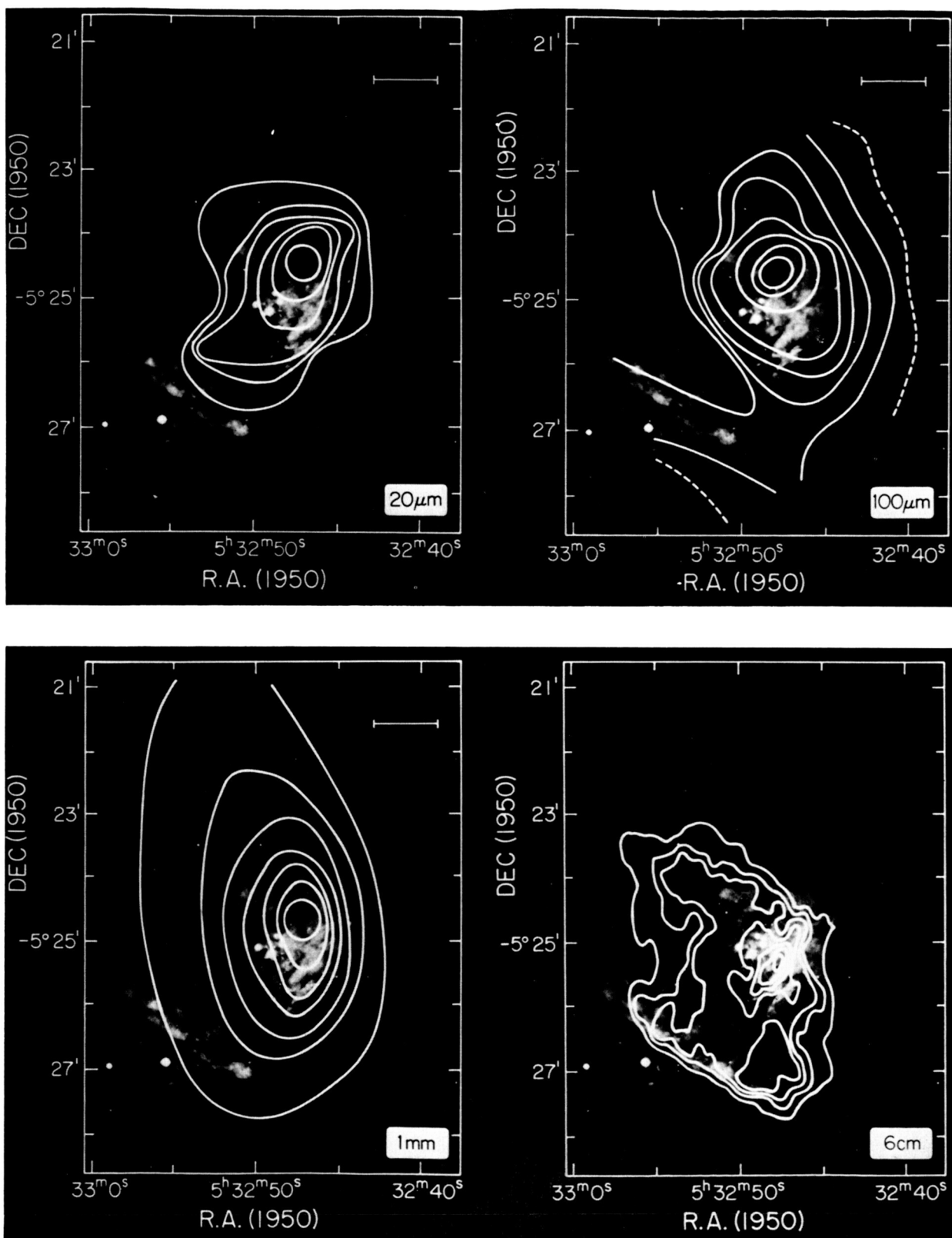


Figure 3-6. Continuum emission from the Orion Nebula complex at 20 μm , 100 μm , 1 mm, and 6 cm.

Table 3-4. Molecular Lines Detected in Interstellar Clouds

H_2
CARBON MOLECULES

C_2H
 CH_3C_2H
 CH
 CH^+
 C_2H_2

NITROGEN MOLECULES

NH_3 N_2H^+

OXYGEN MOLECULES

H_2O OH SiO

CARBON-NITROGEN MOLECULES

CN HC_3N CH_3CN H_2NCN
 HCN HC_5N C_3N CH_3NH_2
 HNC HC_7N H_2CNH CH_2CHCN
 HC_9N

CARBON-OXYGEN MOLECULES

CO CH_3CH_2OH $HCOOCH_3$
 H_2CO H_2C_2O $HCONH_2$
 $HCOOH$ HCO $HNCO$
 CH_3OH CH_3CHO HCO^+
 $(CH_3)_2O$

NITROGEN-OXYGEN MOLECULES

HNO

SULPHUR MOLECULES

SO OCS
 H_2S SiS
 CS SO_2
 NS H_2CS

DEUTERIUM MOLECULES

N_2D^+ DNC DCN HDO DCO^+ HD NH_2D

represent the reaction products of heavy atoms with the most abundant of all atoms, hydrogen. Table 3-5 lists the hydrides which have been observed to date, as well as others which, we have good reason to believe, should exist. These molecules have small moments of inertia, which causes the main rotational transitions to lie at very short wavelengths; Table 3-6 gives some examples. Even for those hydrides already detected, observations at submillimeter wavelengths are essential. The transitions observed so far are generally relatively weak, and particularly prone to anomalous population ratios, making their interpretation in terms of column densities and gas kinetic temperatures difficult or impossible.

Hydrides may be important in another regard - the detection of molecules involving atoms not previously detected in this way, such as calcium, sodium, magnesium, aluminum, lithium, phosphorus, and chlorine (see Tables 3-5 and 3-6). This would open up to study many aspects of inorganic chemistry, and may relate to such questions as the formation and destruction of grains.

It is becoming apparent that ions play a key role in interstellar chemistry. We are aware of HCO^+ , N_2H^+ and CH^+ by direct observation, and the chemical theories involving ion-molecule reactions predict others whose rotational spectra have not yet been determined. We also know of a growing number of spectral features which have not yet been identified. Thus, we have a need to observe at higher frequencies in order to understand the abundances and excitation of ions we have detected. Also, we need to extend our coverage of frequency space so that, by detecting new spectral lines, we can look for patterns which will lead to the identification of these "mystery" molecules.

In addition to the chemistry of gas, there is the chemistry of solids, the composition of interstellar dust grains and their mantles. The submillimeter spectrum may be useful in determining some of the grain parameters. For all thermal sources observed through atmospheric windows, the energy distribution between 1 mm and 350 μm varies as the third to fourth power of the frequency (Figure 3-7). The shape of the overall spectrum of the sources indicates that we are observing the Rayleigh-Jeans portion of the radiation distribution, and that the emissivity varies as the first to second power of the frequency. It would be desirable to observe this part of the spectrum with some precision, particularly in circumstellar shells such as IRC+10216 and other simple systems, in order to provide additional information on the wavelength dependence of the emissivity, and hence on the nature of grains.

4. Heating and Cooling of Clouds

The internal energy of a cloud is an important factor in its evolution. In a hot cloud, internal pressure forces can prevent the collapse of the cloud, so that a cloud can contract only as rapidly as it can radiate away this energy. Thus, the energy transfer within clouds ultimately bears on the star formation rate.

Table 3-5. Interstellar Hydrides

Observed	Examples of Molecules Not Yet Observed	
CH, CH ⁺	CH ₂ , CH ₃ , (CH ₄)	CH ₂ ⁺ , CH ₃ ⁺
OH, H ₂ O		H ₃ O ⁺
NH ₃	NH ₂ , NH	NH ₄ ⁺ , NH ⁺
H ₂ S	SH	
	PH ₃ , PH ₂ , PH	
	HCl	
	CaH, NaH, MgH, LiH, AlH	AlH ⁺ , MgH ⁺ , H ₃ ⁺ , SiH ⁺

Table 3-6. Typical Transitions for Hydrides

Molecule	Transition		Frequency (GHz)
OH	$2_{\pi 3/2}, J = 5/2 - 3/2$		2508
CH	$2_{\pi 1/2}, J = 3/2 - 1/2$		1620
NH	$N = 0 - 1, J = 1 - 2$		975.2
OH ⁺	$N = 0 - 1, J = 1 - 2$		900
HCl	$0 - 1$		625.9
NH ₃	$1_0 - 0_0$		572.5
H ₂ O	$1_{10} - 1_{01}$		556.9
H ₂ S	$1_{11} - 0_{00}$		452.4
SiH ⁺	1_{Σ}^{+}	$J = 1 - 0$	453.2
LiH	1_{Σ}^{+}	$J = 1 - 0$	444.4
AlH ⁺	2_{Σ}	$N = 1 - 0$	393.7
NH ⁺	$2_{\pi r}$		390.6
PH ₃	$1_0 - 0_0$		266.9

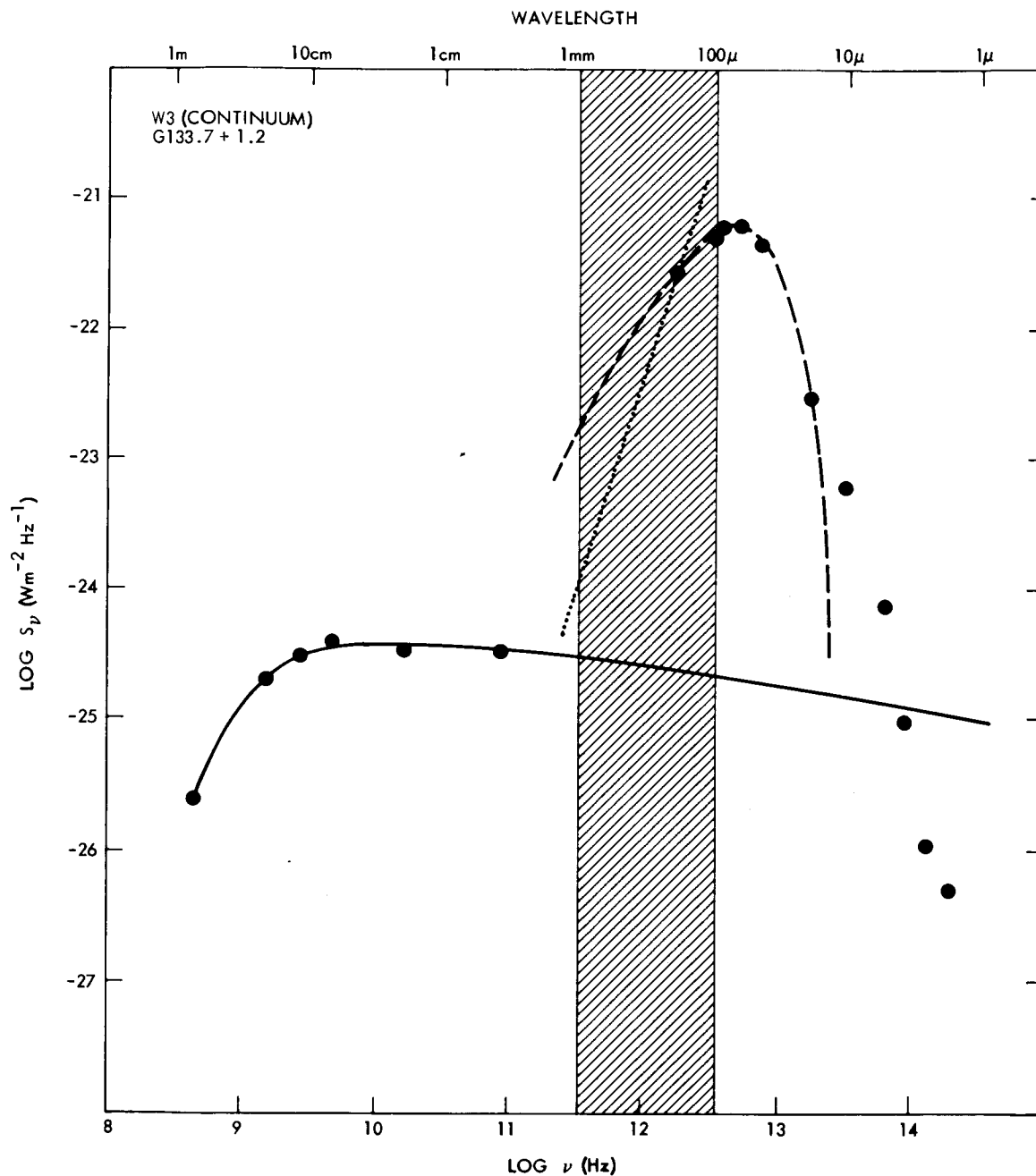


Figure 3-7. Spectrum of the excess infrared emission from an HII region. The dashed line is a black-body curve at 70 K and the solid line the theoretical curve for emission from electron transitions in a plasma (Wynn-Williams and Becklin 1974). The dotted line shows the sub-millimeter spectral dependence, approximately λ^{-3} .

The way in which the dust and the gas in a cloud are coupled energetically is largely a matter for speculation at this time. In one scenario, the rotational transitions of the molecules are normally excited, and the lines in the abundant species are optically thick. Thus, these lines cannot efficiently radiate away the energy, in that the cloud looks like a black body, but only over a very tiny fraction of its total spectrum. However, these transitions can couple to the dust which is mixed with the gas, and the dust in turn can radiate the energy in a continuum. In this case, the dust radiation would control the cooling.

In another scenario, some key transitions of abundant molecules have population inversions. Water, with its highly complex spectrum, is a good candidate. Collisions in the dense cores of clouds could excite the rotational ladder of the molecule in such a way that certain transitions are inverted. The molecule would then radiate the energy very efficiently in the form of powerful masers in the inverted transitions. Masers have been observed extensively in the 22 GHz transition of H_2O ; they appear in a wide variety of sources. The total energy radiated by this transition is not large compared to other heating and cooling processes, but it suggests that other transitions may be strong masers.

In yet another possible scenario, the dust absorbs radiation from powerful infrared sources embedded in the cloud (new stars), transfers this radiation to the gas as suggested above, but without causing maser emission. In this case, the cloud would heat up (Scoville and Kwan 1976). Perhaps this mechanism accounts for why the Orion molecular cloud, at 50-70 K, is so much hotter than most other clouds. Since many of the water transitions cannot be observed even from an airborne platform, because of absorption in the terrestrial atmosphere (see Table 3-8 and Figure A-1), a space platform is needed to pursue these questions.

Similar mechanisms might also operate in other molecules. Sweitzer *et al* (1977) have observed non-metastable inversion transitions of ammonia toward the Orion Nebula up to the (5-4) level. An analysis by Sweitzer (1977) suggests that the infrared radiation field plays a key role in exciting these transitions of ammonia. Observations of the $1_0 - 0_0$ rotational transition of NH_3 at 572.5 GHz will provide important information on the abundance, distribution, and excitation of the molecule, and its role in the energetics of this and similar clouds.

F. STAR FORMATION

The early phase of star formation, the protostellar collapse, is the extension of the cloud studies previously discussed to a small angular scale. We cannot yet claim that we have observed a collapsing protostar. There is little doubt that the intense infrared sources deeply embedded in the dense clouds associated with the major HII regions are very young objects, but we know very little about them. The proposed NRAO 25 m telescope operating to 400 GHz and a complementary space telescope of 10 m operating to 1000 GHz will be powerful tools in the investigation of such phenomena. Both will have many times the angular

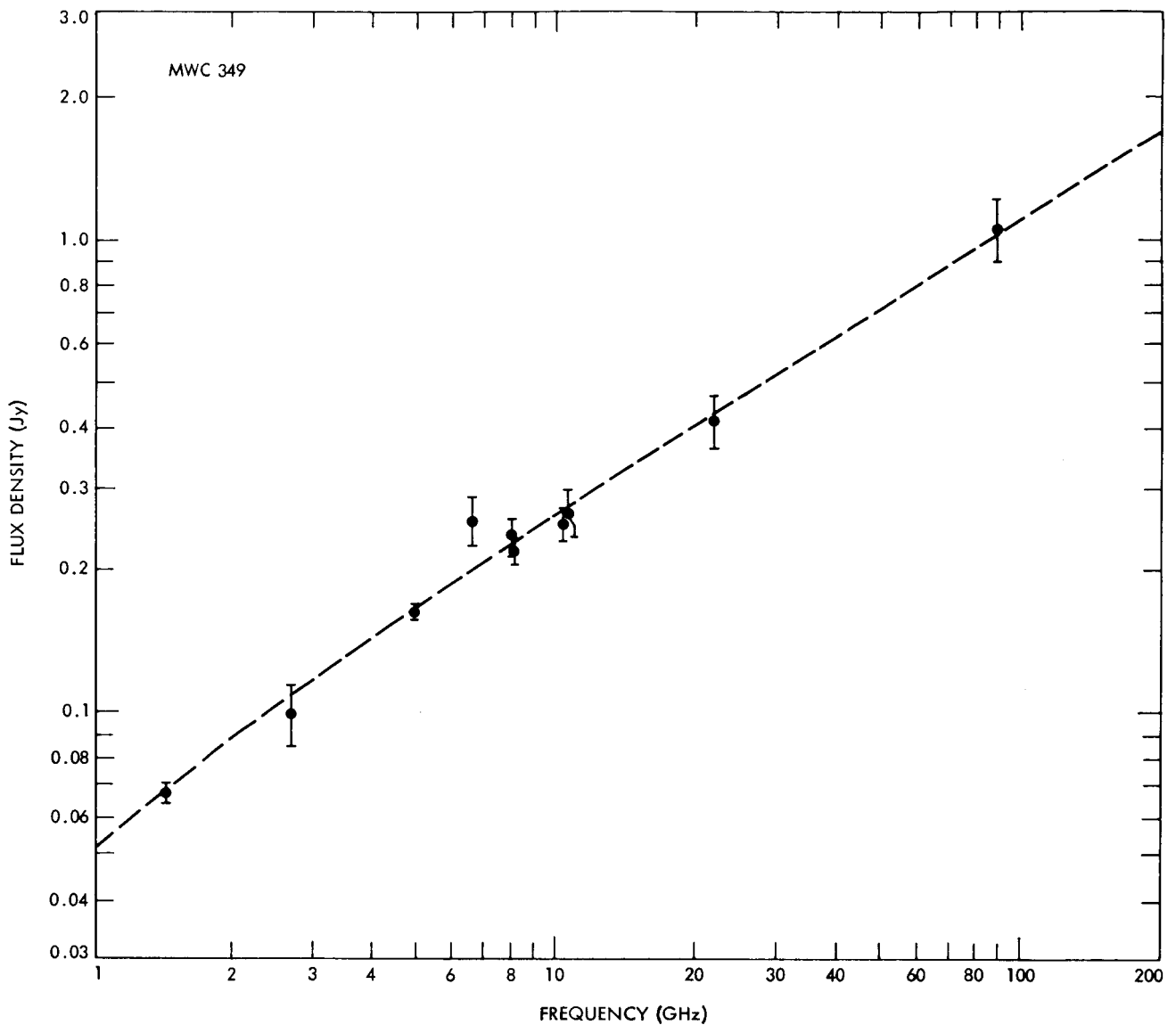


Figure 3-8. Radio Continuum Spectrum of MWC 349

resolution now available, and the space telescope will give access to the high frequency lines whose importance has already been noted previously.

There is a class of young stellar objects apparently undergoing copious mass-loss (Strom *et al* 1975), although the possibility that they are accreting mass is not yet ruled out (Ulrich 1976). These stars have broad emission lines showing (apparently) absorption features in the blue wings. The prototype of this class of stars is P Cygni, which also has a detectable radio continuum (Wendker *et al* 1973). These objects are generally of early spectral type with a rich optical emission

spectrum, and a radio continuum which varies approximately as the frequency to the first power (Figure 3-8). Objects of this type, which are probably at a pre-main sequence stage of evolution, are Lk H 101 (Knapp *et al* 1976), T Tau (Spencer and Schwartz 1973), MWC 349 (Ollnon 1973), M2-9 (Purton *et al* 1975). They are believed to have expanding ionized envelopes. If an envelope is highly centrally concentrated, then the outer, optically thin part will have a flux which is constant with wavelength, and an optically thick core whose flux varies as frequency squared. At higher frequencies, more of the envelope will be optically thin, and the opaque core will be smaller, so that the total spectrum will vary as ν^α , where α is a value between 0 and 2 depending on the frequency and the density structure in the source. From the shape of the observed spectra, approximately ν^1 , it is inferred that the density of the stellar envelope varies as r^{-2} , which is the form of the density law expected for mass overflow at a uniform velocity. It is of considerable interest to extend these spectra until the flat (optically thin) part of the spectrum (if it exists) can be recognized, since this indicates the maximum density (\cong inner radius) of the envelope. The submillimeter spectrum is also useful for extending our observations to higher sensitivities: whereas the presently known sources have fluxes in excess of 100 mJy at 100 GHz, a 10 m space telescope has a 10σ sensitivity limit of (for 1 hour integration) 140 mJy at 300 GHz (where the sources are presumably three times stronger), and 80 mJy at 1000 GHz. Thus, if there are compact sources sufficiently dense that their spectra continue to rise to 1000 GHz, then this instrument would have excellent prospects for detecting them.

A particularly interesting region that is suspected to be at an even earlier stage of evolution is the infrared complex in Orion. In the direction of the center of the Kleinmann-Low nebula we observe lines with large Doppler widths. CO has been observed to extend over 150 km s^{-1} . It has already been shown that such large velocities cannot be due to gravitational collapse: the mass implied would be enormous (Zuckerman *et al* 1976). If the phenomenon is due to mass-loss, its rate is very large. This is another example of a phenomenon seen in a region of suspected star formation which occurs on a scale below the resolving power of current instruments.

The infrared complex in Orion is also interesting because it shows complicated molecules, some of which have not been seen elsewhere. Following a suggestion by Herbig (1970) that interstellar molecules and meteoritic organic compounds might have a common origin, Anders *et al* (1974) have conducted laboratory studies of grain catalytic reactions at temperatures near 400 K which suggest that a large variety of complex molecules might be formed under these conditions. In order to pursue this question we need higher angular resolution to separate the phenomena in the core from those in the surrounding clouds, and higher sensitivity. Both can be achieved at higher frequencies.

The phenomena described here have only very recently begun to be investigated. As our experience grows, these studies will likely become a powerful tool in the investigation of pre-main sequence evolution.

G. COMETS

A major goal of cometary research is to determine the chemical composition of comets since they may represent frozen samples of primordial material from the solar nebula. A general picture which exists at present is that a comet consists of an icy conglomerate nucleus and a gaseous atmosphere which is formed by evaporation from both the nucleus and the solid grains embedded in the atmosphere. Figure 3-9 shows a schematic diagram of the structure for Comet Encke. The gases which boil off the nucleus are mostly molecular when formed, but their concentration falls off rapidly with increasing distance from the nucleus due to photoionizations. Optical spectra of comets have revealed the presence of a number of molecular fragments and ions, but the parent molecules have been more elusive. Recently a few transitions of the parent molecules H_2O , CH_3CN , and HCN have been reported (Snyder 1976). A 10 m submillimeter telescope will offer a substantial improvement in sensitivity for detecting parent molecules. Furthermore the angular resolution may be sufficient to measure the diameter of the inner coma. Figure 3-9 shows for Comet Encke that the outer coma subtends an angle of 28 arc seconds at 1 A.U. This is the resolution of a 10 m telescope operating at 1 mm. For example in the detection of water vapor, a 3 arc minute ground-based telescope working at the 22 GHz water line will have over 100 times less sensitivity than a 10 m telescope operating at the 556 GHz water line. While at present, the volatile component of the nucleus is identifiable only indirectly because of the ions and radicals in the outer regions of the coma, a space telescope will allow the detection of such molecules as H_2O , NH_3 , HCN , H_2CO and others. These data will provide direct evidence on the abundance and composition of the nucleus.

H. PLANETS

Figure 3-10 gives the signal-to-noise ratio obtained in 1 hour integration over a 500-MHz bandpass with a 10 m antenna and a receiver with its system noise temperature given by $T_{\text{sys}} \text{ (K)} \approx 10 \text{ (GHz)}$. A precise determination of the spectra of all the planets is feasible (except Pluto and a number of smaller bodies) and will provide information on the nature of the atmospheres and/or surfaces of these members of the solar system. Jupiter and Venus will be easily resolvable with a 10-m telescope making possible the study of planetary atmospheric circulation and meteorology. In Figure 3-11 we show a 10 m telescope beam at 500 GHz projected on a Pioneer 10 photograph of Jupiter.

1. Venus

Quantitative data for the Venus atmosphere have been obtained from Earth-based observations and from spacecraft which have entered the Venus atmosphere or passed within several planetary radii of the planet. Spectroscopic measurements in the near-infrared bands have been used to determine the basic constituents of the atmosphere. These measurements have shown that CO_2 is the dominant atmospheric constituent. Other gases identified from spectroscopic analysis are hydrogen chloride (HCl), hydrogen fluoride (HF), carbon monoxide (CO), oxygen (O_2), and

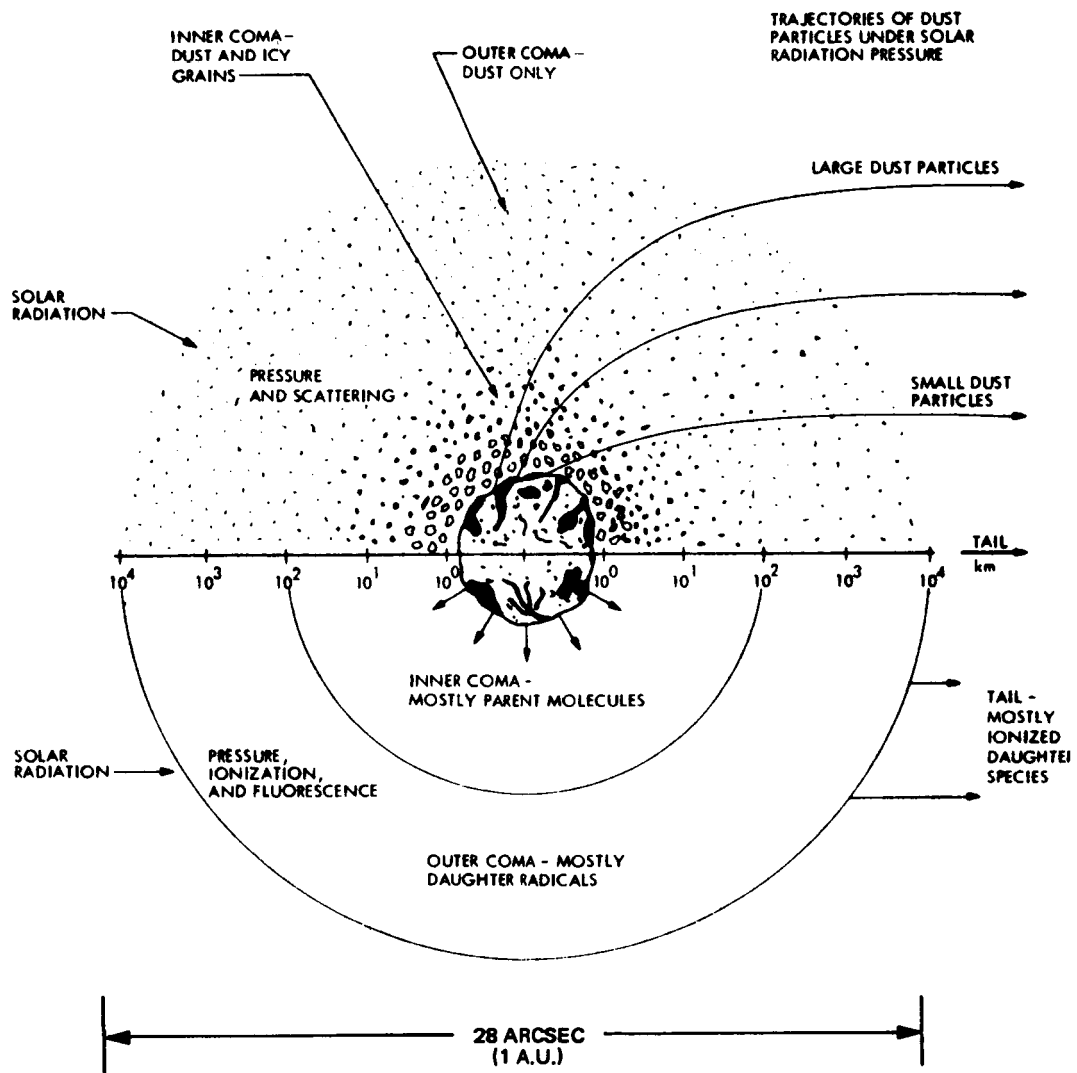


Figure 3-9. Schematic diagram of the structure of Comet Encke.

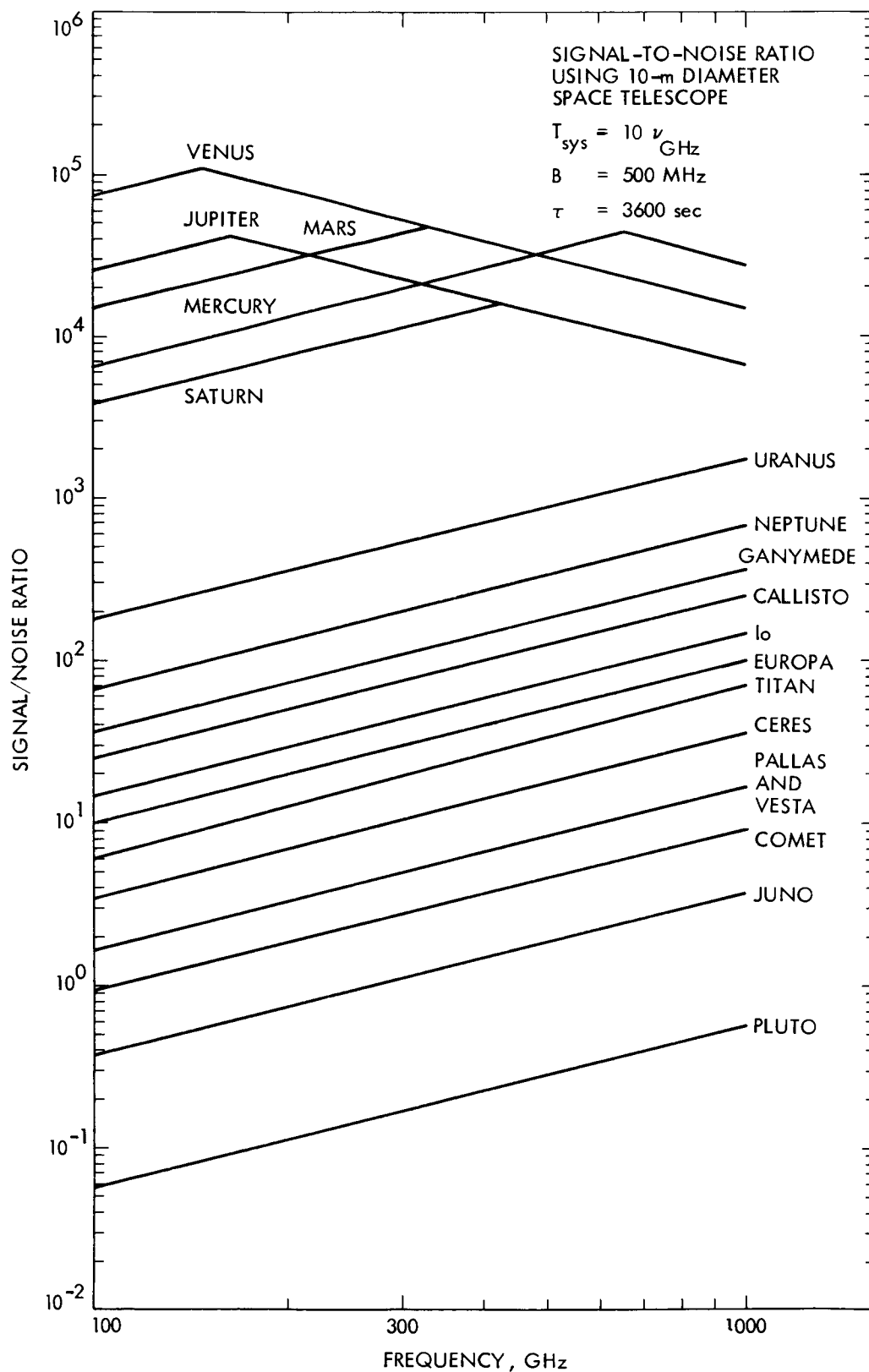


Figure 3-10. Signal-to-noise ratio obtained on various solar system bodies in 1-hour integration with 500 MHz bandwidth.

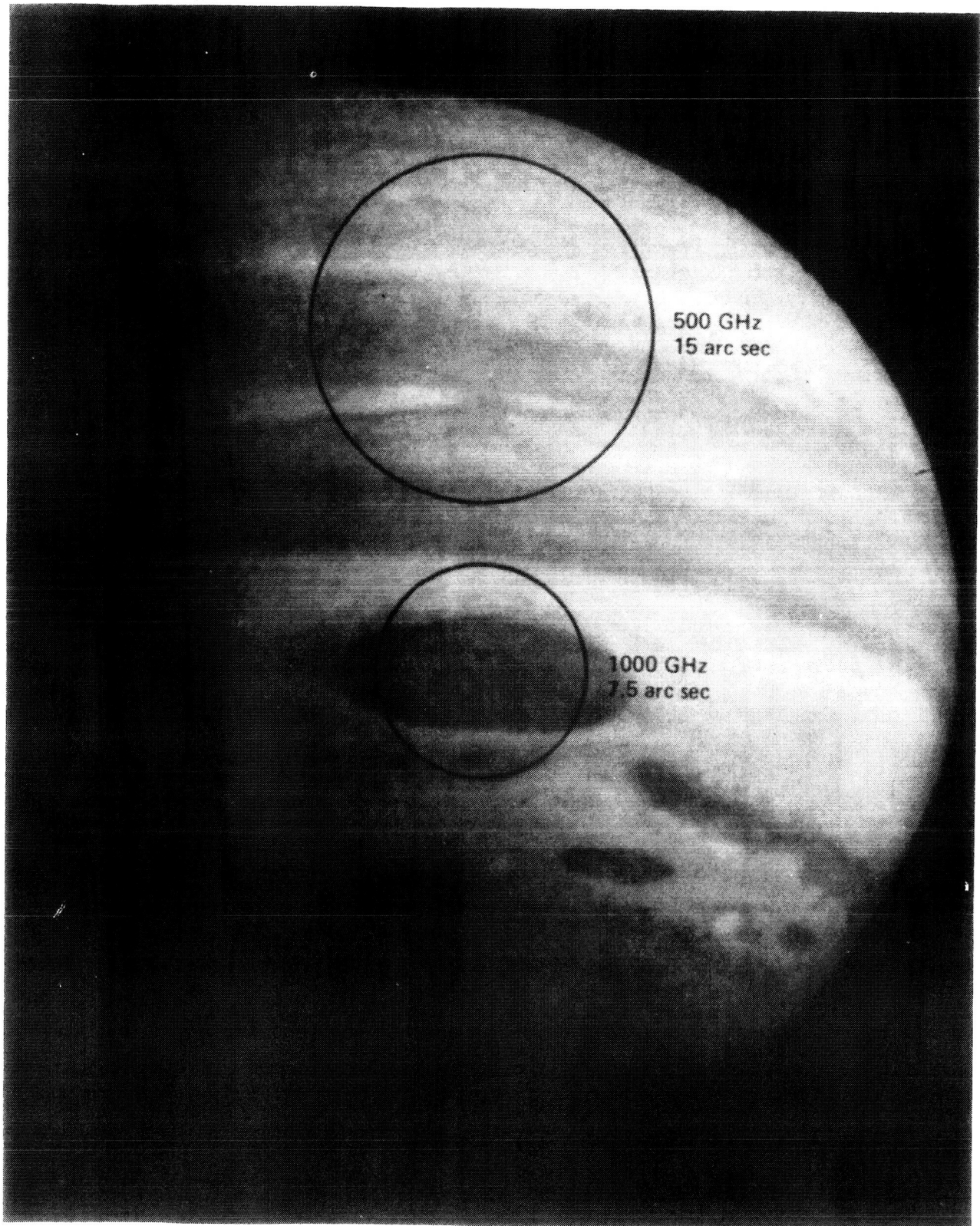


Figure 3-11. Pioneer II Photo of Jupiter. Resolution of 10-m telescope at 500 and 1000 GHz is indicated.

tentatively water vapor (H_2O). The Venera spacecraft reported that the principal inert gas is N_2 , while the H_2O concentration is significantly higher than is reported from ground-based measurements. Table 3-7 shows an estimate on the composition of the Venus atmosphere (Models of the Venus Atmosphere, 1972).

Water vapor is perhaps the most interesting trace species on Venus because of its role in planetary evolution processes, its importance to the thermal radiation budget, its possible direct role in the cloud forming process, and its biological significance. Table 3-8 shows the rotational transitions of water below 1000 GHz which can be observed from space. These will offer the possibility to measure the spatial and temporal variations in water vapor abundance free from strong telluric emission.

Carbon monoxide has been detected in the troposphere by its infrared absorption lines and in the stratosphere by the $J = 1 \rightarrow 0$ microwave absorption at 115.271 GHz. Initial observations as well as theoretical considerations suggest that the CO is produced on the dayside of the planet and swept around to the night side due to the global circulation on Venus. By observing the higher frequency transition shown in Table 3-9 it will be possible to test these theories by spatial mapping of the CO on the day and night sides.

Studies of Venus have suggested pole-to-equator temperature differences, large-scale dynamical features, and variability of stratospheric parameters which can be searched for with a 10 m telescope in orbit. The movement of circulation features around the planet with an apparent period of four days, as indicated by Earth-based observations can be searched for using CO or other molecules as tracers. These observations can provide a key to the understanding of the general circulation of Venus.

2. Outer Planets

The fundamental questions which relate to the outer planets are:

- (1) Are the outer planets primordial objects and what physical and cosmogonical processes account for their differences?
- (2) What processes are currently taking place on these planets and how are these related to the present appearance of the planets?

The answers to these broad questions rest in part on the measurements of the abundance of a large number of molecular species and their distributions in temperature and pressure in the atmosphere. Many of the molecules of interest have strong, rotational lines in the submillimeter spectral range. Examples are NH_3 , PH_3 , H_2O , HCN , and H_2S . Ammonia is known to be present in the atmosphere of Jupiter, but its presence in the spectrum of Saturn, Uranus, and Neptune is not known. A search for the ground state rotational transition at 572.5 GHz should offer approximately a three-order-of-magnitude increase in sensitivity over the inversion transitions near 24 GHz.

Table 3-7. Composition of the Venus Atmosphere

Component	Estimated Percent by volume	Source*
CO ₂	97, +3, -4	Ref. 45
N ₂	<2	Ref. 45
O ₂	<10 ⁻³	Ref. 57
H ₂ O	$\left\{ \begin{array}{l} 10^{-2} - 10^{-1} \\ 10^{-4} - 10^{-2} \end{array} \right.$	Ref. 45 Ref. 2
HCl	10 ^{-4.2}	Ref. 15
HF	10 ^{-6.2}	Ref. 15
CH ₄	<10 ⁻⁴	Ref. 15
CO	10 ^{-2.34}	Ref. 16
COS	<10 ⁻⁶ - 10 ⁻⁴	Ref. 14
NH ₃	<10 ^{-5.5}	Ref. 14
N ₂ O	<5 x 10 ⁻⁵	Ref. 3
He	≈10 ⁻²	Ref. 3
CH ₃ Cl	<10 ⁻⁴	Ref. 15
C ₂ H ₂	<10 ⁻⁴	Ref. 15
HCN	<10 ⁻⁴	Ref. 15
O ₃	<10 ⁻⁶	Ref. 14
C ₃ O ₂	<10 ^{-4.3}	Ref. 14
H ₂ S	<10 ^{-1.7}	Ref. 14
SO ₂	<10 ^{-5.5}	Ref. 14
CH ₃ F	<10 ⁻⁴	Ref. 15

*References in original publication Models of Venus Atmosphere (1972), NASA SP-8011.

Table 3-8. Transitions of Water to 1000 GHz

Transition	Frequency (MHz)
1 ₁₀ - 1 ₀₁	556936.0
2 ₁₁ - 2 ₀₂	752033.2
3 ₁₃ - 2 ₂₀	183310.09
4 ₁₄ - 3 ₂₁	380197.37
4 ₂₃ - 3 ₃₀	448001.08
5 ₁₅ - 4 ₂₂	325152.92
5 ₃₃ - 4 ₄₀	474689.13
5 ₃₂ - 4 ₄₁	620700.81
6 ₁₆ - 5 ₂₃	22235.08*
6 ₄₃ - 5 ₅₀	439150.81
6 ₄₂ - 5 ₅₁	470888.95
6 ₂₄ - 7 ₁₇	488491.13
7 ₅₃ - 6 ₆₀	437346.67
7 ₅₂ - 6 ₆₁	443018.30
10 ₂₉ - 9 ₃₆	321225.64
*Can be observed from the ground	

Oxygen, sulfur, and nitrogen are cosmically abundant and their fully reduced compounds are worth searching for in the outer solar system. Water has been reported on Jupiter but additional measurements are required before the data can be interpreted. H₂S is another molecule which is important in the chemistry of the outer planets and which can be searched for in the submillimeter region.

The probable detection of phosphine in the Jovian atmosphere (e.g., Ridgway *et al* 1976) has important impact on the physics and chemistry of the atmosphere. Thermochemical calculations predict that PH₃ should be absent above the 800 K level of the atmosphere. Its presence suggests the importance of strong dynamical currents or some

Table 3-9. CO Spectral Lines

Frequency (GHz)	Strength
115.271	3.48×10^{-4}
230.537	2.71×10^{-3}
345.795	8.7×10^{-3}
461.040	1.9×10^{-2}
576.267	3.5×10^{-2}
691.473	5.4×10^{-2}
806.651	7.6×10^{-2}
921.793	9.9×10^{-2}

unknown chemistry which is taking place within the atmosphere. Another possibility which has been considered (e.g., Sill 1976) is that PH_3 may be responsible for some of the coloration seen on Jupiter (see Figure 3-11). Table 3-10 gives the frequencies of the lower rotational ladder of phosphine. A theoretical calculation of the Saturn spectrum including ammonia and phosphine is seen in Figure 3-12.

The detections of phosphine, acetylene, and several other molecules on Jupiter suggest that non-equilibrium conditions are present on this planet. Other molecules whose lifetimes probably depend on non-equilibrium conditions and which can be searched for are HCN, CH_3 , CN, OCS, CH_3CCH , HC_3N , HC_5N . Figure 3-13 shows the Jovian spectrum as it is currently known, and many of the lines which may be important are in the unexplored region. Figure 3-11 shows the spatial resolution on Jupiter which can be achieved with a 10 m telescope operating at 500 GHz and 1000 GHz. It can be seen that a 10 m telescope provides sufficient resolution to resolve the belts, zones, and red spot on Jupiter.

I. POST-MAIN-SEQUENCE EVOLUTION

In Subsection F (Star Formation), it was shown that submillimeter observations of the envelopes of young stars are important in understanding their development. The same kinds of observations are relevant to a large variety of stars which have evolved to the red giant stage and beyond. Studies of these kinds of stars address the questions of late stellar evolution, many stages of which are still poorly understood, and of the return of stellar material to the interstellar medium, with important implications for galactic evolution.

Table 3-10. Rotational Transitions of Phosphine

$J \rightarrow J'$	K	ν (MHz)	α
0 \rightarrow 1	1	266944.5	2.2×10^{-3}
1 \rightarrow 2	0	533794.2	7.73 - 3
	1	533814.92	5.81 - 3
2 \rightarrow 3	0	800454.3	1.60 - 2
	1	800485.38	1.42 - 2
	2	800578.62	8.86 - 3
3 \rightarrow 4	0	1066830.0	2.49 - 2
	1	1066871.4	2.35 - 2
	2	1066995.8	1.89 - 2
	3	1067203.0	2.24 - 2

1. Red Giants

A type of stellar envelope being investigated by radio and millimeter techniques is that of Mira variables. Among the long-period variables, oxygen-rich Mira variables show emission in transitions of H_2O , OH , and SiO . On the other hand, S-type Miras appear to be associated only with SiO (Blair and Dickinson 1977). Observations of non-maser SiO in such stars have been used by Morris and Alcock (1977) to determine the amount of SiO being ejected from such stars. They find that the SiO flux is very low, either because the mass loss rate is low ($\sim 10^{-6} M_{\odot} \text{ yr}^{-1}$ assuming $[SiO]/[H_2] = 6 \times 10^{-5}$) or more probably because a major part ($\geq 90\%$) of the silicon is in some other form. It would be of great interest to conduct a similar study of water, because it plays an important role in the radiative transfer, and hence the energetics of the envelope. Unfortunately, only 22 GHz transition can be observed from the ground, and it is a maser. Thus, observations from a large space telescope will be of great interest.

Correlation of the variability of molecular line emissions with variations in the infrared flux can be a very useful approach to studying molecular excitation.

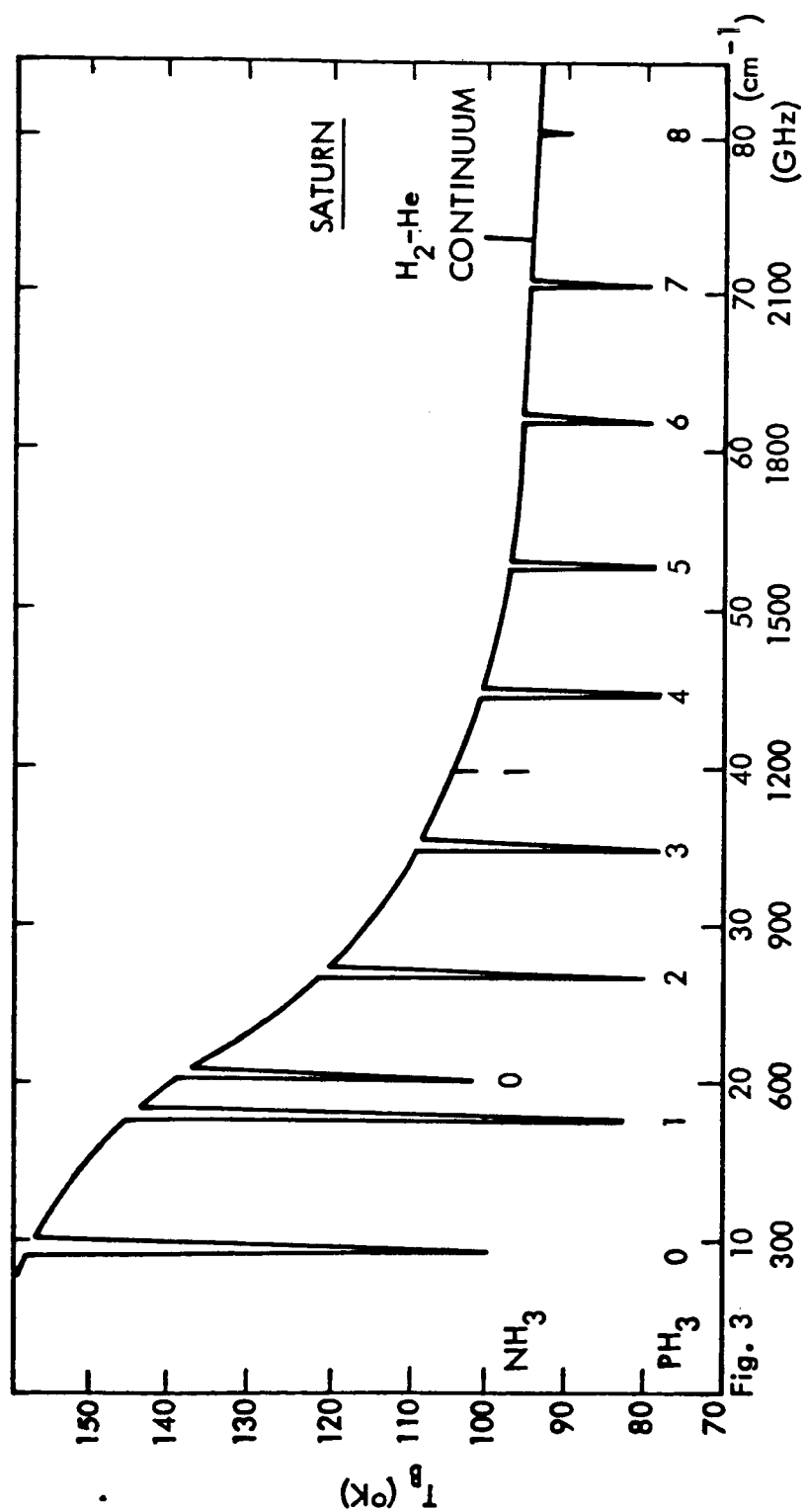


Figure 3-12. Theoretical phosphine and ammonia spectrum on Saturn. (After Encrenaz and Combes (1975).)

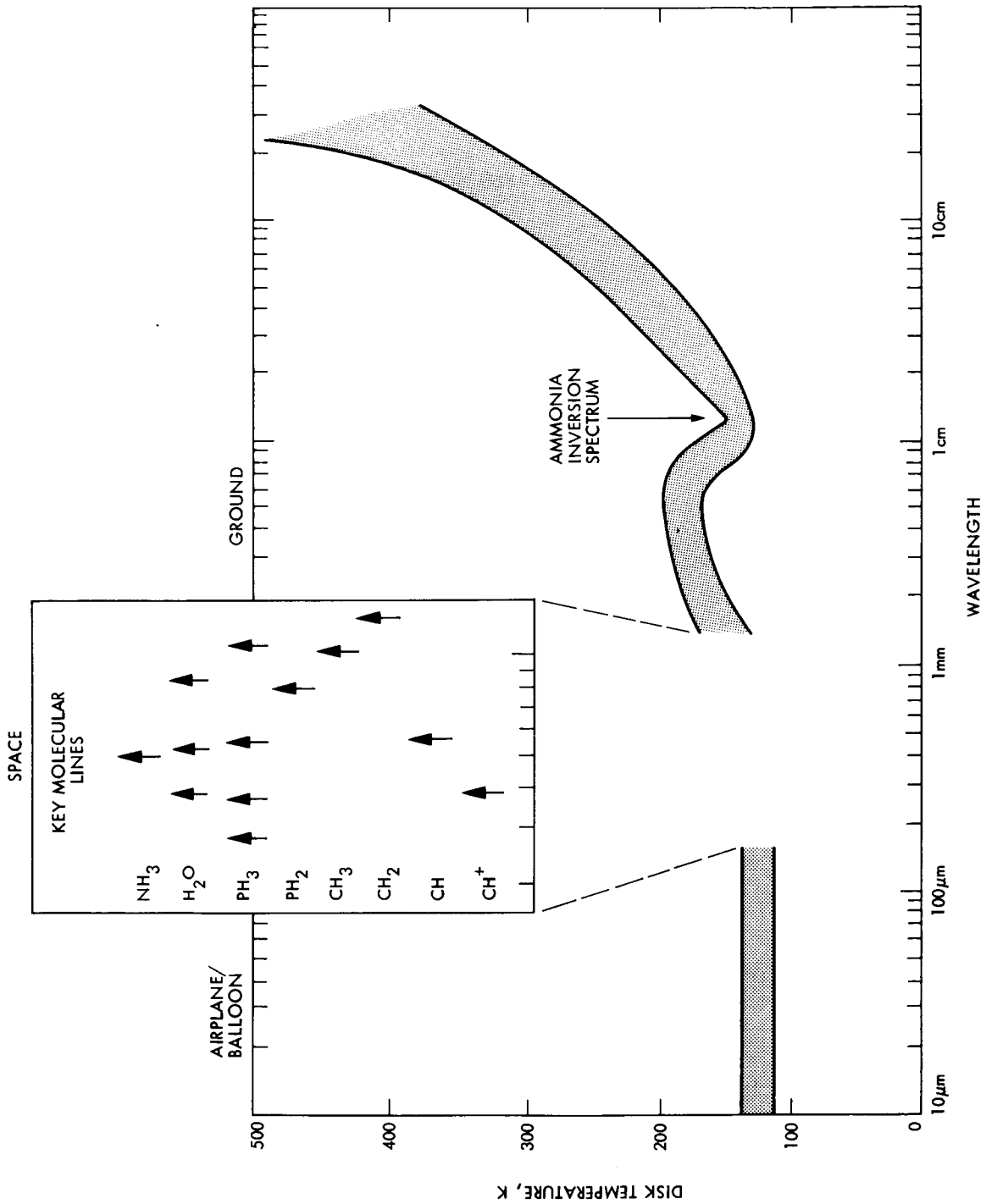


Figure 3-13. Shaded region shows approximate shape of Jovian spectrum. Insert illustrates virtually unexplored spectral region which could be studied with a submillimeter space telescope.

There is a recent report of variable CO emission in X Cygni and Mira (Lo and Bechis 1977). The simultaneous observation in all the lower lines of the CO ladder will be important in the understanding of this phenomenon.

2. Carbon and S-Type Stars

Recently, the envelopes of other evolved stars have begun to be investigated using molecular transitions. These observations are at the very limit of what can be observed with existing technology. Submillimeter observations with a large space antenna will provide increased sensitivity as well as information on molecular excitation.

The prototype of this class of stars is IRC+10216 (see Figure 3-14). All of these stars show wide ($20 - 40 \text{ km s}^{-1}$) CO line profiles (Zuckerman 1977). Mostly, the lines are just barely detected ($T_A < 0.5 \text{ K}$), but in the case of IRC + 10216 ($T_A = 4 \text{ K}$), it has been possible to detect a variety of other molecules besides CO (Morris *et al* 1975). Thus, the chemistry of such envelopes is currently a matter for speculation. Zuckerman *et al* (1977) have noted that the larger fraction of these stars tend to be carbon rich. Also, when the CO flux is normalized to the $0.5 - 20 \text{ m}$ flux, one finds that, for a given intrinsic luminosity, stars with $C/O > 1$ tend to have stronger CO emissions. Zuckerman *et al* (1977) argue that this indicates that carbon-rich stars have greater mass-loss rates. Since 86% of the stars examined did not have detectable CO emissions, and since stars with $C/O > 1$ in their sample tended to have larger IR fluxes, much improved sensitivity in the CO line is needed to substantiate this point.

Prospects for increased sensitivity at higher frequencies are good. An analysis of the excitation of various molecules with optically thin lines in IRC + 10216 (Morris 1975) indicates that infrared radiation excites the molecules into excited vibrational states, from where they decay back to rotational levels of the ground vibrational state. This causes high rotational levels to be populated and predicts brightness temperatures in the higher frequency lines which are comparable to those seen in the lines near 3 mm . Since these sources are generally not resolved (even IRC + 10216 is resolved only in the optically thick line of CO), sensitivity will increase as frequency squared for a given antenna size. The same argument also applies to optically thick lines from unresolved sources, for which the brightness temperature will be approximately the gas temperature.

The nature of the mass-loss is known only in IRC + 10216 (and perhaps CIT 6) from a careful examination of the shapes of the line profiles. In IRC + 10216, the phenomenon is unmistakably mass-loss at a uniform velocity (Kuiper *et al* 1976). In all other instances, only the width of the line indicates a probable outflow. Higher sensitivity is therefore needed to examine the shapes of the lines. Higher angular resolution is needed in order to map the brightness distribution, at least for the larger sources, to confirm the interpretation of the line shapes.

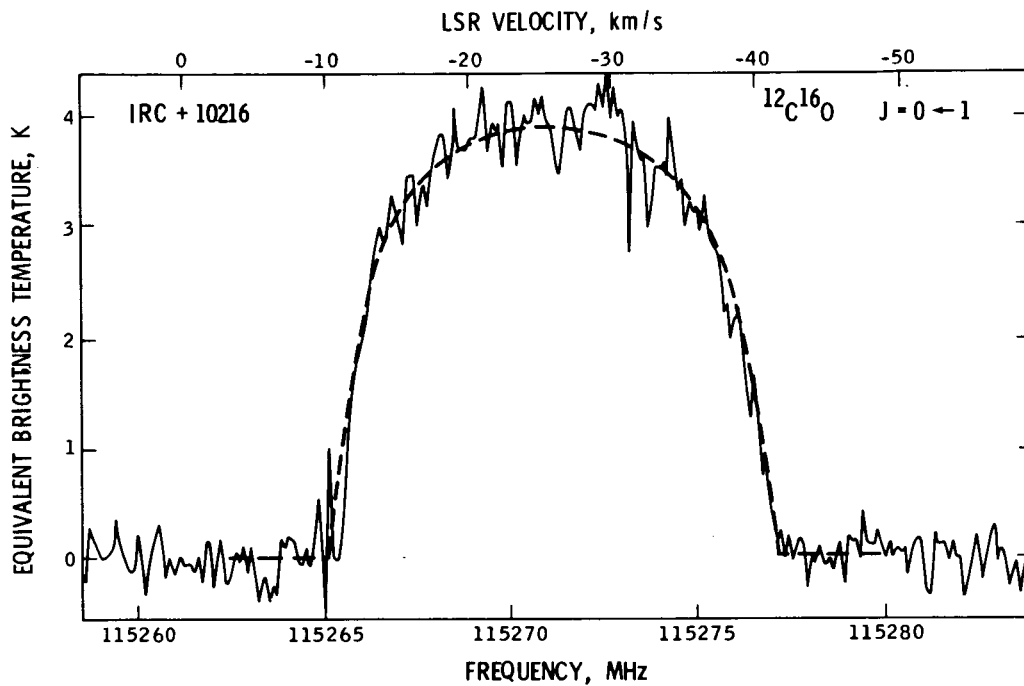


Figure 3-14a. J=0-1 profile of $^{12}\text{C}^{16}\text{O}$ in IRC+10216

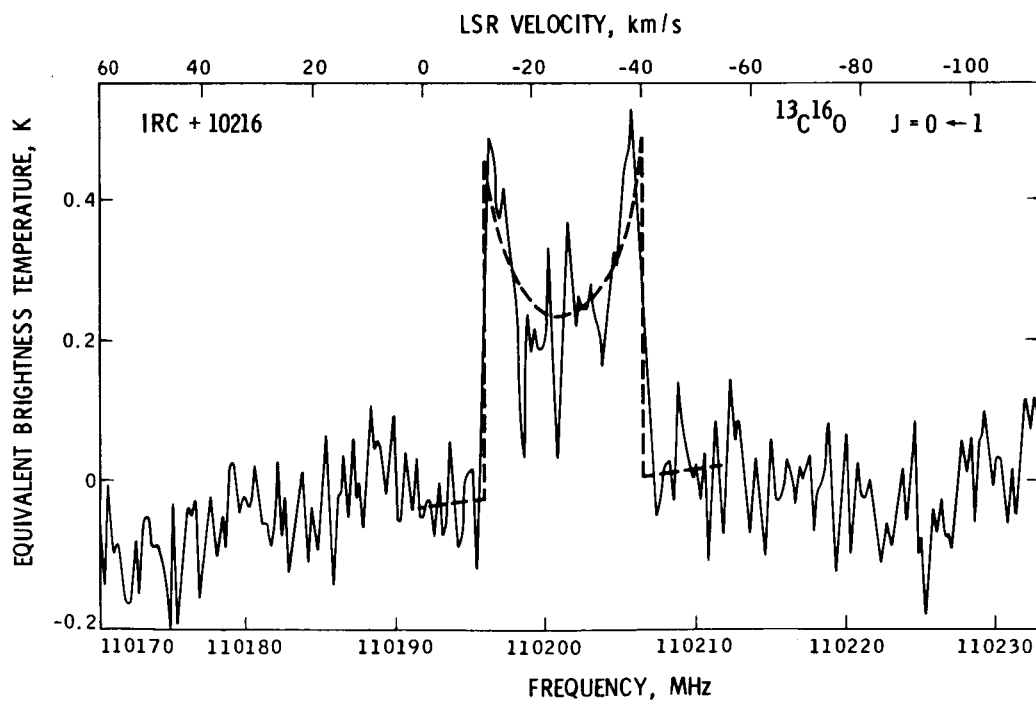


Figure 3-14b. J=0-1 profile of $^{13}\text{C}^{16}\text{O}$ in IRC+10216

3. Early-Type Emission Line Stars

Zuckerman *et al* (1975) and Bechis and Lo (1975) have suggested that at least some of the carbon stars may represent a state of stellar evolution preceding planetary nebulae; a similar suggestion has been made for an entirely different class of objects, which are similar to the young stars previously discussed. V 1016 Cygni is the prototype of this class. It shows a radio spectrum which varies as the first power of the frequency (Marsh *et al* 1976). Prior to 1965, it was a late M star, but it has since undergone 5 magnitudes of brightening and its spectrum has changed to an early type with a complex emission line spectrum indicating both high and low excitation components in the stellar envelope. Many lines show doubling, indicating an expansion at 35 km s^{-1} (Fitzgerald 1973). It has been suggested that this object is a planetary nebula in its formative stages (Ahern *et al* 1977), which is now in the first stages of ejecting its shell. This object, and others like it, shows a flattening of its radio continuum spectrum at millimeter wavelengths, which suggests that the shell has an inner boundary, indicating that the mass-loss phase terminated some time ago. Could it be that the central star in IRC + 10216 will one day cross the H-R diagram and experience the kind of change seen recently in V 1016 Cygni? Submillimeter observations, by their increased sensitivity and angular resolution, may provide answers.

4. Novae

Submillimeter observations of novae with a 10-m space telescope will be achievable for at least a few years after an outburst, and important new data about nova shells can be obtained. The few radio novae which have been observed to date show a nearly thermal spectrum (see, for example, Figure 3-15) which is consistent with the evolution of an expanding thermal source, still optically thick at 100 GHz. In the submillimeter wavelength range it will be possible to measure the optically thin spectral region and hence determine the product of the emission measure and the source solid angle. Hjellming has indicated how such measurements may be used to study the evolutionary properties of the novae. Because of the thermal spectra of novae, there is a tremendous advantage in working at short wavelengths. We note that a 10-m space telescope will achieve a minimum detectable flux density of 10 mJy in about one hour, which is approximately the same sensitivity that is achieved observing with the NRAO three element interferometer. However, since novae are generally optically thick at centimeter wavelengths, one gains relative sensitivity by working at short wavelengths. Thus it should be possible to detect more novae and also to follow the evolution of novae for longer periods of time.

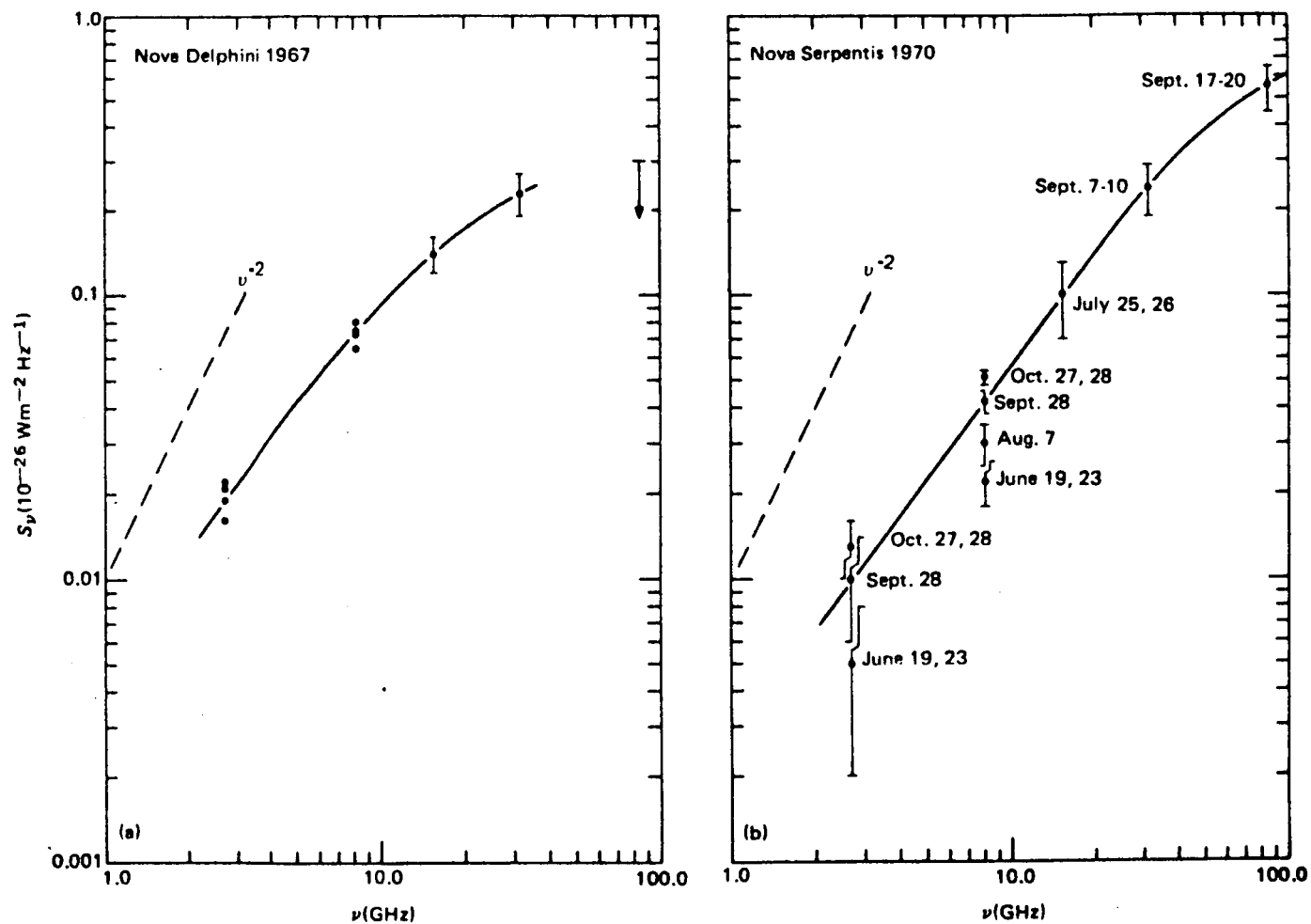


Figure 3-15. Radio Spectra of Nova Delphini 1967 and Nova Serpentis 1970 as measured from June to October, 1970. (C. M. Wade and R. M. Hjellming, 1971. *Astrophys. J.* 163:L65).

SECTION IV

TECHNICAL REQUIREMENTS AND FEASIBILITY

A. GENERAL CONSIDERATIONS

Several important underlying considerations have influenced our thoughts on a submillimeter telescope. These, along with scientific considerations, have been used to develop the technical requirements presented in this section. We acknowledge that the scientific problems of today will not be the same as those a decade from now. To account for these inevitable but unknown changes, we were guided to an instrument concept capable of attacking today's problems but at the same time designed to insure enough flexibility for tomorrow's opportunities. Space technology is rapidly changing. New materials and techniques for space applications are becoming available with great regularity. With this thought in mind, we visualize a telescope and associated instrumentation which can be built with today's technology, but which can also be modified, improved, and upgraded as new technology becomes available. Because any orbiting astronomical telescope is an expensive and complicated device, it must be large enough to make substantial improvements over competing telescopes and be operated for extensive periods of time to justify the cost. Finally, we noted that the possibilities for building very large submillimeter antennas in space are great and that early submillimeter telescope designs should be constantly alert to this growth potential.

B. SCIENCE CONSIDERATIONS

Section III describes some of the science objectives for the space telescope. These objectives translate into telescope requirements necessary to perform the required experiments. The most important requirement is that the telescope should operate over the frequency range from 300 GHz to 3000 GHz (1 mm to 100 μ m) in order to cover the gap between the millimeter spectral region at the low frequency end and the infrared at the high frequency end. In addition, the telescope should have good flux sensitivity, a narrow beam for detailed mapping, and be capable of high spectral resolution over a very broad frequency range.

The requirements for sensitivity over a wide frequency range suggest a reflecting antenna rather than an array. While the requirements on aperture size are difficult to quantify, since there are always smaller or weaker sources to be observed, an instrument capable of mapping with 10 arc-second resolution and with a gain greater than 80 dB will provide a significant improvement over any proposed space or airborne telescope and would have a resolution comparable to the next generation of ground-based millimeter telescopes.

C. SUBMILLIMETER TELESCOPE CONCEPT

We believe that scientific requirements and general considerations point toward a 10 m class reflecting telescope orbiting as a free-flyer (Figure 4-1) and designed to provide a long term space observation capability. (If a permanent space station were established, it might be preferable to attach the telescope to it.) The frequency range of operation should be between 300 - 3000 GHz (1 mm - 100 μ m) to cover the gap between the millimeter and the infrared regions. The lowest frequency of operation would normally be ≥ 400 GHz, since this is approximately the frequency at which ground-based observations begin to suffer severely from atmospheric attenuation (Appendix A). However, observations at longer wavelengths (for example, the 60 GHz oxygen band and the 183 GHz water line) may be desirable to overlap ground-based measurements. The upper frequency limit of the telescope will undoubtedly be limited by the reflector surface accuracy. As a design goal, at 3000 GHz (100 μ m) the telescope would operate in an incoherent mode, that is as a "light bucket." This would be accomplished by having the panels quite precise (6 μ m) on a small scale, although not achieving this accuracy on the scale of the entire telescope. The maximum frequency for coherent operation would be achieved at 1000 GHz where the rms surface irregularities would be $\lambda/16$ or 19 μ m. The antenna effective area for coherent detection would begin to decrease rapidly above 1000 GHz; however, maximum gain would not be realized until ≈ 1250 GHz.

We envision that the telescope will be delivered to orbit by the Space Shuttle. The telescope should also be capable of being serviced by the Shuttle (Figure 4-2) and be retrieved by the Shuttle. All instrumentation should be fully automated. Data would be sent to the earth via a telemetry downlink and commands to the pointing and data acquisition subsystems would be done on an uplink. The receiver packages would be built with a modular design. Instruments should be designed to operate for at least one year without servicing. (Except possibly for the cryostat, it should be possible to operate the telescope for considerably longer.)

The mode of major refurbishment could be to return the telescope to the ground. In orbit, servicing for minor repairs and replacements should be possible as well as replenishment of cryogenics as required.

D. ANTENNA

Table 4-1 gives a comparison between a 10 m submillimeter space telescope and a number of other existing or proposed telescopes. The table lists diameter, maximum usable frequency and effective collecting area when taking into account a typical atmospheric absorption for the location of the instrument.

A 10-m space telescope is seen to have a smaller collecting area than the proposed NRAO 25 m and U.K. 15 m at 300 GHz, but rapidly gains advantage at higher frequencies. At 1000 GHz, LIRTS, a proposed European

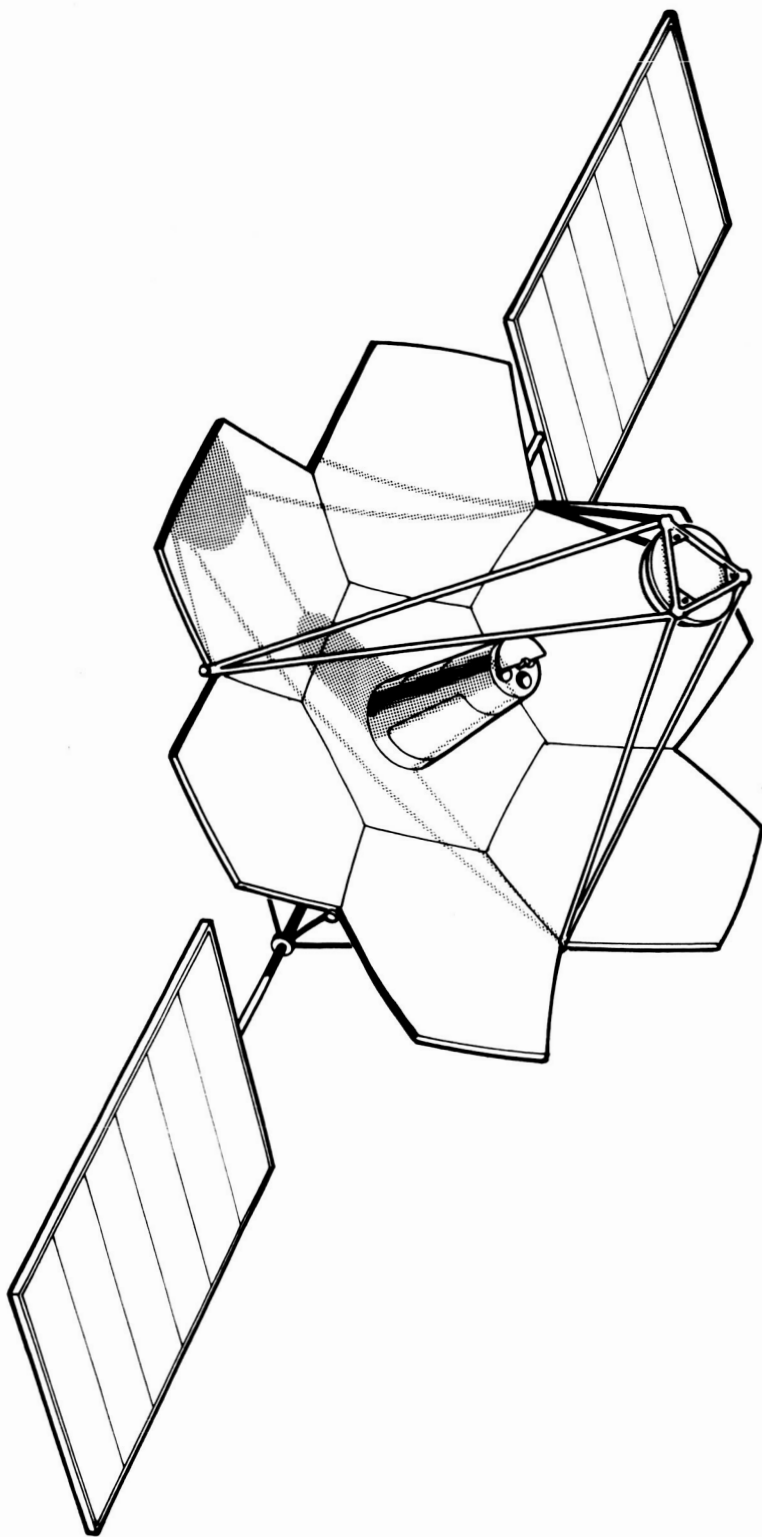


Figure 4-1. 10-m Diameter Orbiting Submillimeter Telescope Concept

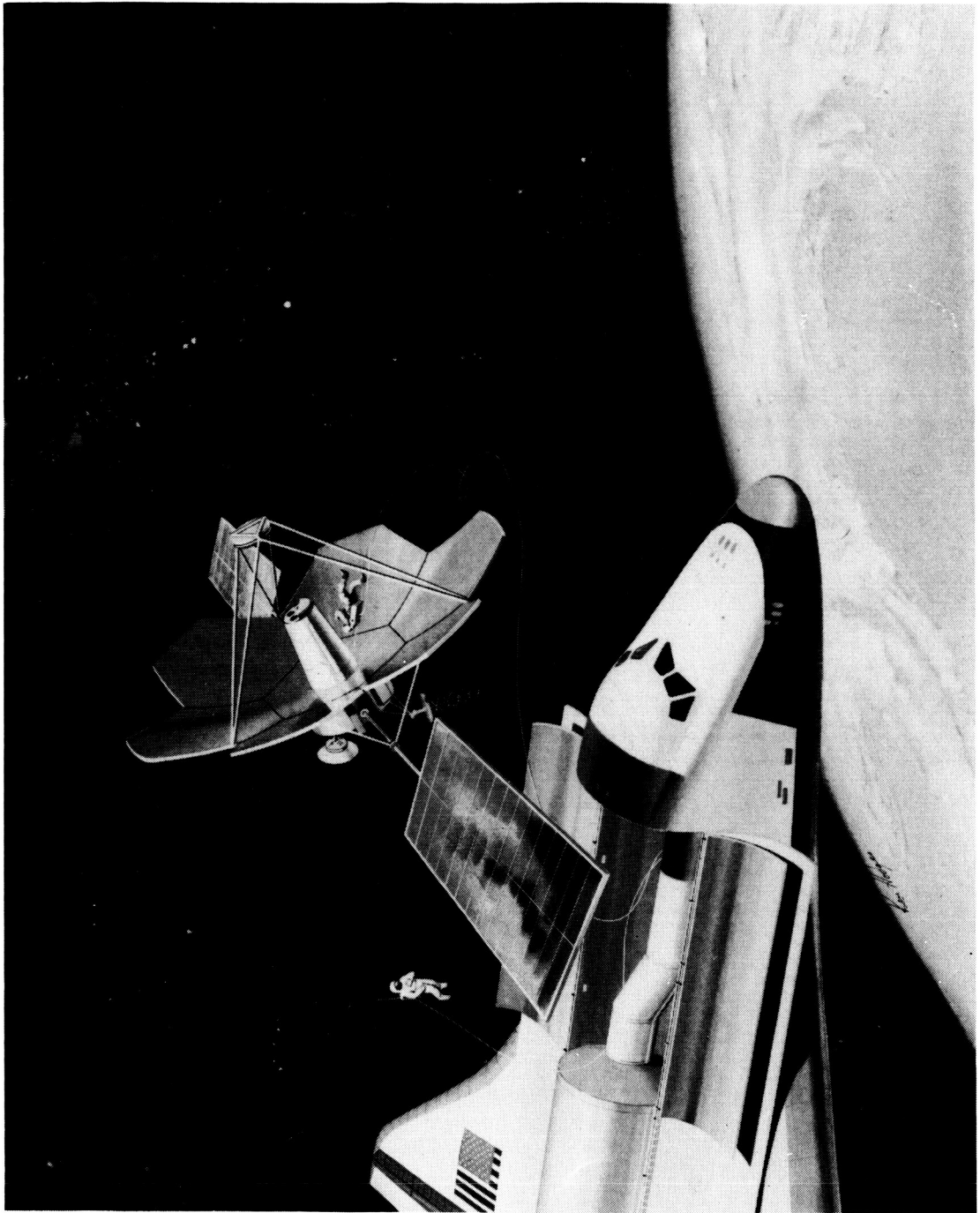


Figure 4-2. 10-m Diameter Orbiting Submillimeter Telescope Being Serviced by Shuttle

Table 4-1. Parameters of Some Submillimeter Telescopes

Existing Telescopes	Diameter (m)	Maximum Frequency (GHz, $\lambda/16$)	Effective Aperture (Through Atmosphere) (m ²)		
			300 GHz	500 GHz	1000 GHz
Kuiper Airborne Observatory	0.9	IR	0.3	0.3	0.3
Bell Telephone Lab	7	300	10	<1	-
Hale Telescope (Palomar)	5	Optical	9	.5	<0.1
Owens Valley	10	350	15	1-2	0.1
<u>Proposed Telescopes</u>					
NRAO	25	250	120	9	0.1
United Kingdom	15	380	90	?	-
LIRTS	2.8	IR	3	3	3
<u>Submillimeter Space Telescope</u>					
	10	1000	40	40	20

infrared telescope for Shuttle, has $\approx 1/7$ of the collecting area of the submillimeter telescope. This translates into a factor of 50 in integration time to obtain equivalent data on unresolved sources.

A precision deployable 10 m antenna with a 20 μ m rms surface accuracy is a technological challenge but is thought to be possible with today's technology. During the last 5 years, R. Leighton has developed several prototype antenna of 10.4-m diameter, 4.1-m focal length, and a surface accuracy of less than 50 μ m rms. Design improvements are expected to yield a two-to-three-fold improvement in the surface figure. Leighton's success (Figure 4-3) gives us confidence that the surface accuracy can be achieved; his unique design offers a method by which the antenna can be stowed in the Shuttle bay and deployed in space. Deployable antennas designed for operation at lower frequencies have been extensively studied by industry. We expect that the materials and deployment technology learned in these studies can be transferred to a precision deployable antenna.



Figure 4-3. 10-m millimeter wavelength telescope at Owens Valley Radio Observatory, constructed of hexagonal modules

The maximum frequency at which an antenna can be used coherently is determined by its surface accuracy. When the rms surface irregularities are $\lambda/16$, the antenna effective area is decreased by a factor of 1/2, although operation at higher frequencies is possible at a further reduced effective aperture. In fact, since gain is proportional to λ^{-2} , maximum gain is achieved when the surface irregularities are $\lambda/4\pi$. By convention, the highest usable frequency is defined where the rms surface irregularities are $\lambda/16$. For 1000 GHz (300 μm), the surface requirement is for a true parabola within an rms value of 19 μm . The maximum gain is achieved when $\lambda = 4\pi \times 19 = 239 \mu\text{m}$ (1250 GHz).

A 10 m antenna delivered into orbit via Space Shuttle must be deployable, since the maximum width of the cargo bay is just over 4 m. One possible configuration, again based on Leighton's 10 m antennas, is that of seven closely packed hexagonal panels, each nearly 4 m in diameter (see Figure 4-1). The individual panels could be made up of graphite-epoxy skins, separated by an aluminum honeycomb to facilitate temperature equalization. A method of hinging the panels to each other and maintaining the required tolerance must be developed, bearing in mind that the required accuracy of 20 μm is just under 0.001 in., about what one might expect in a high quality door hinge.

The antenna requirements and parameters discussed above are summarized in Table 4-2.

Three aspects of telescope design must be studied in more detail:

- (1) Accuracy with which individual panels can be manufactured. Leightons's experience indicates that present techniques can already achieve an accuracy of $\sim 20 \mu\text{m}$ with aluminum honeycomb, and he has identified promising techniques for improving the accuracy. Also, the techniques must be adapted for graphite-epoxy (or a similar composite material), a material more suited to space applications. The accuracy that can be achieved will determine the minimum frequency in the "light-bucket" mode of operation.
- (2) Methods of deployment, by which the panels can be set in space to achieve the necessary overall accuracy and rigidity. This would involve engineering and studying prototype structures. The degree of precision that can be achieved in deployment will probably limit the wavelength to which the entire reflector can be used coherently.
- (3) Surface deformations, which may be expected due to thermal and mechanical stresses when the entire structure is locked into its deployed position. These may be more important in limiting the maximum frequency of coherent operation.

We feel that in-depth studies in these areas, and perhaps in other areas we have overlooked, are an essential prelude to any design activities and should be started as soon as possible.

Table 4-2. Antenna Requirements and Parameters

Diameter: 10 m

Overall Surface accuracy ($\lambda/16$ at 1000 GHz): 19 μm rms

Type: paraboloid of revolution, Cassegrain fed

$\theta_{3\text{dB}}$ at 500 GHz: 15 arc seconds

$\theta_{3\text{dB}}$ at 1000 GHz: 7.6 arc seconds

Gain at 500 GHz: 91 dB

Gain at 1000 GHz: 94 dB

Pointing accuracy: $\theta_{\text{min}}/10$: 0.8 arc second

E. ANTENNA POINTING AND CONTROL

The antenna pointing system should be able to control the telescope position to within 0.1 of the minimum half-power beamwidth for accurate mapping and positioning on point sources. If we take the half-power beam-width, $\theta_{3\text{dB}}$ in degrees, as

$$\theta_{3\text{dB}} = \frac{70\lambda}{d}$$

where λ is the shortest operating wavelength (300 μm) and d is the antenna diameter (10 m), we get $\theta_{3\text{dB}} = 8$ arc seconds and a required pointing accuracy of 0.8 arc seconds. Existing star tracking systems with 1 arc-second accuracy are presently in use and planned pointing systems for the Space Shuttle have accuracies of ≈ 0.3 arc second. The pointing accuracy requirements for a 10-m submillimeter observatory are less severe than the requirements on the planned optical Space Telescope. Because of activities already being carried out in space instrument pointing systems, we feel that further consideration can be deferred until a telescope design is imminent.

F. RECEIVERS

There are two basic types of measurements to be made from a sub-millimeter observatory: (1) narrow band spectroscopy with high frequency resolution of well-defined spectral lines, and (2) broad-band flux density (or brightness temperature) measurements.

Spectroscopy is generally accomplished at millimeter wavelengths by the use of coherent detectors which are now almost exclusively crystal mixers with an IF frequency of a few GHz. Crystal detectors are the oldest and most widely used radio detectors. Prototype receivers using quasi-optical techniques indicate that reliable crystal detectors operating to 600 GHz are now being constructed. We believe that further development and the construction of such receivers for use in astronomy should receive increased financial support.

Other types of detectors for both spectroscopy and broad band detection which may be used in the submillimeter range are masers, parametric amplifiers and down converters, the hot-electron bolometers, and various Josephson junction devices. Active research is presently being carried out on all of the above devices for use at millimeter wavelengths. It is premature to speculate on what will be the "best" technique for space use in the 1980's. However, successful developments at millimeter wavelengths should be followed immediately by work to extend these devices to shorter wavelengths. Appendix C discusses the current state of the art in submillimeter detectors.

Crystal mixers can and are used as broad band detectors although, at frequencies in the submillimeter region, incoherent detectors, such as helium cooled bolometers, offer a sensitivity advantage. Bolometers operating throughout the submillimeter range are presently available and have high sensitivity. However, the technology could benefit from additional development at submillimeter wavelengths.

Even with limited knowledge of future receiver technology, we can specify many of the expected and required receiver parameters. Figure 4-4 is a plot of receiver noise temperature vs frequency for many existing radiometers. With some hesitation, one can extrapolate into the submillimeter region (bounded by vertical lines in the figure) to determine what sort of noise performance might be expected from future instruments. These noise performance extrapolations for coherent detectors are listed under T_{sys} in Table 4-3. The sensitivity for incoherent detectors (bolometers) of 10^{-14} W/Hz- $1/2$ in Table 4-3 is based on present technology.

The exact frequencies for spectral line measurements depends upon what particular transitions are of scientific interest at the time. A versatile telescope should therefore be capable of tuning to any frequency in its intended range of operation. It seems reasonable to anticipate coherent spectral line receivers which are each continuously tunable over, say, a 10% bandwidth. Then, using both the sidebands, six tunable receivers could cover the entire 300-1000 GHz range. The instantaneous bandwidth should be large enough to cover a range of Doppler shifts of 600 km/s (± 300 km/s). Table 4-3 lists the instantaneous bandwidth required for 600 km/s, along with the frequency resolution obtainable with a nominal 1000-channel spectrometer for three arbitrary center frequencies. The minimum detectable temperature is calculated for the given receiver temperature, bandwidth of one channel, and one hour of integration time.

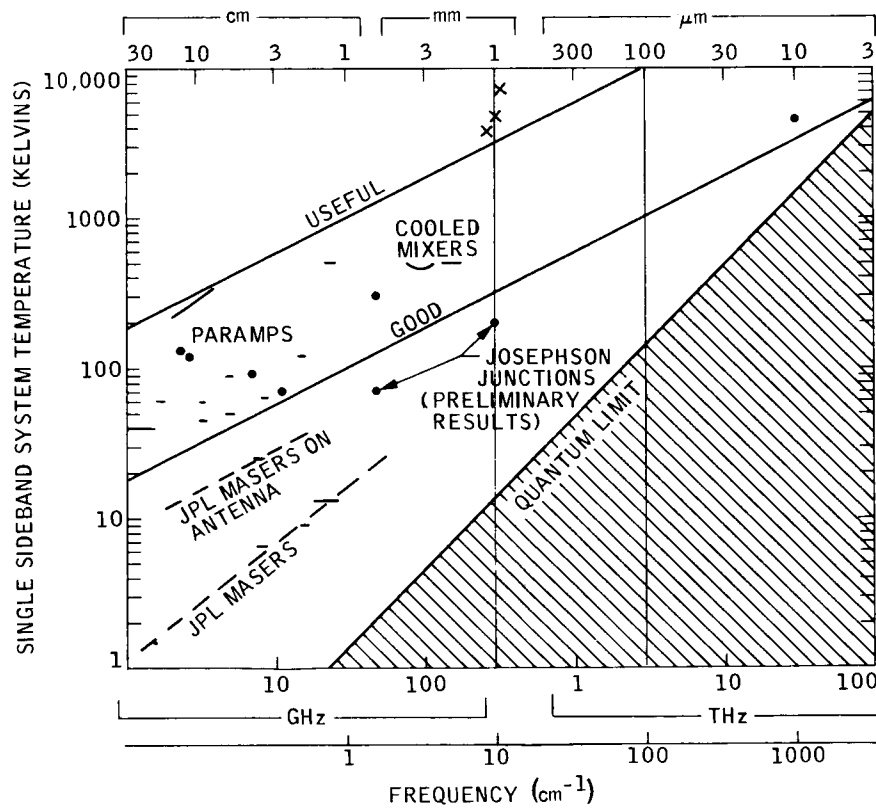


Figure 4-4. Receiver noise temperature versus frequency for a number of receivers

Complete frequency coverage is not necessary for broadband flux density measurements. Possibly four continuum radiometers with a 10% instantaneous bandwidth would be sufficient for the range 300-3000 GHz. Table 4-3 lists four arbitrary frequencies for broad-band coverage along with the minimum detectable power, 10% instantaneous bandwidth and calculated minimum detectable flux density for a 10 meter antenna and one hour of integration.

In a heterodyne receiver, the IF is processed by multi-frequency filter banks or digital methods to obtain high frequency resolution. Electro-acoustical and opti-acoustical interference devices are also becoming available for spectrum analysis at intermediate frequencies. Of all of these, the digital devices have the advantage of stability and flexibility and it seems probable that the system selected for use in space would be digital. The technology to build a prototype system exists. It is desirable to build such a system in order to perfect its design and controlling software for use in space.

Bolometric receivers gain their high continuum sensitivity partially by their broad bandwidth. In the range of intermediate frequency resolution, Fourier transform spectroscopy combines the broad-band properties of a bolometer with some type of filter and a dual path interferometer to give spectral resolution of 10^{-3} to 10^{-5} . This allows for a coarse spectral line survey over a large spectral range by tuning the interferometer over the bandwidth of the bolometer. One or all of the broad-band bolometers could be configured for Fourier transform spectroscopy so that the whole submillimeter spectrum could be mapped for strong unknown spectral lines, or line bands.

Table 4-3. Submillimeter Receiver Sensitivity
Based on Expected Noise Performance,
Required Bandwidth and a 10 m Antenna

Spectroscopy Receivers					
Frequency (GHz)	Expected T_{sys} (K)	Instantaneous IF Bandwidth, $d\nu$ (± 300 km/s)	Frequency Resolution (1000 Channels) (MHz)	Minimum Detectable Temperature, ΔT	
				$1h$, max $d\nu$ (K)	$1h$, 1 Ch. (K)
300	800	750 MHz	1	0.001	0.03
500	1500	1 GHz	1	0.0015	0.05
1000	2000	2 GHz	2	0.0015	0.05

Continuum Receivers				
Frequency (GHz)	Minimum Detectable Power, ΔP ($d\nu=10\%$) (W/ $\sqrt{\text{Hz}}$)	Instantaneous Bandwidth $d\nu$ (10%) (GHz)	Minimum Detectable Flux Density, S ($1h$, $d=10$ m, $S/N=1$) (mJy)	Minimum Detectable Temperature, $\Delta T(1h)$ (mK)
300	10^{-14}	30	14	0.4
500	10^{-14}	50	8	0.2
1000	10^{-14}	100	8	0.1
2000	10^{-14}	200	8	0.06

SECTION V

FOLLOW-UP POSSIBILITIES

In previous sections we focused our attention on the scientific problems which could be addressed with a 10 m telescope using current receiver technology. This discussion is of immediate value from a practical viewpoint, but it nevertheless ignores the growth potential of the system. In this section we consider potential new devices and techniques that might be considered in any follow-up activity.

A. ANTENNAS

Leighton has pioneered the construction of large-aperture antennas constructed of hexagonal panels for submillimeter wavelengths, and we have employed his concepts in the 10 m design discussed in the previous section. In this design, the individual panels of the antenna would be stowed in the Shuttle payload bay in a folded configuration for launch and the antenna would be deployed in space. An immediate extension of this concept to achieve a larger aperture is to increase the number of panels. The largest such antenna that could be easily accommodated in the Shuttle would be one consisting of 37 panels for a total diameter of ~25 meters (assembled). Figure 5-1 shows how the 25 m diameter telescope would be assembled from the 37 panels.

An alternative approach to the preformed surface panels has been proposed by Melcher and Staelin of MIT, based on electrostatically-controlled precision reflector surfaces made of a very thin elastic conducting sheet. Such antennas would be comprised of four major subsystems: (1) deployable structure system, (2) position and shape measurement system, (3) feedback command generation system, and (4) command execution system.

The present concept is that the deployable structure will consist of two large parallel curved surfaces, one (the controlled surface) which is the reflector, and a backup surface (the command surface). This second surface could vary slowly with time due to thermal or other causes without penalty. Electric forces between these two surfaces shape the controlled surface. Both surfaces would be ~5 μm thick and suspended as diaphragms from a rigid rim.

Position and shape measurement can be accomplished by scanned optical systems. The controlled surface can, in principle, be measured with an accuracy better than ~1 μm using a laser interferometer. System measurement times of ~1 s are sought. The surface can be optically referred to both the antenna feed assembly and celestial coordinates. Although this concept is not sufficiently developed to provide the first generation submillimeter wave telescope, the concept has the potential for leading to very large (>30 m) submillimeter antennas.

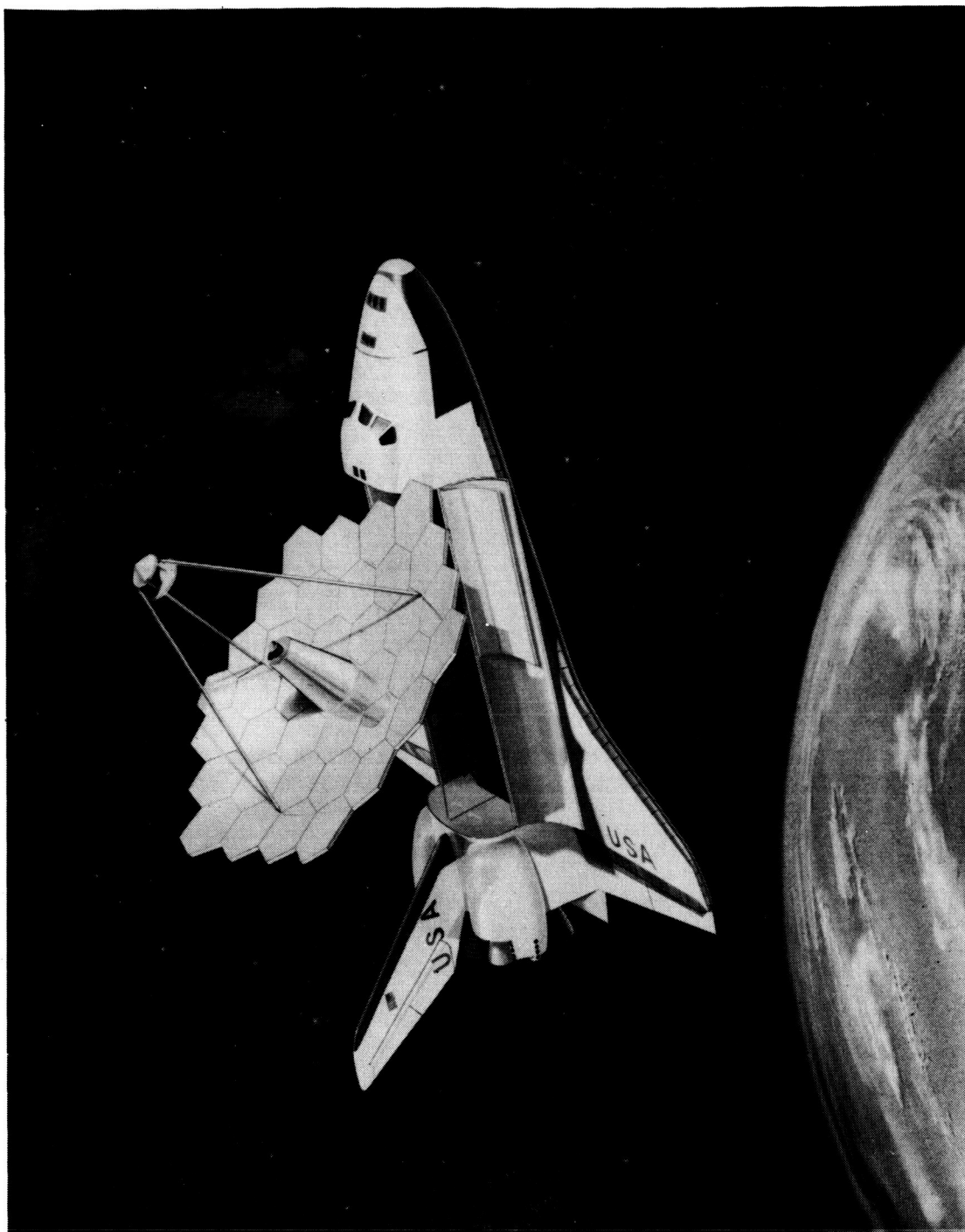


Figure 5-1. 24 m diameter Space-Erectable Antenna Consisting of 37 Hexagonal Panels

B. COHERENT RECEIVERS

The noise level of an ideal coherent receiver amplifier of electromagnetic waves is:

$$\zeta = h \frac{1}{e^{h\nu/kT_{-1}}} + 1$$

where

ζ = noise power density (W hz⁻¹)

h = Planck's Constant

k = Boltzmann's constant

ν = frequency

T = temperature of source (internal plus external source of noise)

The first term in parentheses is black-body radiation; the second term arises from spontaneous emission in the amplifier. In the limit of low temperatures and high frequencies, the noise power density is given by

$$\zeta = h\nu$$

and the equivalent noise temperature by

$$T_R = \frac{h\nu}{k}$$

This is the quantum limit shown in Figure 4-4. It can be seen in this figure that even the "good" receivers are an order of magnitude less sensitive than is theoretically possible. Thus we anticipate that order-of-magnitude improvement in receiver noise performance is possible within the framework of fundamental limitations. This improvement factor is not available from the ground because atmospheric fluctuations and emissions do not allow the quantum limit to be reached. We can already anticipate that masers and Josephson junction detectors can give us a factor of three improvement over the "good" receivers used as a baseline in this report.

SECTION VI
BIBLIOGRAPHY

- Ahern, F.J., Fitzgerald, M.P., Marsh, K.A., Purton, C.R. 1977, Astron. Astroph., 58, 35.
- Anders, E., Hayatsu, R., Studier, M.H. 1974, Astroph. J., 192, L101.
- Blair, G.N., and Dickinson, D.F. 1977, Astroph. J., 215, 552.
- A 25-Meter Telescope for Millimeter Wavelengths. (1975). National Radio Astronomy Observatory, Charlottesville, VA.
- Carpenter, R., Gulkis, S., Sato, T. 1973, Astroph. J. (Let) 182, L61.
- Christiansen, W.N., Hogbom, J.A., Radiotelescopes. Cambridge Univ. Press (1969).
- Cogdell, J.R., McCue, J.J.G., Kalachev, P.D., Salomonovich, A.E., Moisev, I.G., Stacey, J.M., Epstein, E.E., Altschuler, E.E., Feix, G., Day, J.W.B., Hvatum, H., Welch, W.J., Barath, F.T., IEEE Trans. Ant. Prop., AP-18, 515 (1970).
- Cohen, M.H., Kellermann, K.I., Shaffer, D.B., Linfield, R.P., Moffett, A.T., Romney, J.D., Seielstad, G.A., Pauliny-Toth, I.I.K., Preuss, E., Witzel, A., Schilizzi, R.T., Geldzahler, B.J., 1977, Nature, 268, 405.
- Conklin, E.G., and Bracewell, R.N., 1967, Nature, 216, 777.
- Elias, J. H., Ennis, D. J., Gezari, D. Y., Hauser, M. G., Lo, K. Y., Nadeau, D., Neugebauer, G., Werner, M. W., Westbrook, W. E. 1978, Ap. J., 219, in press.
- Encrenaz, Th., and Combes, M., private communication (1975).
- Fitzgerald, M.P., 1973, Nature Phys. Sci., 245, 58.
- Glassgold, A.E., Langer, W.D., 1975, Astroph. J., 197, 347.
- Herbig, G.H., 1970, Mem. Soc. Roy. Sci. Liege, 19, 13.
- Hildebrand, R.H., Whitcomb, S.E., Winston, R., Stiening, R.F., Harper, D.A., and Moseley, S.H., 1977, Ap. J., 216, 698.
- Hoyle, F., Wickramasinghe, N.C., 1977, Nature, 266, 241.
- Johnson, Mori, T.T., and Shimabukuro, F.I., 1970, IEEE Trans., AP-18, 512.
- Knapp, G.R., 1977, private communication.
- Kleinmann, D.E., and Low, F.H., 1970a, Ap. J. (Letters), 159, L165.

- Knapp, G.R., Kuiper, T.B.H., Knapp, S.L., Brown, R.L., 1976, Astroph. J., 206, 443.
- Kuiper, T.B.H., Knapp, G.R., Knapp, S.L., Brown, R.L., 1976, Ap. J. 204, 408.
- Lo, K.Y., Bechis, K.P., 1976, Astroph. J., 205, L21.
- Marscher, A.P., 1977, Astroph. J., 216, 244.
- Marsh, K.A., Purton, C.R., Feldman, P.A., 1976, Astron. Astroph., 49, 211.
- Mezger, P.G., 1975. Proc. Conf. on Far-Infrared Astronomy, Windsor Great Park, England, to be published.
- Morris, M., 1975, Ap. J., 197, 603.
- Morris, M., and Alcock, C. 1977, Ap. J., 218, 687.
- Morris, M., Gilmore, W., Palmer, P., Turner, B.E., Zuckermann, B., 1975, Ap. J., 199, L47.
- Mufson, S.L., and Liszt, H.S., 1975, Ap. J., 202, 183.
- Models of the Venus Atmosphere. NASA SP-8011, 1972.
- Novikov, Id. D., Zel'dovich, Ya. B., 1973, An. Rev. Astr. Astroph., 11, 387.
- Oppenheimer, M., Dalgarno, A., 1975, Astroph. J., 200, 419.
- Ollnon, F.M., 1975, Astron. Astroph., 39, 217.
- Owen, F.N. and Porcas, R.W., 1978, Astroph. J., in press.
- Pacholczyk, A.G., and Wisniewski, W.A., 1967, Ap. J., 147, 394.
- Parijskii, Y.N., 1973a, Ap. J. (Letters), 180, L47.; 1973 b, Sov. Astron-AJ 17, 291.
- Peebles, P.J.E., and Yu, J.T., 1970, Ap. J., 162, 815.
- Penston, M.V. 1970, Astroph. J., 162, 771.
- Pigg, Jr., J.C., "A Limit on the Inhomogeneity of the Cosmic Microwave Background Radiation at an Angular Scale of 1.25 Arc Min" PhD dissertation, California Institute of Technology, 1976.
- Purton, C.R. 1975 Astroph. J., 195, 79.
- Ridgway, S.T., Larson, H.P., and Fink, U., 1976, Jupiter, ed. Gehrels, T., University of Arizona Press, 384.
- Rickard, L.J., Turner, B.E., Palmer, P. 1977, Ap. J., 218, L51.

- Rieke, G.H., and Low, F.J., 1972, Ap. J., (Letters), 176, L95.
 . 1975a, Ap. J., 197, 17.
 . 1975b, Ap. J. (Letters), 199, L13.
 . 1975c, Ap. J. (Letters), 200, L67.
- Sachs, R.K., Walfe, A.M., 1967, Astroph. J. 147, 73.
- Scoville, N.Z., Kwan, J. 1976, Ap. J., 206, 718.
- Shimazaki, and Laird, A.R., (1970) J. Geophys. Res., 75, 3221.
- Shimabukuro, F.I., and Epstein, E.E., (1970) IEEE Trans., AP-18, 485.
- Silk, J. 1974, Ap. J., 194, 215.
- Silk, J. and Ames, S., 1972, Ap. J., 178, 77.
- Sill, G.T., 1976, Jupiter, ed. T. Gehrels, University of Arizona Press, 372.
- Snyder, L.E., 1976, in The Study of Comets, Proc. IAU Coll. 25, NASA SP-393, p. 232.
- Spencer, J.H., Schwartz, P.R., 1974, Astroph. J., 188, L105.
- Strom, S.E., Strom, K.M., Grasdalen, K.M., 1975, An. Rev. Astr. Astroph., 13, 187.
- Sunyaev, R.A., and Zeldovich, Ya., B. 1970, Astrophys. Space Sci., 7, 3.
- Sweitzer, J.S., 1977, B.A.A.S., 9, 373.
- Sweitzer, J.S., Palmer, P., Morris, M., Turner, B.E., Zuckerman, B., 1977, B.A.A.S., 9, 373.
- Telesco, C.M., Harper, D.A. and Loewenstein, R.F. 1976, Ap. J. (Letters), 203, L53.
- Ulich, B. L., and Hass, R.W., (1976) Astroph. J. Suppl., 30, 247.
- Ulrich, R.K., 1976, Astroph. J., 210, 377.
- U.S. Standard Atmosphere, 1962. U.S. Government Printing Office, Washington, D.C.
- Von Hoerner, S. 1967, Astron. J., 72, 35.
- Waters, J.W., (1976) in Methods of Experimental Physics, Vol. 12: Astronomy Observatory, Charlottesville, VA.
- Waters, J.W., Gustincic, J.J., Kakar, R.K., Kuiper, T.B.H., Swanson, P.N., Kerr, A.R., Thaddeus, P., presented at 149th Meeting of the American Astronomical Society, Honolulu, HI (1977).

Wendker, H.J., Baars, J.W.M., Altenhoff, W.J., 1973, Nature Phys. Sci., 245, 58.

Werner, M.W. 1970, Astron. J., 6, 81.

Westphal, J.A., (1974), Final Report on the 10-Micron Sky Noise Survey.
California Institute of Technology, Pasadena, CA.

Wynn-Williams, C.G., and Becklin, E.E. 1974, Proc. Astron. Soc. Pacific, 86, 5.

Zuckerman, B., 1977, preprint (Paper presented at IAU Symposium No. 76: Planetary Nebulae).

Zuckerman, B., Gilra, D.P., Turner, B.E., Morris, M., Palmer, P., 1976, Astroph. J., 205, L15.

Zuckerman, B., Kuiper, T.B.H., Rodriguez Kuiper, E.N., 1976, Astroph. J., 209, L137.

Zuckerman, B., Palmer, P., Morris, M., Turner, B.E., Gilra, D.P., Bowers, P.F., Gilmore, W., 1977, Ap. J. 211, L97.

APPENDIX A

EFFECT OF THE ATMOSPHERE ON GROUND BASED
AND AIRBORNE OBSERVATIONS

We are concerned with two effects when considering intensity measurements of astronomical objects from within the atmosphere: absorption of incident radiation, and an increase in noise due to emission by atmospheric gases. Absorption by the atmosphere may be expressed as

$$T(\nu) = T^*(\nu)e^{-\tau_\nu(h, \theta)}, \quad (1)$$

where $T(\nu)$ is the observed antenna temperature, $T^*(\nu)$ is the equivalent antenna temperature as it would be observed outside the atmosphere, and $\tau_\nu(h, \theta)$ is the optical depth through the atmosphere from a height, h , above mean sea level at a zenith angle of θ . Waters (1976) has described in detail the absorption and emission of microwave radiation by atmospheric gases. Treating the atmosphere as plane-parallel (accurate to 1% for $\theta < 70^\circ$),

$$\tau_\nu(h, \theta) = \sec \theta \int_h^\infty K_\nu(h') dh' \quad (2)$$

where $K_\nu(h')$ is the volume absorption coefficient at a frequency ν and a height h' .

In computing the models for atmospheric transparency (Figure A-1) and effective system temperature for earth-based receivers (Figure A-2), we have used the U.S. Standard Atmosphere (1962) for the temperature and pressure variation with altitude. We have calculated the capacity due to O_2 transitions using a kinetic line shape, and due to H_2O transitions including an empirical line-shape correction as described by Waters (1976). The mixing ratio of water was taken as 4×10^{-6} in the altitude range of 15 - 70 km. Below 15 km, the mixing ratio of water was assumed to have a scale height of 2 km, with the surface volume density treated as a parameter (see Table A-1). The calculation was terminated at an altitude of 70 km.

In Figure A-1, we have plotted $\tau_\nu(h, \theta = 45^\circ)$ for parameters characteristic of Mauna Kea, Hawaii (or perhaps White Mountain, California) and the typical operating conditions of the Kuiper Airborne Observatory. The parameters are given in Table A-1. The horizontal line for $\tau = 1$ may be considered the point at which observations become difficult, while the line for $\tau = 2.3$ (or 10 dB of absorption) represents nearly impossible observing conditions. Except in the cores of the atmospheric lines, the atmosphere is essentially transparent above the tropopause but, except for a few small windows, ground based observations are limited to frequencies less than 440 GHz.

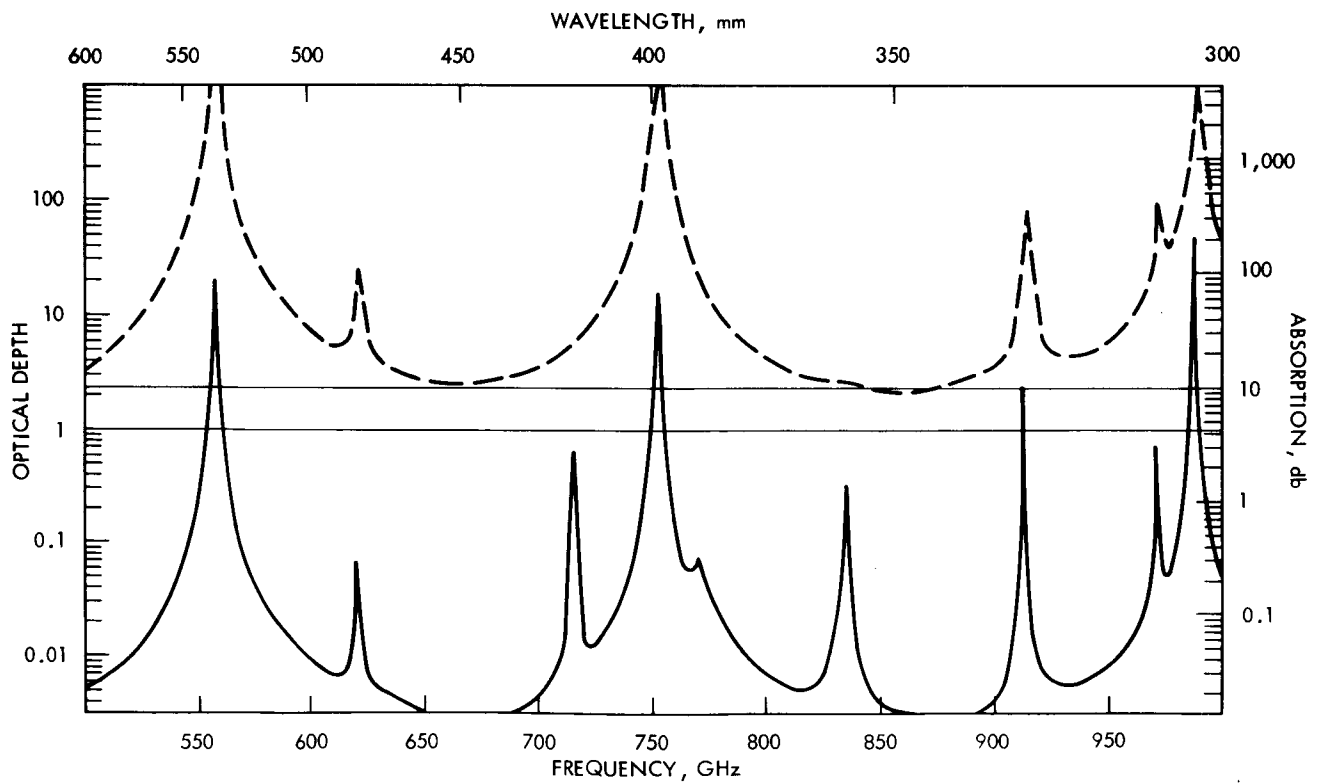
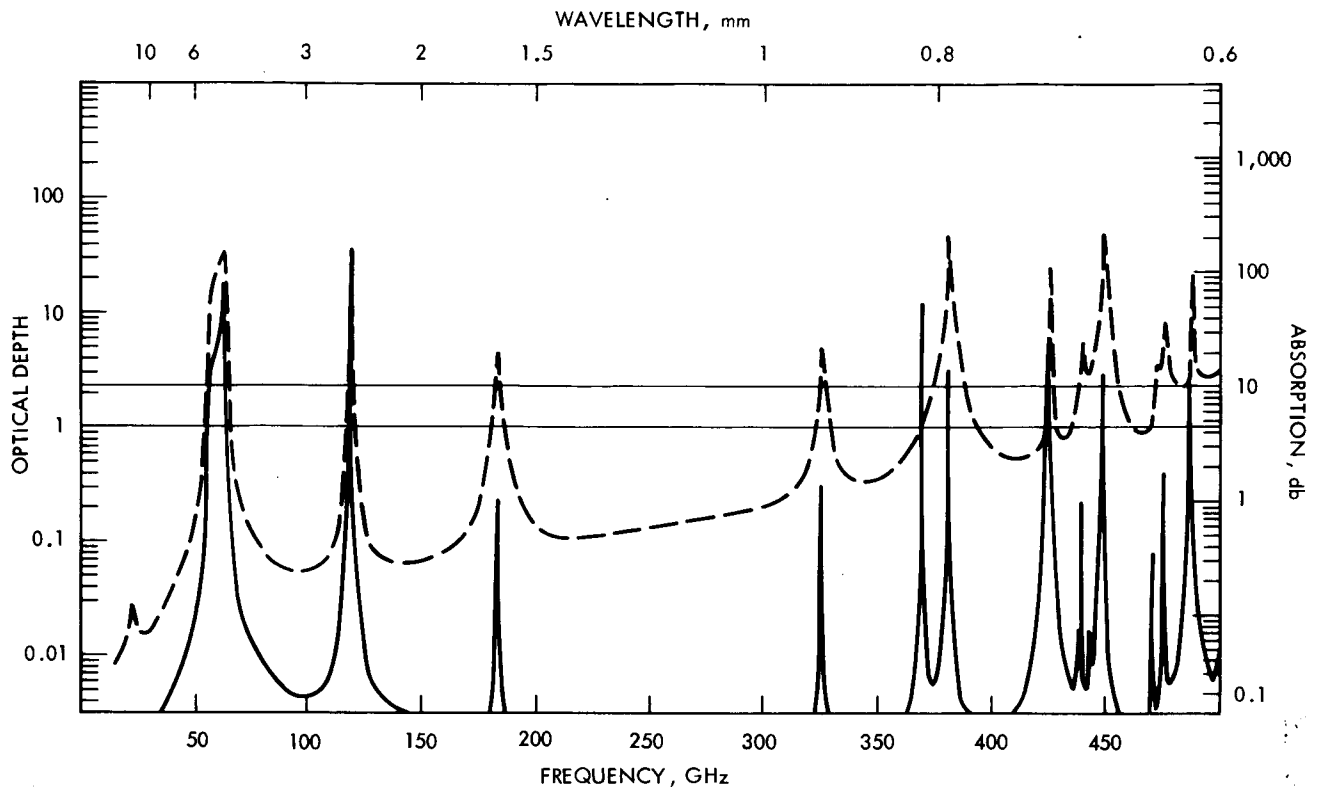


Figure A-1. Vertical Atmospheric Opacity from Sites
Given in Table A-1

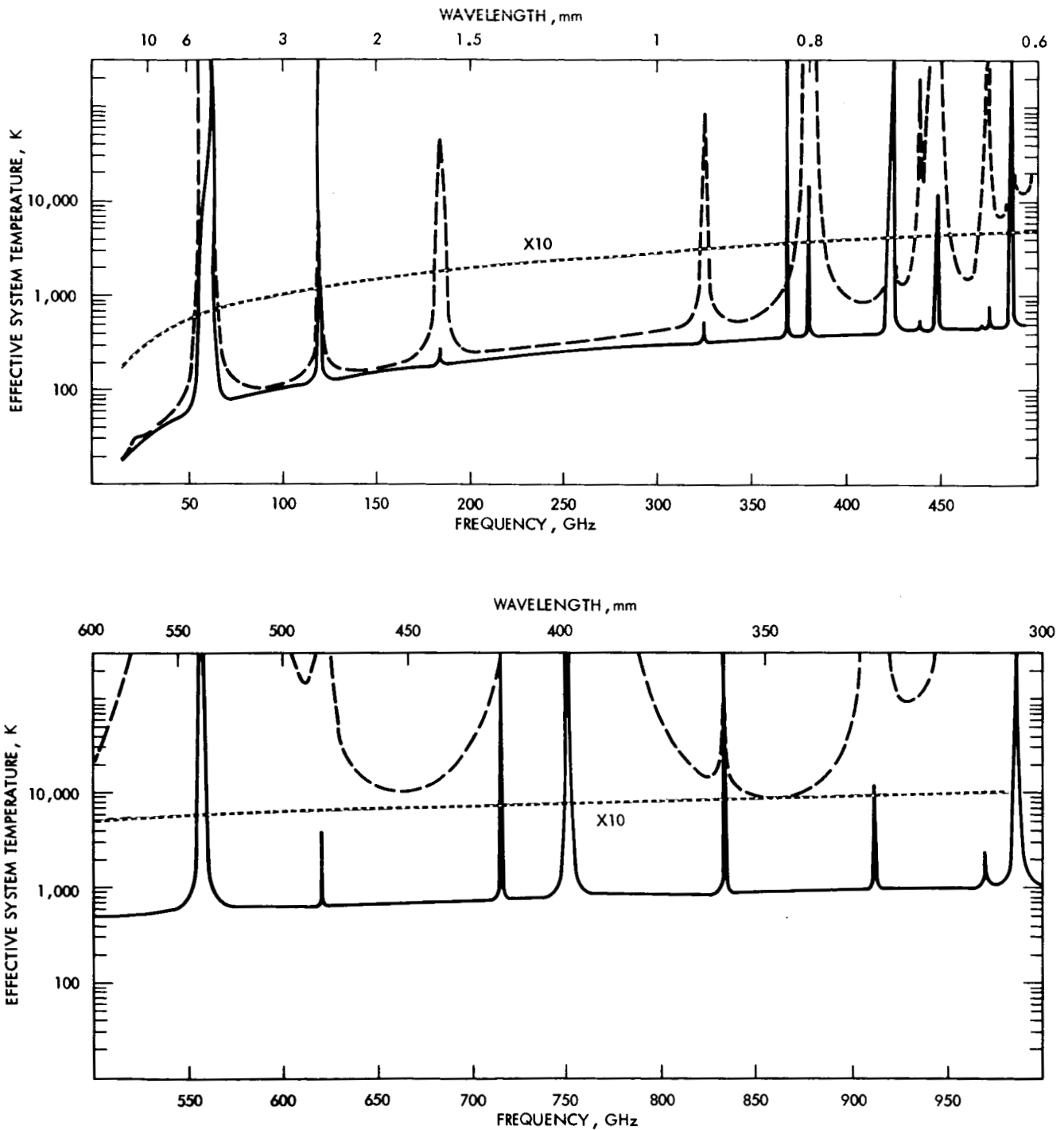


Figure A-2. Effective System Temperature for a Highly Sensitive Receiver ($T_{\text{rec}} \text{ (K)} = \nu \text{ (GHz)}$) Located at the Sites Given in Table A-1.

Table A-1. Parameters of Sites used in Atmosphere Model Calculations

Location	Altitude	Water Volume Density at Sea Level	Precipitable Water
Mauna Kea, HI	4.08	10.0	1.5 mm
NASA C-141	12.5	5.0	6 μ m

In addition to weakening the incoming signal, emission by atmospheric gases contributes to the total system temperature which temperature averaged over all the sources in the beam (≈ 3 K, since contributions from discrete sources can generally be ignored), and $T_{ATM}(\nu)$ is the atmospheric brightness temperature

$$T_{ATM}(\nu) = \sec \theta \int_h^\infty T_{KIN}(h') e^{-\tau_\nu(h, h', \theta)} K_\nu(h') dh' \quad (4)$$

where $T_{KIN}(h')$ is the kinetic temperature of the atmospheric gases at height h' and $\tau_\nu(h, h', \theta)$ is the optical depth between height h and height h' along a path of zenith angle θ ,

$$\tau_\nu(h, h', \theta) = \sec \theta \int_h^{h'} K_\nu(h') dh$$

for a plane-parallel atmosphere. If we have a signal $T^*(\nu)$ outside the atmosphere, we can then define a signal-to-noise ratio as

$$SNR = \frac{T^*(\nu) e^{-T(h, \theta)}}{T_{rec} + 2.7 e^{-\tau_\nu(h, \theta)} + T_{ATM}(\nu)} \quad (5)$$

This may be compared to the signal-to-noise ratio which the same receiver would have outside the earth's atmosphere

$$SNR^* = \frac{T^*(\nu)}{T_{REC} + 2.7} \quad (6)$$

If we compare Equations (5) and (6), we may define an "effective" system temperature for a receiver in the atmosphere,

$$T_{\text{sys}}^* = [T_{\text{REC}} + T_{\text{ATM}}(\nu)] e^{\tau(h, \theta)} + 2.7 \quad (7)$$

which may be thought of as the effective system temperature of a receiver outside the atmosphere which obtains the same signal-to-noise ratio. As we increase the altitude of our receiver, τ_ν and T_{ATM} decrease, and Equation (A-5) reduces to the extra-atmospheric case

$$T_{\text{sys}}^* = T_{\text{rec}} + 2.7 \quad (8)$$

In Figure A-2, we have plotted this effective system temperature for different locations within the earth's atmosphere. For the intrinsic receiver noise temperature, we have adopted a formula suggested by Penzias (private communication, 1975) that receiver developments within the near future should lead to receiver temperatures approximately equal to the operating frequency in GHz. Figure A-2 represents the ideal case of a receiver looking directly at the zenith; in the case of a receiver looking obliquely through the atmosphere, the performance will degrade in proportion to $\sec \theta$. The lower envelope of the curve for the C-141 represents the receiver performance in space (Eq. 8).

Figure A-2 is also useful for a cost-benefit analysis. If, for example, it were determined that observations from the Shuttle were 100 times as expensive as ground-based observations, we would then require our receiver to be $\sqrt{100}$ times more sensitive in space than on the ground. Then, at any frequency at which the effective system temperature exceeded the value of an equivalent receiver in space by 10 or more, observations in space would be more cost effective. Again, this represents an ideal case. In real life, however, atmospheric extinction will be variable, and this in turn will limit the ability of receivers to reduce noise by integration. (Millimeter observers have all experienced very irregular spectral baselines caused by clouds; for example, under such circumstances, longer integrations will not improve the quality of the spectra.)

A graphic way of looking at the effect of atmospheric attenuation is to consider the attenuation as decreasing the effective area of the antenna. The dashed line in Figure A-3 shows the maximum usable frequency plotted against maximum practical antenna diameter from the information given for ground-based telescopes. When observing through a lossy atmosphere with, for example, a 20-dB loss, the amount of signal is reduced by a factor of 100, and the antenna would be equivalent to an antenna outside the atmosphere with 1/100 of the area or 1/10 the diameter. The solid line in Figure A-3 shows the "effective diameter" of a ground-based telescope looking through a lossy atmosphere typical of that at the Kitt Peak site. For instance, the largest antenna that could be constructed on the ground, usable at 400 GHz, would be about 12-m diameter. When looking through the atmosphere, it would receive

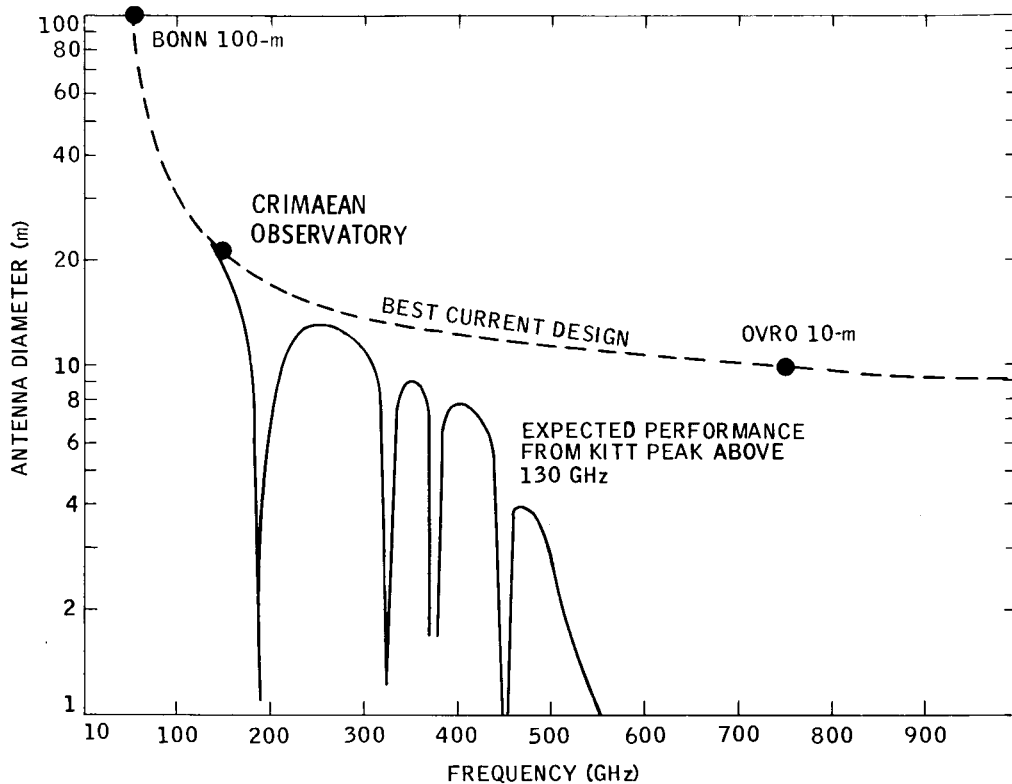


Figure A-3. Effective Antenna Diameter of the Largest Antennas Possible with Present Technology, when Such Antennas are Located on Kitt Peak

only as much energy as an 8-m antenna outside the atmosphere. An 11-m antenna at 600 GHz would receive only as much energy as a 10-cm antenna in space!

In the previous discussions, we have assumed that the molecules H_2O and O_2 are the sole source of the opacity. Ozone is the next most important source of opacity. There are some 65 transitions of ozone between 60 and 300 GHz. At sea level, the strongest has an optical depth of ~ 0.3 , giving a sky brightness of ~ 60 K, which is not much worse than the effect of the 22 GHz water line. Other atmospheric constituents have even less effect on atmospheric transparency.

APPENDIX B

THE PHYSICAL LIMITATIONS OF GROUND-BASED ANTENNAS

Cogdell *et al* (1970) have completed a survey of millimeter antennas now in use, which is listed with some additions in Table B-1. The physical limitations of these antennas are determined primarily by the accuracy of their reflecting surfaces, which determines the shortest wavelength at which the antennas can operate. Gravity loading, wind loading, and thermal gradients all act to distort the surface of a ground-based antenna. A parabolic antenna with an rms deviation of the surface, ϵ , has an effective area given by the approximate expression.

$$A_{\text{effective}} = A_{\text{geometric}} \cos^2(4\pi\epsilon/\lambda)$$

where λ is the operating wavelength (Christiansen and Hogbom 1969). Figure B-1 shows the loss in effective aperture as a function of ϵ/λ . As a rule-of-thumb, the wavelength equal to 16 times the rms surface deviations ($\lambda = 16\epsilon$) is defined as the shortest wavelength at which a telescope can operate. There is a 3-dB loss in antenna gain at this wavelength and the gain is rapidly decreasing.

Figure B-2 shows, for a variety of antennas, a plot of antenna diameter as a function of minimum usable wavelength. It can be seen that there is a definite correlation between antenna diameter and minimum usable wavelength. Von Hoerner (1967) has interpreted this figure in terms of three natural limits for the size of ground-based steerable antennas. These are a thermal-deflection limit, a gravitational-deflection limit, and a maximum-stress limit. The gravitational and thermal limits derived by von Hoerner are shown in Figure B-2 as dotted and dashed lines, respectively. These limits are in no sense absolute since they can be overcome by design. Thus, a special "homologously deforming" design permits the Bonn 100-m to operate in excess of the gravity limit, while shielding the antenna from direct sunlight improves the performance of the NRAO 11-m telescope.

Based on the results obtained with ground-based antennas, a 10-m antenna operating to wavelengths of 300 μm should require no engineering breakthroughs. The engineering challenge lies in using the gravity-free space environment to design even larger antennas.

Table B-1. Performance Parameters of Selected Filled Aperture Millimeter Radio Telescopes

<u>Organization</u>	<u>Diameter</u> (m) D	<u>RMS</u> <u>Surface</u> <u>Error</u> (mm)	<u>D/ε</u>	<u>Minimum</u> <u>Wavelength</u> (mm) $\lambda_m = 16\epsilon$	<u>Minimum</u> <u>Beamwidth</u> (arc/sec) $1.2\lambda_m/D$
Crimaen Observatory	22	0.12	1.8×10^5	1.9	21
Lebedev Physics Institute	22	0.50	4.4×10^4	8.0	90
Nat. Rad. Astr. Obs.	11	0.15	7.2×10^4	2.4	54
Owens Valley Rad. Obs.	10	0.025	4×10^5	.4	10
Aerospace Corp.	4.6	0.05	9.1×10^4	.8	43
Univ. of Texas	4.9	0.1	4.9×10^4	1.6	81
Air Force Cambridge Res. Labs	8.8	0.15	5.9×10^4	2.4	67
Bonn University	10	0.34	2.9×10^4	5.4	133
Communic. Res. Ctr	9.1	0.53	1.7×10^4	8.5	230
Univ. Calif. Berkeley	6.1	0.15	4.1×10^4	2.4	97
JPL Table Mtn Obs.	5.5	0.18	3.05×10^4	2.9	131
MIT Lincoln Labs	8.5	0.2	4.3×10^4	3.2	93

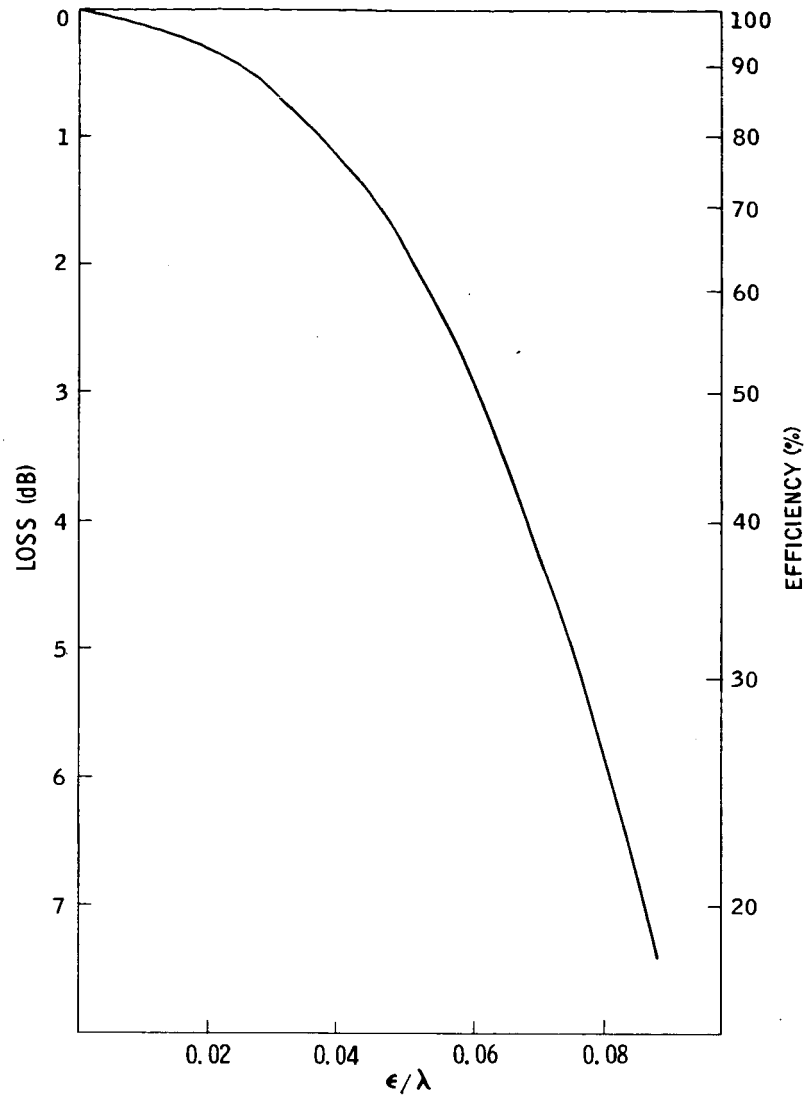


Figure B-1. Efficiency of a Reflecting Antenna as a Function of its Surface Irregularities

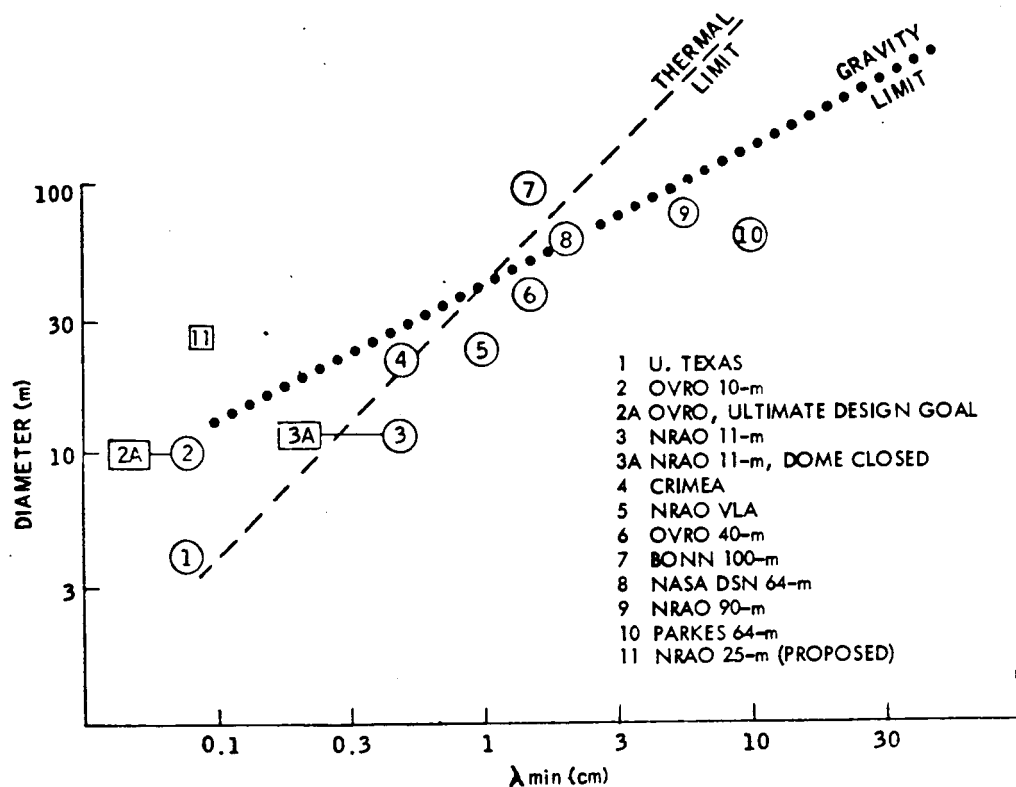


Figure B-2. Relationship between the Diameter of a Reflecting Antenna and its Minimum Operating Wavelength

APPENDIX C

REVIEW OF SUBMILLIMETER WAVE MIXERS*

Malcolm McCall
The Ivan A. Getting Laboratories
The Aerospace Corporation
El Segundo, CA 90245

Abstract

A survey of heterodyne mixers is presented for the wavelengths of 40 μm to 1000 μm as reported in the literature to date.

I. Introduction

The principle concerns in the choice of a heterodyne mixer are its sensitivity, bandwidth, and operating temperature. The Schottky-barrier diode mixer, discussed in Section II, is a room temperature wide bandwidth device. These features plus its high sensitivity have made it the most widely used mixer element at microwave and millimeter wavelengths and the most extensively explored mixing device at submillimeter wavelengths. The Josephson junction mixer, a cryogenic device, has yielded outstanding sensitivities well into the submillimeter and is discussed in Section III. Photoconductive mixers, which must also be cooled to liquid helium temperatures, are discussed in Section IV. Section V covers several other types of mixing devices, two of which, the hot carrier diode and the super-Schottky diode, may be strong contenders in the submillimeter in the near future.

As a general rule mixers require the order of 1 milliwatt of local oscillator (LO) power (delivered to the diode) for efficient mixing. The super-Schottky, hot electron photoconductive and Josephson junction mixers are, however, notable exceptions. Their LO requirements fall one, or more, orders of magnitude below the milliwatt level and could be provided by harmonic generation. The availability and quality of LO sources are not considered in this paper; for discussions on recent submillimeter/FIR laser developments, the reader is referred to several articles on the subject in this Proceedings.

II. Schottky-Barrier Mixers

Of the various devices explored as mixers at submillimeter wavelengths, the Schottky-barrier diode has received the greatest attention. Its inherent sensitivity, wide bandwidth, room temperature operation, and mechanical stability make it an attractive choice for a variety of system applications.

A Schottky-barrier diode consists of a metal contact deposited on a semiconductor substrate. The diode current voltage (I-V) characteristic is given to a good approximation by⁽¹⁾

$$I = i_o \left[\exp \left(\frac{qV}{nkT} \right) - 1 \right] \quad (1)$$

where q is the electronic charge, T is the temperature, k is Boltzman's constant, i_o is the saturation current and is determined by the area and material parameters of the diode, and n is the ideality factor which is approximately unity for low- to moderately-doped materials. This highly nonlinear relationship between I and V is responsible for the success of the Schottky diode as a detector and mixer.

This diode operates as a mixer in a fashion typical of the rectifying type of diode⁽²⁾. A large LO voltage is impressed on the diode to obtain a heavily-modulated time-dependent conductance $g(t)$, a function which is periodic in the LO frequency f_1 . In the presence of a signal voltage at frequency f_s , currents and voltages are generated at the intermediate frequency $f_{IF} = |f_1 - f_s|$. (For example, analytically a sinusoidal IF current is produced from the product of the sinusoidal signal voltage and the fundamental Fourier component of $g(t)$.) For low LO powers, the efficiency of this conversion process is a strong function of qV_1/nkT where V_1 is the amplitude of the LO voltage. With large LO power the conversion efficiency of the device saturates at a value determined by the impedance terminations on its input and output ports.

The sensitivity of a mixer (receiver) is expressible in terms of either its minimum detectable power MDP_M (MDP_R) or its mixer (receiver) noise temperature T_M (T_R). These quantities are related by the expression

$$MDP_{M,R} = k T_{M,R} B_{IF} \quad (2)$$

where k is Boltzman's constant and B_{IF} is the IF bandwidth. T_M and T_R are given by

$$T_M = L_c T_d \quad (3)$$

* This work was supported by The Aerospace Corporation on company-financed funds.

and

$$T_R = L_c (T_d + T_{IF}) \quad (4)$$

where L_c is the conversion loss of the mixer, defined as the ratio of available power from the RF source to the power absorbed in the IF load. T_d and T_{IF} are the noise temperatures of the mixer diode and IF amplifier, respectively. Hence in fabricating a mixer, utmost attention must be paid to minimizing L_c .

Conversion loss L_c of a mixer in a tunable mount is conveniently expressed as the product of three terms^(3,4,5)

$$L_c = L_0 L_1 L_2. \quad (5)$$

The intrinsic conversion loss L_0 is the loss arising from the conversion process within the nonlinear resistance of the diode and includes the impedance mismatch losses at the RF and IF ports. Analysis of L_0 as a function of qV_1/nkT for a properly-terminated sinusoidally-pumped broadband mixer yields the result shown in Fig. 1. The L_0 of a Schottky-barrier mixer has been recently analyzed as a function of diode diameter, impedance, temperature and the Richardson constant of the semiconductor and found to increase as any one of these quantities is reduced⁽⁶⁾. The RF and IF parasitic losses, L_1 and L_2 , respectively, are the losses associated with the parasitic elements of the diode. These losses are given by

$$L_1 = 1 + \frac{R_s}{R} + \omega^2 C^2 R R_s \quad (6)$$

$$L_2 = 1 + \frac{R_s}{R_2} \quad (7)$$

where R_s and C are the parasitic spreading resistance and junction capacitance, respectively, as shown in Fig. 2, and ω is the signal angular frequency. R_s is the resistance which results from the crowding of the current in the semiconductor near the metal contact. R is the signal input impedance of the local oscillator pumped nonlinear resistance, and R_2 is the IF load impedance. The ω^2 dependence of the third term in (6) is responsible for the degradation in the performance of Schottky-barrier mixers at high frequencies. However, both L_1 and L_2 are geometry and material dependent, and it is by the manipulation of these dependencies in the design of the diode that one reduces L_c at high frequencies. (Note added in proof: The skin effect resistance^(8,9) is being neglected relative to R_s . In general, this is an oversimplification but an acceptable one for optimum diode geometries^(5,19).)

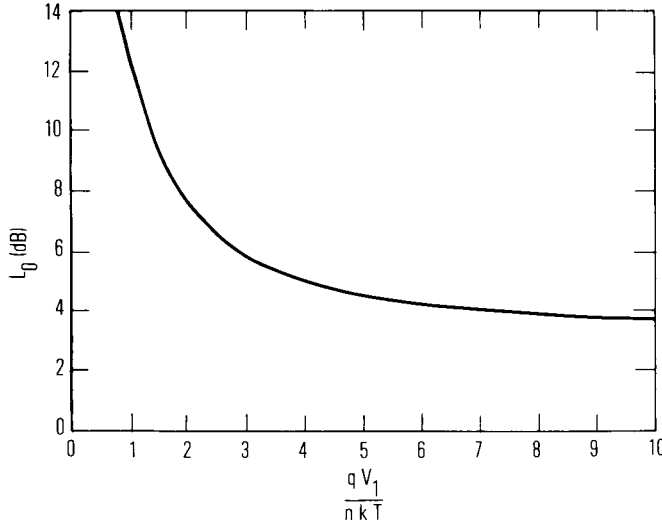


Fig. 1. Intrinsic conversion loss as a function of local oscillator drive for a Schottky-barrier mixer with optimum coupling.²

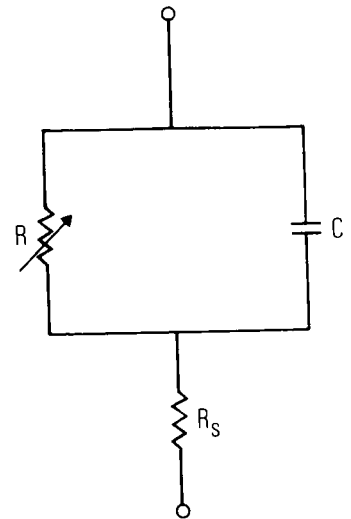


Fig. 2. Equivalent circuit of a Schottky-barrier diode.

A straightforward method for minimizing the third term in (6) is reducing C . Capacitance is proportional to area, and contact diameters of 1 to 2 μm obtained by photolithographic techniques are common at millimeter and submillimeter wavelengths. A dimension of 1 μm , however, is near the photolithographic limit. Using electron lithography, diameters as small as 0.1 μm have been obtained.⁽⁵⁾ Submicron-size diodes are useful in open or nontunable mounts as single contact diodes and in tunable mounts as multiple contact (contact array) diodes. This latter geometry is discussed below.

The loss terms in (6) and (7) are proportional to R_s , which in turn is inversely proportional to the mobility of the semiconductor. N-type GaAs has a large mobility, operates at room temperature, and is

commercially available. For these reasons nearly all millimeter and submillimeter wave Schottky-barrier mixers utilize this material.

The epitaxial diode structure shown in Fig. 3 is the standard design in high frequency Schottky-barrier mixers.⁽⁷⁻¹¹⁾ The epitaxial layer is grown very thin (as small as 1000Å) and the substrate is very heavily doped in order to reduce the diode spreading resistance. Moderate doping is chosen for the epitaxial layer so as to minimize the diode noise temperature T_D .⁽¹²⁾ For usage at millimeter and submillimeter wavelengths, diode diameters with micron dimensions are used to reduce the effects of C.

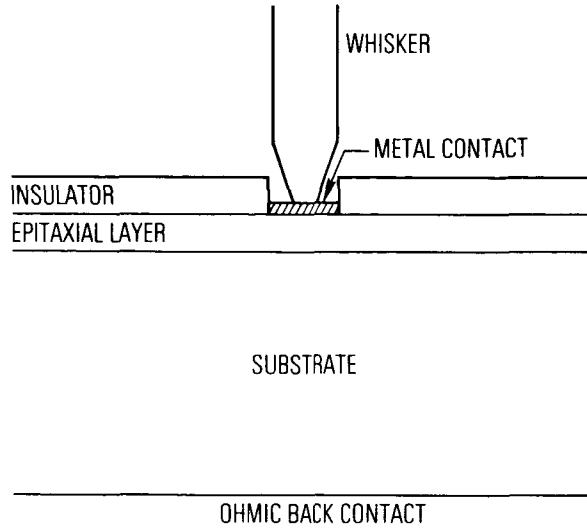


Fig. 3. The structure of an epitaxial Schottky-barrier diode. With n-GaAs the epilayer doping is 1 to $4 \times 10^{17} \text{ cm}^{-3}$ and the substrate doping is 2 to $5 \times 10^{18} \text{ cm}^{-3}$.

Contact to a Schottky-barrier diode is made by a whisker, as shown in Fig. 3. The whisker functions as an antenna to couple RF radiation to the junction, couple IF power out, and supply the required DC bias.

The contact array diode has been proposed as a favorable alternative to the epitaxial diode as a sensitive high frequency mixer.⁽⁵⁾ This diode achieves a low spreading resistance, and hence low L_j , by utilizing a structure consisting of a large number of small Schottky-barrier diodes connected in parallel. The number chosen is sufficiently large to maintain a low value of L_0 . Arrays with more than 100 diodes, each $0.35 \mu\text{m}$ in diameter, have been fabricated but not yet tested. Figure 4 is a sketch of the cross section of the diode, and Fig. 5 shows a scanning electron microscope (SEM) photograph of several linear contact-array diodes recently fabricated.⁽⁵⁾

For operation at wavelengths less than $50 \mu\text{m}$, special attention must be paid to the choice of the majority carrier concentration because of plasma frequency considerations.⁽¹³⁾ Calculations by Aukerman show excessive RF parasitic losses for frequencies near the plasma resonance of the semiconductor.⁽¹⁴⁾ The plasma resonance of n-type GaAs at a doping of $1 \times 10^{17} \text{ cm}^{-3}$ is approximately $34 \mu\text{m}$; for $5 \times 10^{18} \text{ cm}^{-3}$ it is near $15 \mu\text{m}$.⁽¹⁵⁾ Consequently, Schottky diodes uniformly doped to the latter concentration would appear to be the proper choice in the vicinity of $40 \mu\text{m}$. Another advantage of heavily doped Schottky diodes at high frequencies is that conduction in the device is the result of a tunneling process⁽¹⁶⁾; classical transit-time limitations which would attenuate the signal and local oscillator harmonics are avoided^(17, 18).

The function of the mixer mount is to both couple the radiation to the diode and provide a method to reactively tune out the capacitive C. The use of single mode waveguide mixer mounts is the standard method at microwave and millimeter wavelengths, and these are available commercially for frequencies up to 325 GHz.

A group at The Aerospace Corporation is developing a 600 GHz single mode waveguide mixer mount integrated with a horn antenna to couple incident radiation to the waveguide structure. At Lincoln Laboratory a group is designing a diode-mount configuration for 600 GHz operation based on a planar transmission line structure.⁽¹⁹⁾ This approach is covered in detail by Fetterman in an accompanying article in this Proceedings. Gustincic⁽²⁰⁾ is developing a 600 GHz quasi-optical mixer mount consisting of a biconical horn antenna with the diode situated at the gap of the antenna. Incident radiation is focused on the antenna which converts the power to an RF voltage across the diode. Tuning is provided by a curved back-short structure.

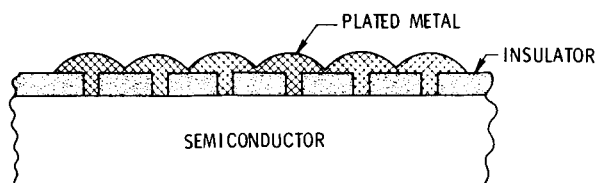


Fig. 4. The structure of a contact array diode. To reduce skin effect losses, ohmic contacts are made on the top surface encompassing the linear array on both sides.

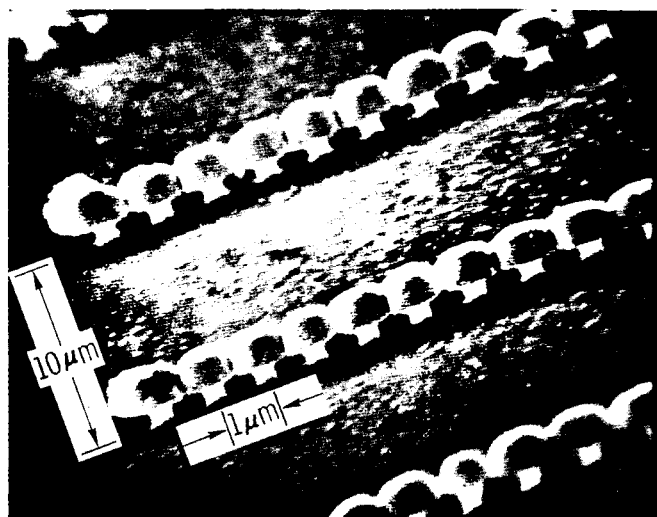


Fig. 5. An SEM photograph of preliminary linear contact-array diodes. The insulating layer normally present has been stripped away to permit viewing of the entire structure.⁽⁵⁾

Table I. Reported results with room temperature n-type GaAs Schottky-barrier mixers.

Wavelength (μm)	f_c (GHz)	Mixer MDP (W Hz^{-1})	References
70-1222	9000		Hodges and McColl ⁽¹³⁾
118	600	10^{-9}	Fetterman, et al. ^(21,22)
170		10^{-12}	
337		5×10^{-15}	
447		10^{-17}	Gustincic ⁽²⁰⁾
891	600	2×10^{-16}	Fetterman, et al. ^(21,22)
1300	1300	1.7×10^{-19}	Schneider and Wrixon ⁽²³⁾
1300	1000	1.2×10^{-19}	Goldsmith and Plambeck ⁽²⁴⁾
337	(Point Contact)	$10^{-15} - 10^{-16}$	Blaney, et al. ⁽²⁷⁾
337		10^{-17}	Zuidberg and Dymanus ⁽²⁹⁾
337		10^{-15}	Reinert ⁽³⁰⁾
500		2×10^{-18}	Packard ⁽²⁵⁾
1000		6×10^{-20}	Bauer, et al. ⁽²⁶⁾

Table I summarizes heterodyne results with Schottky-barrier diodes operating at room temperature. The figure of merit cut-off frequency $f_c = (2\pi R_s C_0)^{-1}$ is calculated from the zero bias capacitance C_0 and the measured dc series resistance R_s of the diode. Fetterman, et al. ^(21,22) using an n-GaAs epitaxial diode approximately 1 micron in diameter observed mixing at wavelengths as short as 118 μm . Hodges and McColl⁽¹³⁾ using 1/2 μm diameter contacts on $5 \times 10^{18} \text{ cm}^{-3}$ n-GaAs were able to extend the Schottky diode as a mixer to 70 μm and as a video detector to 42 μm ⁽⁵⁾. Both of these efforts used an open structure mixer mount with no provision for tuning out the reactances of the diode and whisker antenna. Gustincic's result at 447 μm was obtained using a Lincoln Lab diode mounted in the quasi-optical mount discussed above.⁽²⁰⁾ The result of Schneider and Wrixon⁽²³⁾ at 1300 μm using a single mode waveguide mount was obtained with insufficient LO power. One would conclude that the MDP could have been driven lower if more LO power had been available. Goldsmith and Plambeck⁽²⁴⁾ at 1300 μm employed second harmonic pumping.

Also shown for completeness in Table I are several results with point contact diodes formed on n-GaAs. Since there is always an uncertainty as to the nature of point contact devices, they are shown here as a subclass of Schottky diodes. The results of Packard⁽²⁵⁾ and Bauer, et al.⁽²⁶⁾ were obtained with n-GaAs and single mode waveguide mounts. The 500 μm result of Packard⁽²⁵⁾ used second harmonic pumping and a crossed waveguide configuration for the mount. The results of Blaney, et al.,⁽²⁷⁾ Zwelberg and Dymanus,⁽²⁹⁾ and Reinert⁽³⁰⁾ were with an n-GaAs diode in an open structure.

III. Josephson Junction Mixers

Proposed by Josephson⁽³¹⁾ in a theoretical article in 1962, the Josephson junction was originally envisioned as consisting of two superconductors separated by a thin insulating barrier. The insulator thickness was to be properly chosen to provide weak coupling for the superconducting electron pairs via tunneling. This type of coupling has since been demonstrated with a variety of barriers and structures, but the predominate configuration for high frequency mixing has consisted of a Nb point contact to a flat Nb surface.

The I-V characteristic of such a Josephson device is shown in Fig. 6 as curve A.⁽³²⁾ Up to a critical current I_c , current flows through the junction in the absence of a corresponding voltage drop. For currents

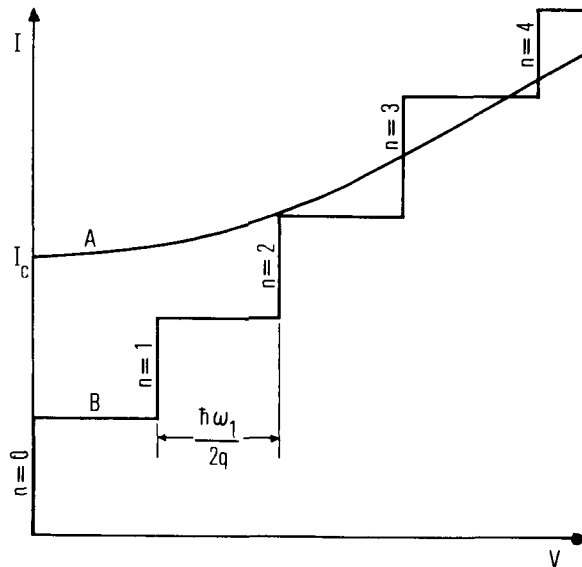


Fig. 6. Current voltage characteristics of a Josephson junction. Curves A and B are with and without local oscillator power, respectively.

greater than I_c , wherein a dc junction voltage does result, an oscillation in current and voltage is produced with an angular frequency given by

$$\omega_J = \frac{2q V_0}{\hbar} \quad (8)$$

where V_0 is the applied dc voltage and \hbar is Planck's constant divided by 2π .

If the device is biased with a dc voltage V_0 and an ac local oscillator voltage $V_1 \cos \omega_1 t$, the resulting supercurrent is

$$I = I_c \sin \frac{2q}{\hbar} \left[V_0 t + \frac{V_1}{\omega_1} \sin (\omega_1 t) + \alpha \right] \quad (9)$$

Hence the supercurrent is frequency modulated. Expanding this expression in harmonics, one obtains

$$I = I_c \sum_{-\infty}^{\infty} J_n \left(\frac{2q V_1}{\hbar \omega_1} \right) \sin \left[\left(n \omega_1 + \frac{2q V_0}{\hbar} \right) t + \alpha \right] \quad (10)$$

Thus the magnitudes of the harmonic components are determined by Bessel functions of order n .

The interaction between these harmonics and the self oscillation produce the zero frequency beats shown as steps in Fig. 6. These constant voltage steps are separated by multiples of the voltage $V = \hbar \omega_1 / 2q$.

The Josephson mixer is biased with a constant current between the $n = 0$ and $n = 1$ steps and with the zero voltage current diminished by approximately two. If a small signal with a frequency close to ω_1 is superimposed on this device, the result is, in effect, an amplitude modulation of the LO at the IF frequency.⁽³³⁾

The Josephson junction operates as an efficient mixer with small LO powers. However, another mode of operation for the Josephson junction is obtained by eliminating the external LO altogether and using the self oscillation of the junction in its stead. The main source of difficulty with this self-pumping mode is the noise introduced in the conversion process from a troublesomely large Josephson self-oscillation linewidth (≈ 1 GHz)^(34, 35). This mode of operation clearly needs further development; however, its goal is particularly desirable at FIR wavelengths where adequate LO source power is held at a premium.

Table II. Reported results with Josephson junction mixers at 4.2 K.

<u>Wavelength</u> (μm)	<u>MDP</u> (W Hz^{-1})	<u>References</u>
337	10^{-17}	Blaney ⁽³⁶⁾
950	3×10^{-21}	Edrich, et al. ⁽³⁷⁾

As summarized in Table II, the Josephson junction mixer has yielded very good sensitivities at sub-millimeter wavelengths. Blaney⁽³⁶⁾ using Nb-Nb point contacts at 4.2 K reports a receiver MDP of $1 \times 10^{-17} \text{ W Hz}^{-1}$ at $337 \mu\text{m}$ using 10^{-4} watts of LO power. Output noise was dominated by a room temperature amplifier with a noise temperature of 500 K. The smallest observed conversion loss of the junction was approximately 29 dB, a value which includes the signal input matching loss.

Edrich, et al.⁽³⁷⁾ also using Nb-Nb contacts at 4.2 K, report considerably better performance for the junction by subtracting off a number of system losses. They find the junction itself exhibits a conversion loss of 9.5 dB and a mixer noise temperature of 223 K at $950 \mu\text{m}$. This performance corresponds to a mixer MDP of 3×10^{-21} watts/Hz.

Tinkham, et al.⁽³⁸⁾ reason that the above theoretical treatment of the Josephson junction is inadequate at wavelengths shorter than $\approx 100 \mu\text{m}$. They attribute simple bolometric heating as the appropriate mixing mechanism at these wavelengths and estimate that the bandwidth of this type of mixing should be as large as the energy gap frequency.

IV. Photoconductive Mixers

Photoconductive detectors derive their radiation sensitivity from the change in semiconductor conductivity induced by the radiative transitions within the crystal. There are three different types of transitions: intrinsic, extrinsic and free carrier.⁽³⁹⁾

Intrinsic photoconductivity results from the photoexcitation of electrons from the valence band to the conduction band. For the wavelengths of interest here, this type of photoconductivity is not applicable. Extrinsic photoconductivity is derived from transitions from impurity levels within the gap to conduction band for n-type material and to the valence band for p-type material.

Free carrier photoconductivity results from a change in the conductivity of electrons already within the conduction band. By cooling the crystal to very low temperatures to weaken the coupling between the electrons and the lattice, the radiation absorbed by the electrons raises their temperature resulting in a change in mobility, and hence, a change in conductivity. Free carrier photoconductivity is applicable only at long wavelengths, i.e., greater than approximately $400 \mu\text{m}$.⁽²⁸⁾

Cryogenic cooling of all these photoconductors is a necessity at the wavelengths of interest. Only in the near infrared ($1 - 3 \mu\text{m}$) is room temperature operation permissible. As the detector wavelength increases, increased cooling is necessary to reduce the competition between carriers generated by incident signal photons and those generated thermally. In general, liquid helium temperatures are required for wavelengths longer than $100 \mu\text{m}$.

A photoconductive detector is adaptable to heterodyne mixing because of the nonlinearity present in its square law behavior. That is, the output current is proportional to the power absorbed in the crystal, and hence, proportional to the square of the electric field of the impressed radiation. In the presence of both signal and local oscillator power, this nonlinearity yields the IF, or difference frequency.

The bandwidth capability of the heterodyne photoconductor is limited by the majority carrier lifetime τ of the material. This lifetime is responsible for the degradation of mixer performance at high IF frequencies. τ is found to vary considerably with the semiconductor and dopant constituents. Consequently, for applications where a wide IF bandwidth is desirable, some semiconductors are more suitable for the task than others. However in general, photoconductive mixers in the FIR are characterized by bandwidths less than 10 MHz.

Table III. Reported results with extrinsic photoconductive mixers.

<u>Material</u>	<u>Wavelength</u> (μm)	<u>Bandwidth</u> (MHz)	<u>Temp. of</u> <u>Operation</u> (K)	<u>MDP</u> (W Hz^{-1})	<u>References</u>
Ge:Ga	119	≈ 5	4.2		Seib ⁽⁴⁰⁾
GaAs	337	> 4	4.2		Fetterman, et al. ⁽⁴¹⁾
Si (D^- state)	119	≈ 150	2	3×10^{-16}	Norton, et al. ⁽⁴³⁾
GaAs	337		4.2	1.4×10^{-14}	De Graauw, et al. ⁽⁴²⁾

Table III summarizes the results of three heterodyne experiments with extrinsic detectors. Seib's results with gallium-doped germanium at 119 μm were hampered by insufficient LO power.⁽⁴⁰⁾ In the experiments of Fetterman, et al.⁽⁴¹⁾ and DeGraauw, et al.⁽⁴²⁾ with GaAs at 337 μm , the detection mechanism is photo ionization of shallow donor states. The mechanism utilized in the experiments of Norton, et al.⁽⁴³⁾ is based on an unusual type of bound electron states in n-type Si. At low temperatures ($\approx 2\text{K}$) very weakly bound electron states can be formed between an electron and a neutral donor impurity. The observed photoconductivity results from the excitation of the electrons from these negative donor ion states to the conduction band. A measured response time of 10^{-9} seconds would indicate a 150 MHz heterodyne bandwidth, a value substantially larger than those typically encountered with extrinsic mixers. Their reported receiver MDP of 3×10^{-16} watts/Hz is an amplifier limited result.

Table IV. Reported results with hot electron photoconductive mixers at 4.2 K.

<u>Materials</u>	<u>Wavelength</u> (mm)	<u>Bandwidth</u> (MHz)	<u>MDP</u> (W Hz^{-1})	<u>References</u>
GaAs	4			Fetterman, et al. ⁽⁴¹⁾
InSb	1.3	2	4×10^{-21}	Phillips and Jefferts ^(44, 45)

Table IV summarizes the heterodyne results of two hot electron (free carrier absorption) photoconductive detectors. The results of Phillips and Jefferts^(44, 45) with an InSb hot electron bolometer are outstanding. With only 4×10^{-7} watts of LO power, they obtained an MDP of 4×10^{-21} W Hz^{-1} at 1.3 mm. They forecast that the device can be extended to about 600 μm before the bolometer element ceases to respond to radiation.

V. Other Detectors

Table V. Reported results with MOM and pyroelectric mixers.
Operating temperature is at room ambient.

<u>Detector Type</u>	<u>Wavelength</u> (μm)	<u>MDP</u> (W Hz^{-1})	<u>References</u>
Pyroelectric	337		Gebbie, et al. ⁽⁴⁰⁾
MOM	337	$10^{-15} - 10^{-16}$	Blaney, et al. ⁽²⁷⁾

Table V shows results of two other room temperature mixers. The pyroelectric detector is a ferroelectric device wherein incident radiation changes the spontaneous polarization of the lattice resulting in a net electric field across the crystal. Response times are limited by the electrical circuitry and the provisions for heat sinking. Nanosecond response times are possible but at the expense of a severe loss in sensitivity. Room temperature operation is the principle attraction of the pyroelectric detector. However, as a mixer, the large local oscillator powers necessary for high sensitivity may demand that cooling be a requirement.⁽²⁸⁾

The metal-oxide-metal (MOM) diode consists of a very light contact of a metal whisker onto a flat metal surface.⁽⁴⁷⁾ It is believed that this configuration produces a metal-oxide-metal structure whose I-V behavior is dominated by electron tunneling. The nonlinearity of its I-V characteristic, although weak, and its unusually wide bandwidth has allowed its use as a harmonic mixer to wavelengths as short as 2 μm .⁽⁴⁸⁾ The device is very unstable, but because of its wide bandwidth it has been an essential ingredient in precision frequency metrology experiments at FIR wavelengths.⁽⁴⁸⁻⁵⁰⁾

Two devices which have not yet been extended into the 40 μm - 1000 μm region, but may be in the near future, are the hot carrier (thermoelectric) diode⁽⁵¹⁻⁵³⁾ and the super-Schottky diode.⁽⁵⁴⁻⁵⁶⁾ The hot carrier diode is a metal semiconductor contact device in which incident radiation, coupled to the diode by a whisker antenna, is absorbed by majority carriers in the vicinity of the contact. These "warmed" carriers in turn generate a thermoelectric output voltage which is proportional to the absorbed incident power. The

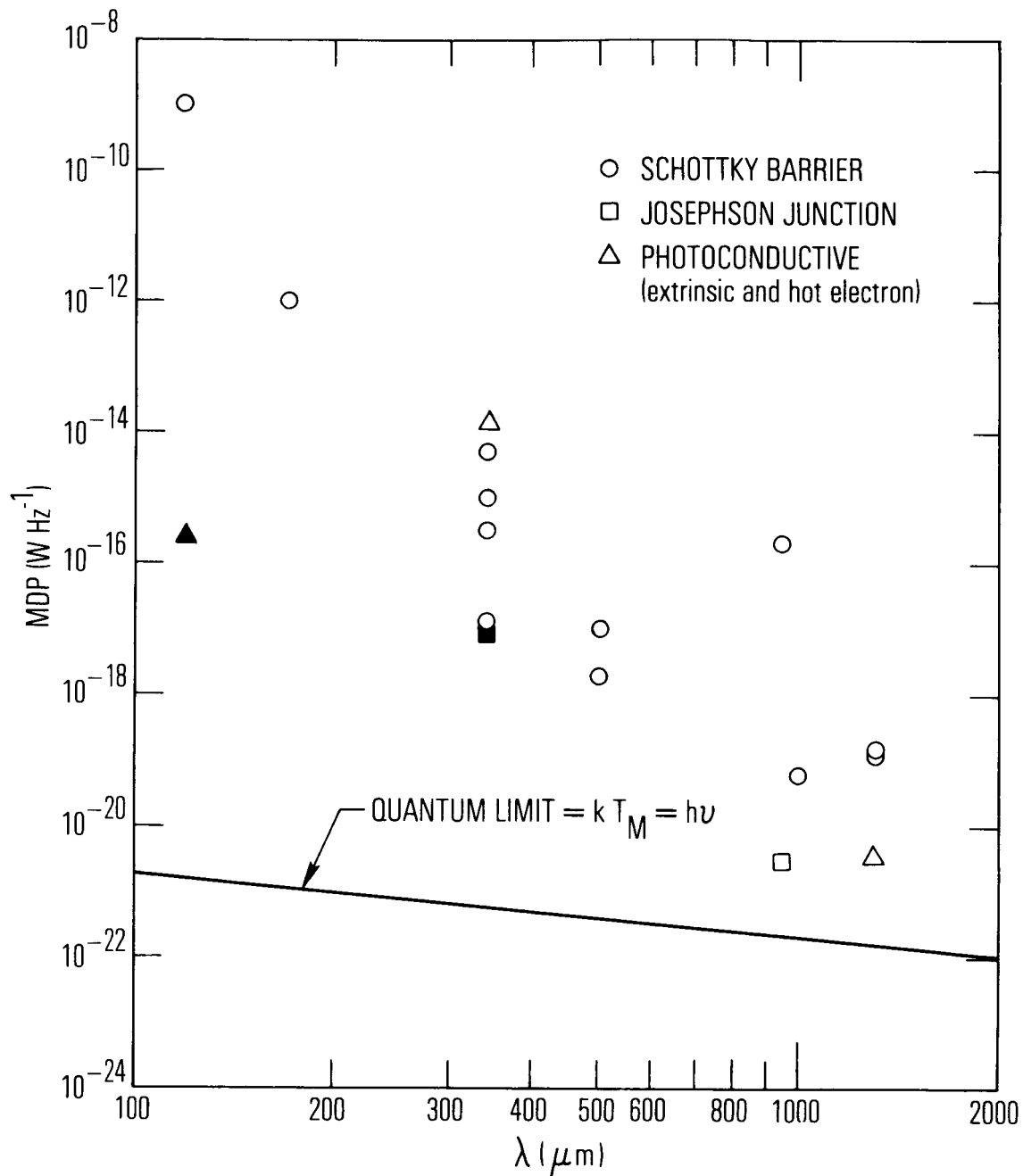


Fig. 7. Reported values of mixer minimum detectable power (MDP) as a function of wavelength. The two filled-in data points refer to values of receiver MDP. The Schottky-barrier mixer results were obtained with room temperature operation. The remaining devices were cooled to 4.2 K, or below.

bandwidth of this device is determined by the relaxation time τ_e for the hot carriers to thermalize with the lattice. For the semiconductors of interest, τ_e is the order of 10^{-11} s to 10^{-12} s at room temperature, indicating that bandwidths near 100 GHz are possible. Erlar and Aukerman⁽⁵³⁾ have recently observed room temperature mixing at $10.6 \mu\text{m}$ with an IF frequency of 55 GHz using a point contact to n-type InAs. (This material is particularly suited to the hot carrier device since metal contacts to n-InAs are characterized by the absence of a Schottky-barrier.) Because of a demonstrated sensitivity at $10 \mu\text{m}$, its wide bandwidth, room temperature operation, and its adaptability to microfabrication techniques developed for Schottky-barrier diodes, the hot carrier thermoelectric diode appears to have good potential in the submillimeter.

The super-Schottky diode is the most sensitive detector of microwave radiation yet developed,⁽⁵⁴⁻⁵⁶⁾ As a mixer at 10 GHz, it has delivered an MDP of $8 \times 10^{-23} \text{ WHz}^{-1}$ ($T_M = 6 \text{ K}$) at a liquid helium bath temperature of 1 K. The LO requirements are only 2×10^{-8} watts. A Schottky-barrier type of device, it consists of a superconducting contact to a heavily doped semiconductor. Experiments reported to date have used Pb contacts on p-type GaAs. The high solubility of GaAs for acceptor impurities fulfills the heavy doping requirement of the device but the mobility of p-GaAs is relatively low. The low mobility results in a loss in sensitivity at high frequencies due to the effects of the parasitic loss L_1 via the third term in (6). Development efforts to extend this device to millimeter and submillimeter wavelengths are centering on techniques to lower the spreading resistance of the device. The contact array method, discussed above in Section II, and the use of Schottky-barrier contacts to semiconductors with very high mobilities, e.g., n-InSb and n-InGaSb, are being actively pursued.^(5, 57)

VI. Conclusion

The above sections cover the major efforts reported on mixers operating in the $40 \mu\text{m}$ to $1000 \mu\text{m}$ range. A summary of reported sensitivities is presented in Fig. 7 along with the quantum limit for these types of mixers $kT_M = h\nu$.⁽⁵⁸⁾ This limit is applicable only for photon energies $h\nu$ much greater than kT , and hence, only for mixers cooled to cryogenic temperatures for the wavelengths under discussion.

Figure 7 illustrates in relative terms the excellent performance the Josephson junction mixer has yielded at submillimeter wavelengths. However, problems associated with the reproducibility of its properties and parameters and the mechanical stability of the device remain a major concern.

One would conclude that because of the many desirable features of the Schottky-barrier diode, this device will attract the bulk of the attention in the years to come. Its sensitivity, wide bandwidth, room temperature operation, and mechanical stability make the device an attractive choice. One can speculate that room temperature Schottky-barrier mixers with MDP's of 1×10^{-18} watts/Hz in the vicinity of $500 \mu\text{m}$ will be achieved in the very near future. At shorter wavelengths effective mixer mounts must be devised if efficient coupling to the diodes is to be achieved. This problem is common to all of the diode type of mixers and must be addressed if truly significant advances are to be made. It is clear that work is in its infancy and that much remains to be done.

References

1. Sze, S.M., Physics of Semiconductor Devices, New York: Wiley, 1969, pp. 393-394.
2. Torrey, H.C. and Whitmer, C.A., Crystal Rectifiers (M.I.T. Radiation Lab. Ser., vol. 15), New York: McGraw-Hill, 1948.
3. Messenger, G.C., and McCoy, C.T., "Theory and Operation of Crystal Diodes as Mixers," Proc. IRE, vol. 45, pp. 1269-1283. 1957.
4. Kerr, A.R., "Low-Noise Temperature and Cryogenic Mixers for 80-120 GHz," IEEE Trans. Microwave Theory Tech., Vol. MTT-23, pp. 781-787. 1975.
5. McColl, M., Hodges, D.T., and Garber, W.A., "Submillimeter-wave Detection with Submicron-size Schottky-barrier Diodes," in Conf. Digest, Second Int. Conf. and Winter School on Submillimeter Waves and Their Applications, San Juan, Puerto Rico, Dec. 1976, pp. 62-63; IEEE Trans. Microwave Theory Tech., Vol. MTT-25, June, 1977 (in press).
6. McColl, M., "Conversion Loss Limitations on Schottky-barrier Mixers," IEEE Trans. Microwave Theory Tech., Vol. MTT-25, pp. 54-59. 1977.
7. Leedy, H.M., Stover, H.L., Morehead, H.G., Bryan, R.P., and Garvin, H.L., "Advanced Millimeter-wave Mixer Diodes, GaAs and Silicon, and a Broadband Low-noise Mixer," in Proc. 3rd Biennial Cornell Engineering Conf. (Ithaca, N.Y.), pp. 451-462. 1971.
8. Clifton, B.J., Lindley, W.T., Chick, R.W., and Cohen, R.A., "Materials and Processing Techniques for the Fabrication of High Quality Millimeter Wave Diodes," in Proc. 3rd Biennial Cornell Engineering Conf. (Ithaca, N.Y.), pp. 463-475. 1971.
9. Wrixon, G.T., "Low-noise Diodes and Mixers for the 1-2 mm Wavelength Region," IEEE Trans. Microwave Theory Tech., Vol. MTT-22, pp. 1159-1165. 1974.
10. Schneider, M.V., and Carlson, E.R., "Notch-front Diodes for Millimeter-wave Integrated Circuits," to be published.
11. Schneider, M.V., and Linke, R.A., "Low-noise Millimeter-wave Mixer Diodes Prepared by Molecular Beam Epitaxy (MBE)," to be published.
12. Viola, T.J., Jr. and Mattauch, R.J., "Unified Theory of High-frequency Noise in Schottky Barriers," J. Appl. Phys., Vol. 44, pp. 2805-2808. 1973.
13. Hodges, D.T. and McColl, M. "Extension of the Schottky Barrier Detector to $70 \mu\text{m}$ (4.3 THz) Using Submicron Dimensional Contacts," Appl. Phys. Lett., Vol. 30, pp. 5-7. 1977.

14. Aukerman, L.W., private communication.
15. For a survey of this subject, see Schumann, P.A., "Plasma Resonance Calibration Curves for Silicon, Germanium and Gallium Arsenide," Solid State Tech., Vol. 13, pp. 50-51, Jan. 1970.
16. Millea, M. F., McColl, M. and Mead, C.A., "Schottky Barriers on GaAs," Phys. Rev., Vol. 177, pp. 1164-1172. 1969.
17. Thornber, K.K., McGill, T.C. and Mead, C.A., "The Tunneling Time of an Electron," J. Appl. Phys., Vol. 38, pp. 2384-2385. 1967.
18. van der Ziel, A., "Infrared Detection and Mixing in Heavily Doped Schottky-barrier Diodes," J. Appl. Phys., Vol. 47, pp. 2059-2068. 1976.
19. Murphy, R.A., Bozler, C.O., Parker, C.D., Fetterman, H.R., Tannenwald, P.E., Clifton, B.J., Donnelly, J.P., and Lindley, W.T., "Submillimeter Heterodyne Detection with Planar GaAs Schottky-barrier Diodes," IEEE Trans. Microwave Theory Tech., Vol. MTT-25, June 1977 (in press).
20. Gustinic, J.J., "A Quasi-optical Radiometer," presented at the Second Int. Conf. and Winter School on Submillimeter Waves and Their Applications, San Juan, Puerto Rico, Dec. 1976, pp. 106-107.
21. Fetterman, H.R., Clifton, B.J., Tannenwald, P.E., and Parker, C.D., "Submillimeter Detection and Mixing Using Schottky Diodes," Appl. Phys. Lett., Vol. 24, pp. 70-72. 1974.
22. Fetterman, H.R., Clifton, B.J., Tannenwald, P.E., Parker, C.D., and Penfield, H., "Submillimeter Heterodyne Detection and Harmonic Mixing Using Schottky Diodes," IEEE Trans. Microwave Theory Tech., Vol. MTT-22, pp. 1013-1015. 1974.
23. Schneider, M.V., and Wrixon, G.T., "Development and Testing of a Receiver at 230 GHz," IEEE S-MTT Int. Microwave Symp. Dig. Tech., (Atlanta, Ga.), 1974, pp. 120-122.
24. Goldsmith, P.F. and Plambeck, R.L., "A 230-GHz Radiometer System Employing a Second-harmonic Mixer," IEEE Trans. Microwave Theory Tech., Vol. MTT-24, pp. 859-861. 1976.
25. Packard, R.F., "A Superheterodyne 600 Gc Radiometer Receiver," presented at the 1965 G-MTT Symposium, Orlando, Fla.
26. Bauer, R.J., Cohn, M., Cotton, J.M., Jr., and Packard, R.F., "Millimeter Wave Semiconductor Diode Detectors, Mixers, and Frequency Multipliers," Proc. IEEE, Vol. 54, pp. 595-605. 1966.
27. Blaney, T.G., Bradley, C.C., Edwards, G.J., and Knight, D.J.E., CPEM 74 Digest, IEEE Conference Publication, No. 113, p. 99, 1974, as referenced in Ref. 28.
28. De Graauw, Th., "Detectors for Infrared Heterodyne Mixing and Detection", Space Science Reviews, Vol. 17, pp. 709-719. 1975.
29. Zuidberg, B.F.J., and Dymanus, A., "Heterodyne Spectroscopy in the THz Region with a Laser Local Oscillator", in Conf. Digest, Second Int. Conf. and Winter School on Submillimeter Waves and Their Applications, San Juan, Puerto Rico, Dec. 1976, pp. 185-186.
30. Reinert, W., "Investigation of a Superheterodyne Mixing System with an 'Open Structure' Mixer at 337 μm Wavelength," Space Science Reviews, Vol. 17, pp. 703-707. 1975.
31. Josephson, B.D., "Possible New Effects in Superconductive Tunneling," Phys. Lett., Vol. 1, pp. 251-253. 1962.
32. For a concise review of superconductivity and the Josephson junction, see Mercereau, J.E., "Superconductivity" in Topics in Solid State and Quantum Electronics, W.D. Hersberger, Ed., New York: Wiley, 1972, pp. 224-240.
33. Taur, Y., Claassen, J.H. and Richards, P.L., "Josephson Junctions as Heterodyne Detectors," IEEE Trans. Microwave Theory Tech., Vol. MTT-22, pp. 1005-1009. 1974.
34. Vernet, G. and Adde, R., "Josephson Frequency Conversion in the Range 145 - 1600 GHz with Nb-Nb Superconducting Point Contacts Used as Oscillator-mixer," J. Appl. Phys., Vol. 45, pp. 2678-2688. 1974.
35. Vernet, G., Hénau, J-C., and Adde, R., "The Josephson Self-Oscillator Mixer as a Submillimeter and Far-Infrared Detector", in Conf. Digest, Second Int. Conf. and Winter School on Submillimeter Waves and Their Applications, San Juan, Puerto Rico, Dec. 1976, pp. 183-184.
36. Blaney, T.G., "Heterodyne Laser Radiation Detection at 891 GHz using Josephson Point Contacts," Rev. Phys. Appl., Vol. 9, pp. 279-284. 1974.
37. Edrich, J., Sullivan, D.B., and McDonald, D.G., "Results, Potentials and Limitations of Josephson Mixer Receivers at mm and Long Submm Wavelengths," IEEE Trans. Microwave Theory Tech., Vol. MTT-25, 1977 (in press).
38. Tinkham, M., Octavio, M. and Skocpol, W.J., "Heating effects in high-frequency metallic Josephson devices," J. Appl. Phys., Vol. 48, pp. 1311-1320. 1977.
39. For an excellent review of FIR photoconductivity, see: Putley, E.H., "Far Infra-red Photoconductivity," Phys. Stat. Sol. Vol. 6, pp. 571-614. 1964.
40. Seib, D. H., "Heterodyne Detection Experiments at 118.6 μm in Ge:Ga", IEEE J. Quantum Electron., Vol. QE-10, pp. 130-131. 1974.
41. Fetterman, H.R., Tannenwald, P.E., and Parker, C.D., "Millimeter and Far Infrared Frequency Mixing in GaAs," Proc. Symp. Submillimeter Waves, J. Fox (ed.), Polytechnic Press, Brooklyn, N.Y., 1970, pp. 591-594.
42. De Graauw, Th., Van De Stadt, H., Bicanic, D., and Zuidberg, B., "Heterodyne Detection at 337 μm in Epitaxial GaAs," Infrared Phys., Vol. 16, pp. 233-235. 1976.
43. Norton, P., Slusher, R.E., and Sturge, M., "Heterodyne Detection in the Far Infrared Using Shallow Impurity States in Silicon," in Conf. Digest, Second Int. Conf. and Winter School on Submillimeter Waves and Their Applications, San Juan, Puerto Rico, Dec. 1976, pp. 187-188.
44. Phillips, T.G., and Jefferts, K.B., "A Low Temperature Bolometer Heterodyne Receiver for Millimeter Wave Astronomy," Rev. Sci. Instrum., Vol. 44, pp. 1009-1014. 1973.
45. Phillips, T.G., and Jefferts, K.B., "Millimeter-wave Receivers and Their Applications in Radio Astronomy," IEEE Trans. Microwave Theory Tech., Vol. MTT-22, pp. 1290-1292. 1974.

46. Gebbie, H.A., Stone, N.W.B., Putley, E.H., and Shaw, N., "Heterodyne Detection of Sub-millimetre Radiation," Nature, Vol. 214, pp. 165-166. 1967.
47. Dees, J.W., "Detection and Harmonic Generation in the Submillimeter Wavelength Region," The Microwave Journal, Vol. 9, pp. 48-55. 1966.
48. Jennings, D.A., Petersen, F.R., and Evenson, K.M., "Extension of Absolute Frequency Measurements to 148 THz: Frequencies of the 2.0- and 3.5- μ mXe Laser," Appl. Phys. Lett., Vol. 26, pp. 510-511. 1975.
49. Daneu, V., Sokoloff, D., Sanchez, A., and Javan, A., "Extension of Laser Harmonic-frequency Mixing Techniques into the 9 μ Region with an Infrared Metal-Metal Point Contact Diode," Appl. Phys. Lett., Vol. 15, pp. 398-401. 1969.
50. Sakuma, E. and Evenson, K.M., "Characteristics of Tungsten-Nickel Point Contact Diodes Used as Laser Harmonic-Generator Mixers," IEEE J. Quantum Electron., Vol. QE-10, pp. 599-603. 1974.
51. Harrison, R.I. and Zucker, J., "Hot-carrier Microwave Detector," Proc. IEEE, Vol. 54, pp. 588-595. 1966.
52. Aukerman, L.W. and Erler, J.W., "InAs Hot Carrier Optical Diode at 10.6 μ m," to be published.
53. Erler, J.W. and Aukerman, L.W., "Heterodyne Detection at 10 μ m with a Hot Carrier Diode," Bull. Am. Phys. Soc., Vol. 22, p. 261. 1977.
54. McColl, M., Pedersen, R.J., Bottjer, M.F., Millea, M.F., Silver, A.H., and Vernon, F.L., Jr., "The super-Schottky Diode Microwave Mixer," Appl. Phys. Lett., Vol. 28, pp. 159-162. 1976.
55. McColl, M., Millea, M.F., Silver, A.H., Bottjer, M.F., Pedersen, R.J., and Vernon, F.L., Jr., "The super-Schottky Microwave Mixer," IEEE Trans. Magn., Vol. MAG-13, pp. 221-227. 1977.
56. Vernon, F.L., Jr., Millea, M.F., Bottjer, M.F., Silver, A.H., Pedersen, R.J., and McColl, M., "The super-Schottky Diode," IEEE Trans. Microwave Theory Tech., Vol. MTT-25, April 1977 (in press).
57. McColl, M., and Millea, M.F., "Schottky Barriers on InSb," J. Electronic Materials, Vol. 5, pp. 191-207. 1976.
58. Oliver, B.M., "Thermal and Quantum Noise," Proc. IEEE, Vol. 53, pp. 436-454. 1965.
59. Champlin, K. S. and Eisenstein, G., "Cut-off Frequency of Submillimeter Schottky-Barrier Diodes", submitted for publication.